HYDRAULIC DESIGN CRITERIA

SHEETS 211-1 TO 211-1/2

SLUICE ENTRANCES FLARED ON FOUR SIDES

PRESSURE-DROP COEFFICIENTS

1. Purpose. The objectives in sluice entrance design are positive pressures at all flows to preclude cavitation, smoothly varying pressures to minimize entrance losses, and small size for stop-log closure. Hydraulic Design Charts 211-1 to 211-1/2 give pressure-drop data for several shapes of entrances to rectangular sluices.

2. Theory. The pressure drop (H_d) from the reservoir surface to any point on the pressure gradient for an entrance curve can be expressed as a function of the velocity head in the conduit proper:

$$H_d = C(V^2/2g)$$

where

H_d = pressure drop, ft

C = dimensionless pressure-drop coefficient

V = average velocity in conduit proper, fps.

3. Experimental Data. The pressure data on Chart 211-1 to 211-1/2 were obtained from tests conducted at the Waterways Experiment Station under CW 802, Conduit Intake Model Tests.* The laboratory test section represented a prototype sluice 5.67 ft wide by 10 ft high ($h/w = 1.765$) with the elliptical and combination elliptical entrance curves shown on the charts. The value of D in the curve equations is equal to the conduit height for the top and bottom curves and the conduit width for the side curves. The Pine Flat prototype data** shown on Chart 211-1/2

* Entrances to Conduits of Rectangular Cross Section; Investigation of Entrance Flared in Four Directions. U. S. Army Engineer Waterways Experiment Station, CE, TM 2-428, Report No. 1, Vicksburg, Miss., March 1956.

** Vibration, Pressure and Air-Demand Tests in Flood-control Sluice, Pine Flat Dam, Kings River, California. U. S. Army Engineer Waterways Experiment Station, CE, Miscellaneous Paper No. 2-75, Vicksburg, Miss., February 1954, and subsequent unpublished test data.

are for a 5-ft-wide by 9-ft-high (h/w = 1.80), horizontal sluice with ellipitical entrance curves at the 20-on-1 sloping upstream face. These data are averages obtained for 14 pool elevations between 113 and 302 ft above the sluice center line.

4. The CW 802 data are from laboratory tests in which the discharge was closely controlled. The Pine Flat prototype data are based on a discharge curve developed from stream measurements. The pressure-drop coefficients are sensitive to small inaccuracies in discharge, and the discrepancy between the laboratory and prototype data is attributed to such small inaccuracies. A 2 per cent adjustment in the basic discharge data would result in close agreement.

5. Sluice Entrance Pressures. The dimensionless pressure-drop coefficients given on Charts 211-1 to 211-1/2 can be used to compute the pressure gradient elevations for the given entrance shapes. The pressure gradient for any combination of pool elevation and discharge then can be compared with the entrance profile to determine the pressures on the entrance surfaces. The elliptical shape should normally be used, but for high dams with insufficient back pressures use of the longer combination elliptical curve may be necessary to prevent occurrence of negative pressures.

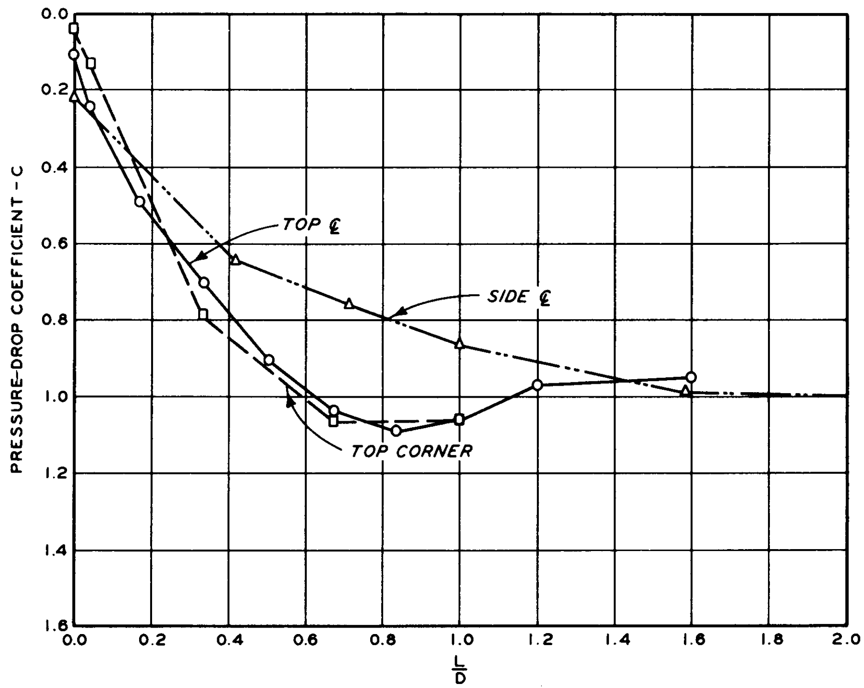

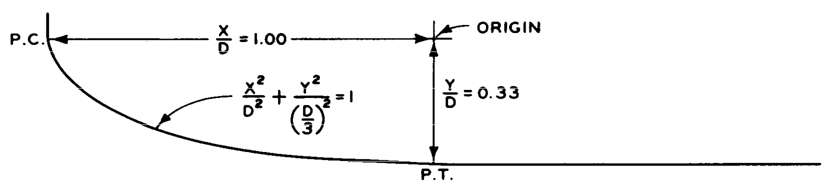

BASIC EQUATION

$$C = \frac{H_D}{\frac{V^2}{2g}}$$

WHERE:

C = PRESSURE-DROP COEFFICIENT
H_D = PRESSURE DROP FROM POOL IN FT
V = AVERAGE VELOCITY IN CONDUIT PROPER IN FT PER SEC

NOTE:

RESULTS BASED ON CW802 TEST DATA (h/w=1.765).

D = DIMENSION OF CONDUIT IN DIRECTION CONCERNED IN FT
L = DISTANCE ALONG CONDUIT IN FT
h = HEIGHT OF CONDUIT PROPER
w = WIDTH OF CONDUIT PROPER

SLUICE ENTRANCES
PRESSURE-DROP COEFFICIENTS
ELLIPTICAL SHAPE

HYDRAULIC DESIGN CHART 211-1

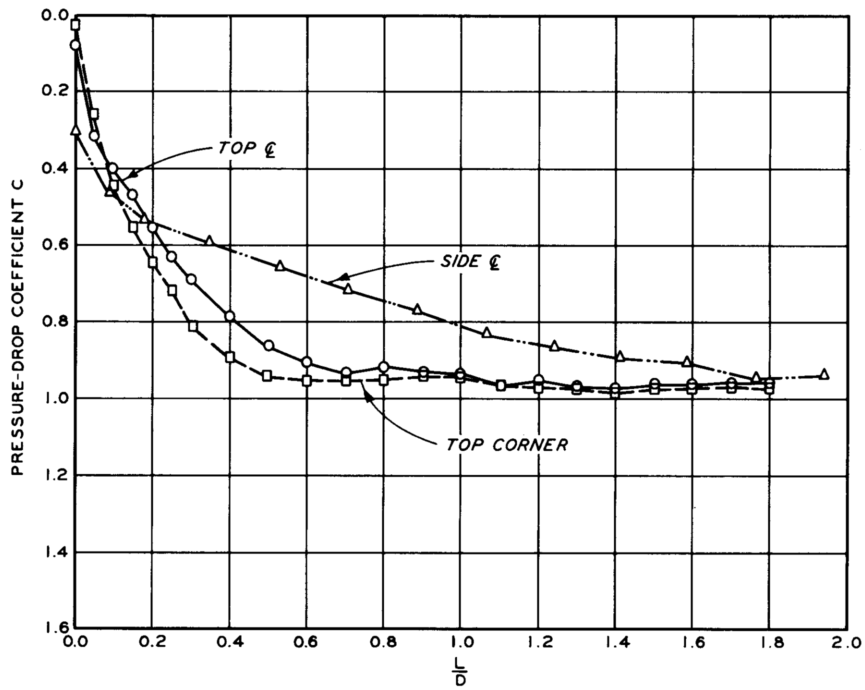

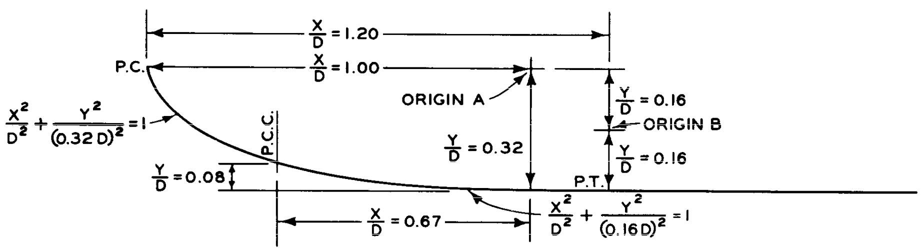

BASIC EQUATION

$$C = \frac{H_D}{\frac{V^2}{2g}}$$

WHERE:

- C = PRESSURE-DROP COEFFICIENT
- H_D = PRESSURE DROP FROM POOL, FT
- V = AVERAGE VELOCITY IN CONDUIT PROPER, FT PER SEC

NOTE:

RESULTS BASED ON ES 802 TEST DATA (h/w = 1.765).

D = DIMENSION OF CONDUIT IN DIRECTION CONCERNED, FT
L = DISTANCE ALONG CONDUIT, FT
h = HEIGHT OF CONDUIT PROPER, FT
w = WIDTH OF CONDUIT PROPER, FT

SLUICE ENTRANCES

PRESSURE-DROP COEFFICIENTS
COMBINATION ELLIPTICAL SHAPE

HYDRAULIC DESIGN CHART 211-1/1

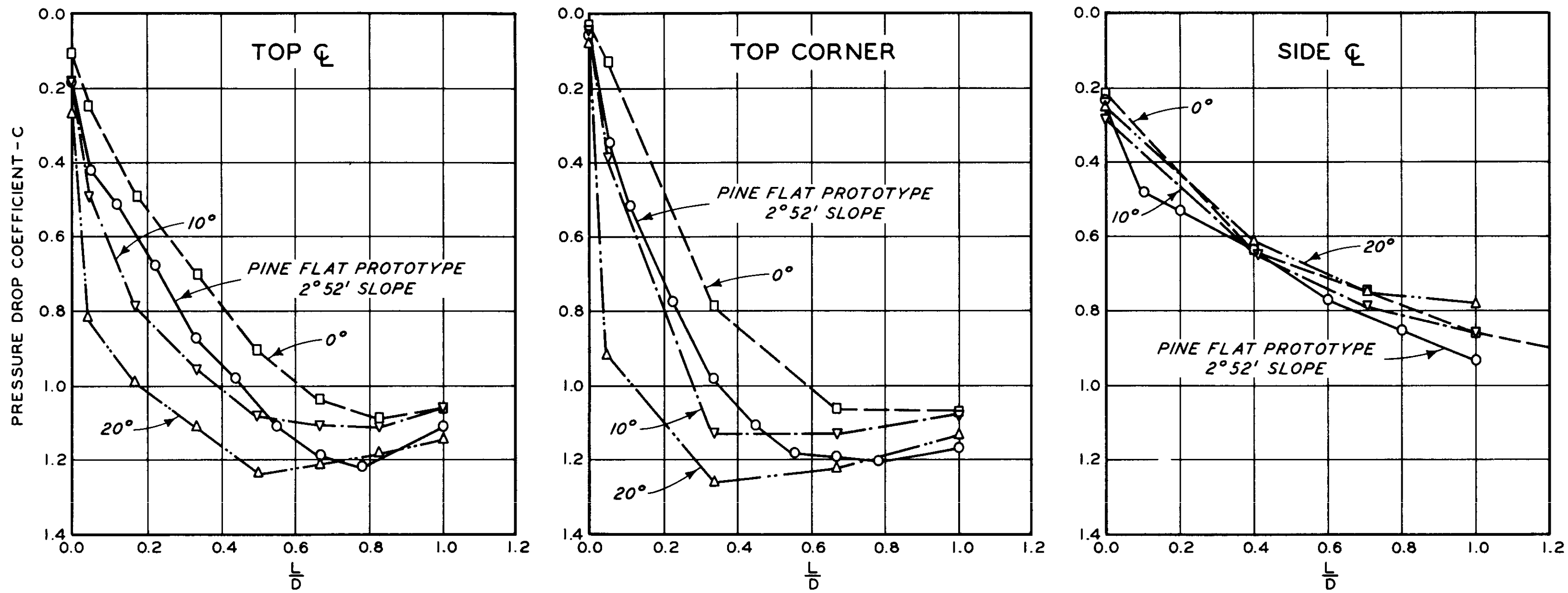

BASIC EQUATION

$$C = \frac{H_D}{\frac{V^2}{2g}}$$

WHERE:

C = PRESSURE DROP COEFFICIENT
H_D = PRESSURE DROP FROM POOL IN FT
V = AVERAGE VELOCITY IN CONDUIT PROPER IN FT PER SEC

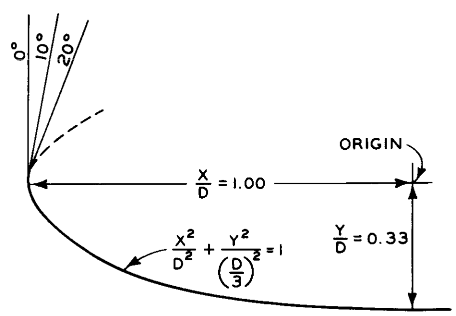

DEFINITION SKETCH

D = DIMENSION OF CONDUIT IN DIRECTION CONCERNED IN FT
L = DISTANCE ALONG CONDUIT IN FT
h = HEIGHT OF CONDUIT PROPER
w = WIDTH OF CONDUIT PROPER

NOTE:

COEFFICIENTS BASED ON CW802 MODEL TEST DATA (h/w = 1.765). PINE FLAT PROTOTYPE DATA FOR HORIZONTAL SLUICE (h/w = 1.800) WITH ENTRANCE AT 20 ON 1 (2°52′) SLOPING UPSTREAM FACE.

SLUICE ENTRANCES

PRESSURE DROP COEFFICIENTS
ELLIPTICAL SHAPE
EFFECT OF ENTRANCE SLOPE

HYDRAULIC DESIGN CHART 211-1/2

WES 6-57

HYDRAULIC DESIGN CRITERIA

SHEETS 212-1 TO 212-1/2

GATE SLOTS

PRESSURE COEFFICIENTS

1. Background. Flow past gate slots results in a decrease in pressure on the conduit walls immediately downstream from the slot. Cavitation erosion can occur downstream from the slot when high-velocity flow is accompanied by insufficient pressure in the general region. One of the variables involved is the ratio of the slot width to depth. Another important variable is the conduit geometry downstream from the slot. Undesirable pressure conditions on the conduit walls can be improved to some degree by offsetting the downstream edge of the slot and returning gradually to the original conduit wall alignment.

2. Basic Data. Hydraulic Design Chart 212-1 presents pressure coefficients for rounded corner gate slots with a width-depth ratio equal to 2.1. Similar data for a ratio of 1.8 are presented in Chart 212-1/1 for slots with the rounded downstream corners combined with a 1:12 taper to the original conduit alignment. The coefficients shown were computed using the equation

$$H_d = CH_v$$

where

H_d = pressure difference from reference pressure, ft

C = pressure coefficient

H_v = conduit velocity head at reference pressure station, ft

The reference pressure station noted above is shown in the definition sketch in each chart. The coefficients shown in the charts result from U. S. Army Engineer Waterways Experiment Station (WES) laboratory tests made on 1-to-6-scale models of gate slot designs for Bull Shoals Dam.[1]

3. Chart 212-1/2 presents coefficients for computing the minimum pressure in and downstream from square-edged slots with ratios of width to depth ranging from 0.5 to 2.5. The chart is based on tests by the U. S. Bureau of Reclamation (USBR)[2] with supporting data by Spengo.[3] The USBR tests also included study of the effects of rounding the upstream corner of the gate slot, decreasing the downstream wall convergence rate to 1:24 and 1:36, and using convergences shaped to circular arcs. Rounding of the upstream corner of the slot appears to have little effect on the pressures in or near the slot unless the rounding is appreciable.

In this case expansion of the flow into the slot can result in greater downstream flow contraction accompanied by greater pressure reduction on the downstream walls. Changing the downstream convergence rate to 1:24 and 1:36 effects a downstream movement of the minimum pressure location with no appreciable pressure changes. The USBR tests also showed that convergences shaped to circular arcs are hydraulically superior to those formed by tangents.

4. The coefficients shown in Charts 212-1 through 212-1/2 are based on mean piezometric measurements and do not reflect local pressure fluctuations caused by turbulence in the flow. It is suggested that the minimum computed pressure be limited to at least atmospheric pressure to reduce the possibility of cavitation in the prototype. Prototype data from electric pressure transducers are needed for firm criteria.

5. Design Criteria. Charts 212-1 through 212-1/2 should be used as guides for estimating minimum pressure conditions in the vicinity of gate slots for full tunnel flow. The rounding of the upstream edge of the gate slot shown in the charts can be eliminated with no apparent adverse hydraulic or structural effects. The 1:12 downstream taper shown in Chart 212-1/1 has been generally adopted for design and found satisfactory. In practice, the radius of the downstream corner of the gate slot has been appreciably decreased over that shown in the charts to reduce gate span and slot depth, thereby effecting savings in costs. Experience indicates that for part-gate operation cavitation erosion mainly occurs 6 to 8 in. downstream from the beginning of the 1:12 taper rather than at the end of the taper, as inferred from Chart 212-1/1. If the gates are to be operated appreciably at part-gate openings under high heads, consideration should be given to using stainless steel for the first 6 to 8 in. of the taper. The design criteria above is recommended for high head structures. The simpler gate slot design given in Chart 212-1 should be adequate for low heads when the conduit back pressure results in a minimum computed average local pressure approximating atmospheric pressure.

6. References.

(1) U. S. Army Engineer Waterways Experiment Station, CE, Model Studies of Conduits and Stilling Basin, Bull Shoals Dam, White River, Arkansas. Technical Memorandum No. 2-234, Vicksburg, Miss., June 1947.

(2) Ball, J. W., "Hydraulic characteristics of gate slots." ASCE, Hydraulics Division, Journal, vol 85, HY 10 (October 1959), pp 81-114.

(3) Spengo, A., "Cavitation and Pressure Distribution at Gate Slots." M.S. thesis, University of Iowa, Iowa City, June 1949.

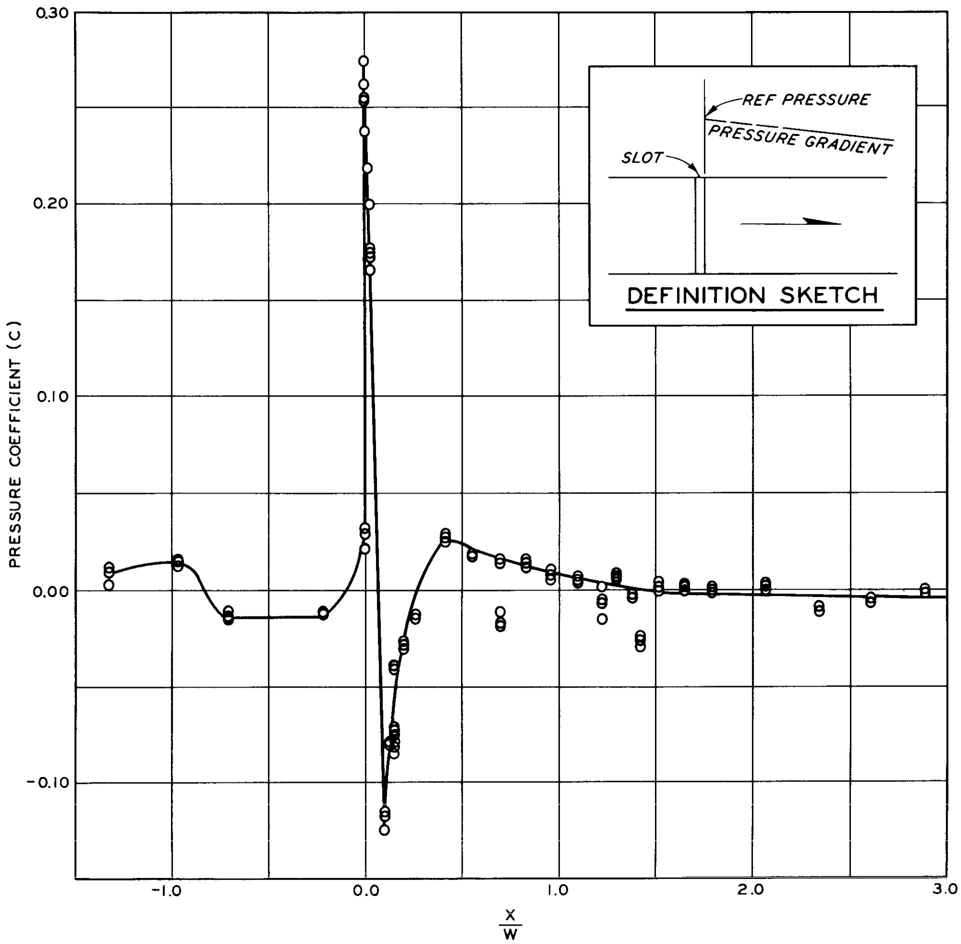

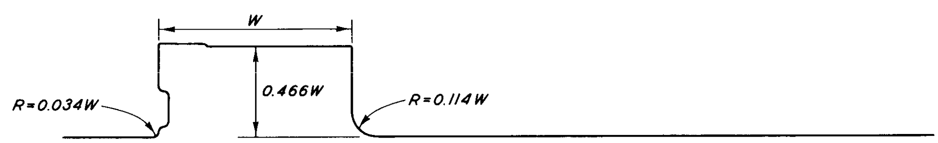

TYPE I GATE SLOT (REFERENCE I)

NOTE: X/W = RATIO OF DISTANCE FROM DOWNSTREAM EDGE OF SLOT TO WIDTH OF SLOT

EQUATION

$$H_d = CH_V$$

WHERE:

H_d = PRESSURE DIFFERENCE FROM REFERENCE PRESSURE, FT

C = PRESSURE COEFFICIENT

H_V = CONDUIT VELOCITY HEAD AT REFERENCE PRESSURE STATION, FT

GATE SLOTS WITHOUT DOWNSTREAM OFFSET

PRESSURE COEFFICIENTS

HYDRAULIC DESIGN CHART 212-1

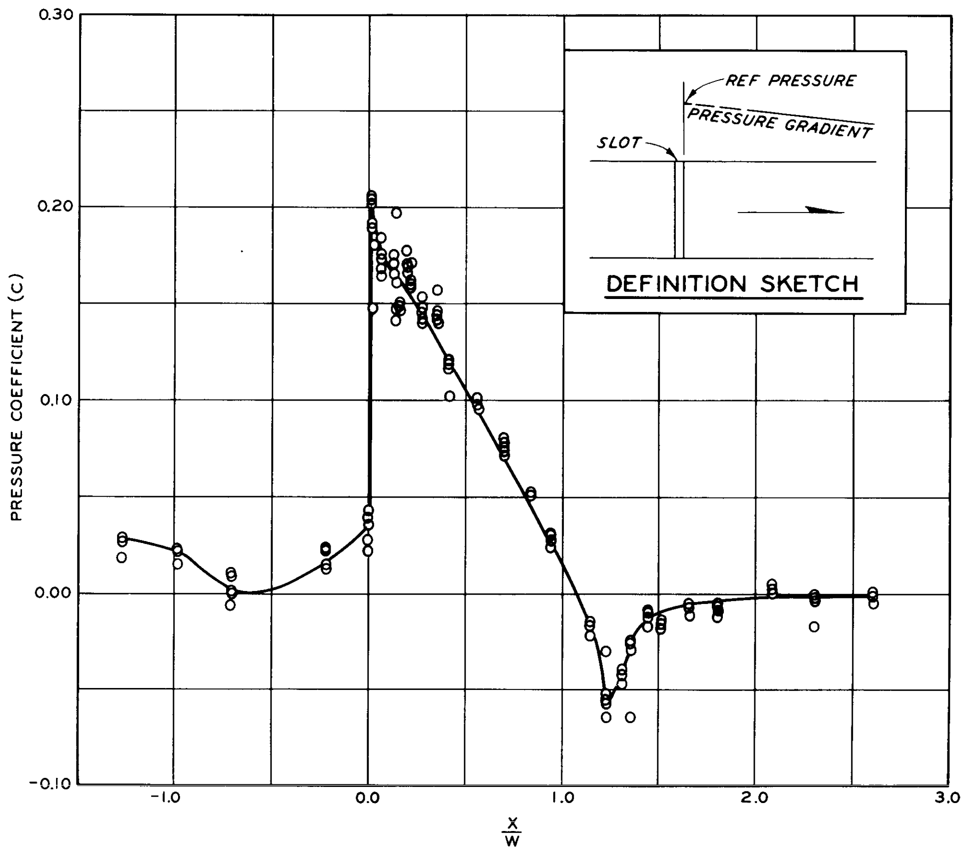

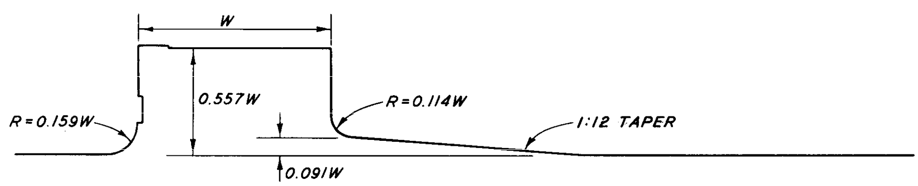

TYPE 2 GATE SLOT (REFERENCE 1)

EQUATION

$H_d = CH_V$

WHERE:

H_d = PRESSURE DIFFERENCE FROM REFERENCE PRESSURE, FT

C = PRESSURE COEFFICIENT

H_V = CONDUIT VELOCITY HEAD AT REFERENCE PRESSURE STATION, FT

NOTE: X/W = RATIO OF DISTANCE FROM DOWNSTREAM EDGE OF SLOT TO WIDTH OF SLOT

GATE SLOTS WITH DOWNSTREAM OFFSET

PRESSURE COEFFICIENTS

HYDRAULIC DESIGN CHART 212-1/1

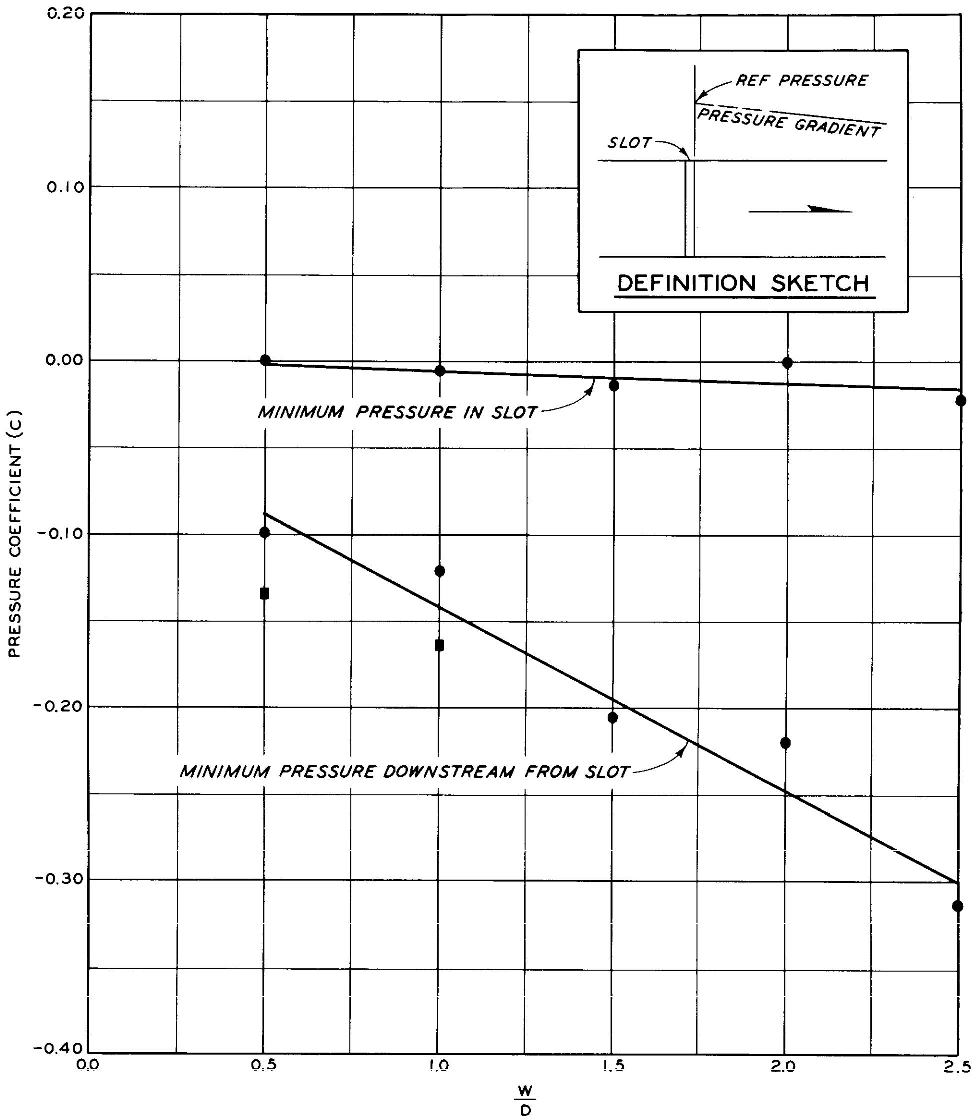

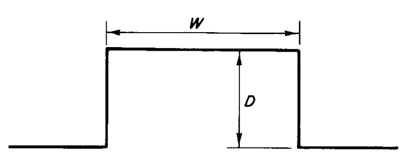

LEGEND

- ● USBR (REF 2)
- ■ SPENGO, SUI (REF 3)

EQUATION

$H_d = CH_v$

WHERE:

H_d = PRESSURE DIFFERENCE FROM REFERENCE PRESSURE, FT

C = PRESSURE COEFFICIENT

H_v = CONDUIT VELOCITY HEAD AT REFERENCE PRESSURE STATION, FT

GATE SLOTS WITHOUT DOWNSTREAM OFFSET

PRESSURE COEFFICIENTS EFFECT OF SLOT WIDTH-DEPTH RATIO

HYDRAULIC DESIGN CHART 212-1/2

HYDRAULIC DESIGN CRITERIA

SHEET 221-1

CONCRETE CONDUITS

INTAKE LOSSES

1. Chart 221-1. The chart presents intake losses determined from model and prototype investigations of single, double, and triple intakes. It is only applicable to conduits flowing full.

2. Theory. For design purposes intake losses include trashrack, entrance, gate-slot, transition, and friction losses throughout the intake section. The total intake loss expressed as a function of the velocity head in the conduit proper is

$$h_e = K_e \, (V^2/2g)$$

where

h_e = intake loss, ft

K_e = loss coefficient

V = average velocity in conduit proper, ft/sec

g = acceleration due to gravity, ft/sec^2

3. Accurate experimental determination of intake losses is dependent upon the conduit being of sufficient length to permit a uniform friction gradient to be established based on fully developed turbulence. The intake loss is the total available head minus the velocity head and the friction loss of the conduit.

4. Basic Data. Chart 221-1, which summarizes the best available data, was developed from results of model and prototype investigations of conduits of sufficient length for turbulence to become fully developed. The data selected from model and prototype investigations for use in determining intake losses for the three types of intakes are described below.

a. Single intake. The Pine Flat Dam[1] data used are prototype pressures observed in a rectangular concrete conduit. Other data[2] were obtained during a laboratory study of the effect of artificial stimulation of the turbulent boundary layer in a rectangular conduit conducted under Corps of Engineers Engineering Studies Item 802, Conduit Intake Model Tests. The laboratory intake section contained no gate slots. Data concerning the effects of gate slots on intake losses were obtained in special tests made during the Bull Shoals Dam[3] model study; the data indicate that these effects are negligible.

b. Double intake. Prototype pressure data were obtained at Denison[4] and Fort Randall Dams.[5] The Denison[6] and Fort Randall[7] models were built to a scale of 1 to 25. The friction losses in the Fort Randall model appeared normal. Those in the Denison model appeared excessively low. However, the relation between model and prototype intake losses is consistent.

c. Triple intake. The Tionesta model[8] data are the only known data resulting from a study of a triple intake to a conduit of sufficient length to permit turbulence to become fully developed.

5. References.

(1) U. S. Army Engineer Waterways Experiment Station, CE, Vibration, Pressure and Air-Demand Tests in Flood-Control Sluice, Pine Flat Dam, Kings River, California. Miscellaneous Paper No. 2-75, Vicksburg, Miss., February 1954.

(2) __________, The Effect of Artificial Stimulation of the Turbulent Boundary Layer in Rectangular Conduits. Miscellaneous Paper No. 2-160, Vicksburg, Miss., March 1956.

(3) __________, Model Studies of Conduits and Stilling Basin, Bull Shoals Dam, White River, Arkansas. Technical Memorandum No. 2-234, Vicksburg, Miss., June 1947.

(4) __________, Pressure and Air Demand Tests in Flood-Control Conduit, Denison Dam, Red River, Oklahoma and Texas. Miscellaneous Paper No. 2-31, Vicksburg, Miss., April 1953.

(5) __________, Flow Characteristics in Flood-Control Tunnel 10, Fort Randall Dam, Missouri River, South Dakota; Hydraulic Prototype Tests. Technical Report No. 2-626, Vicksburg, Miss., June 1963.

(6) __________, Hydraulic Model Studies of the Control Structures for the Denison Dam, Red River. Technical Memorandum No. 161-1, Vicksburg, Miss., April 1940.

(7) __________, Spillway and Outlet Works, Fort Randall Dam, Missouri River, South Dakota; Hydraulic Model Investigation. Technical Report No. 2-528, Vicksburg, Miss., October 1959.

(8) Carnegie Institute of Technology, Report on Hydraulic Model Tests of Spillway and Outlet Works for Tionesta Creek Reservoir Dam, Tionesta, Pennsylvania. Hydraulic Laboratory, Pittsburgh, Pa., September 1938.

SHAPE	PROJECT (1)	CONDUIT PROPER: LENGTH / DIAM (2)	CONDUIT PROPER: REYNOLDS NUMBER (2)	CONDUIT PROPER: VELOCITY HEAD (1)	AVERAGE INTAKE COEFFICIENT K_e
	SINGLE INTAKE (CONCRETE DAM CONDUITS)				
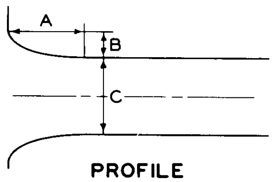 PROFILE	PINE FLAT (PROTOTYPE) A=9.0, B=3.0 C=9.0, E=5.0 F=5.0, G=1.7	54	$2.9-3.6 \times 10^7$ (PROTOTYPE)	65-81	0.16
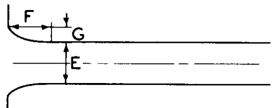 PLAN	ES 802 (1:20 MODEL) A=7.5, B=2.5 C=10.0, E=5.7 F=4.3, G=1.4	83	6.7×10^5 (MODEL)	97	0.07 (3)
	DOUBLE INTAKE (EARTH DAM TUNNEL)				
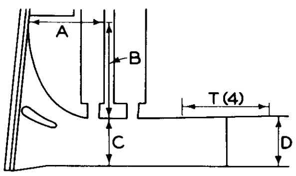 PROFILE	DENISON (PROTOTYPE) A=25.0, B=39.0 C=19.0, D=20.0 E=9.0, T=53.0	40	1.2×10^8 (PROTOTYPE)	66	0.19
	DENISON (1:25 MODEL) (SEE ABOVE)	47	$8.2-9.6 \times 10^5$ (MODEL)	61-82	0.12
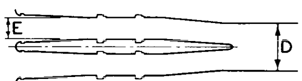 PLAN	FT RANDALL (5) (PROTOTYPE) A=24.0, B=16.0 C=23.0, D=22.0 E=11.0, T=49.0	39	$0.7-1.5 \times 10^8$ (PROTOTYPE)	16-72	0.25
	FT RANDALL (1:25 MODEL) (SEE ABOVE)	39	$0.9-1.0 \times 10^6$ (MODEL)	46-86	0.16
	TRIPLE INTAKE (EARTH DAM TUNNEL)				
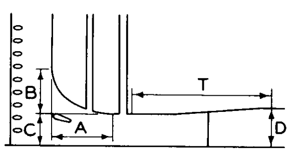 PROFILE 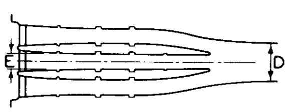 PLAN	TIONESTA (1:36 MODEL) A=30.0, B=22.0 C=16.0, D=19.0 E=7.5, T=66.0	98	$1.5-4.1 \times 10^5$ (MODEL)	7-50	0.33

INTAKE HEAD LOSS

$$h_e = K_e \frac{V^2}{2g}$$

V = VELOCITY IN CONDUIT PROPER

(1) DIMENSIONS IN PROTOTYPE FEET.
(2) EQUIVALENT DIAMETER FOR NONCIRCULAR SECTIONS BASED ON HYDRAULIC RADIUS.
(3) DOES NOT INCLUDE GATE-SLOT LOSSES.
(4) LENGTH OF TRANSITION
(5) ROOF CURVE MAJOR AXIS HORIZONTAL

CONCRETE CONDUITS
INTAKE LOSSES
HYDRAULIC DESIGN CHART 221-1

HYDRAULIC DESIGN CRITERIA

SHEET 224-1

RESISTANCE COEFFICIENTS

CONCRETE CONDUITS

1. General. The Kutter and Manning coefficients have been used extensively in the past by design engineers in the United States. Manning's n has found more favor in flood-control and irrigation design work because of its relative simplicity in the evaluation of resistance (friction) losses. A Manning's n value of 0.013 has been commonly used by engineers in the design of concrete conduits since publication of an article by Horton[1] in 1916 which was subsequently published in King's Handbook of Hydraulics. The Manning coefficient served a useful purpose for the design of conduits with Reynolds numbers that were small compared to those of large flood-control conduits. Tests at very high Reynolds numbers on the Oahe Dam flood-control conduit[2] where all joints and irregularities were ground smooth indicated a Manning's n of about 0.0098, illustrating that the older design values of the Manning's n can result in overdesign. However, because of possible deterioration of interior surfaces with time a Manning's n value of 0.014 is still used for capacity design by some engineers.

2. Effect of Reynolds Number. The variation of the resistance coefficient relative to the Reynolds number is expressed with the Darcy factor "f." This relation is normally plotted in the form of a general resistance diagram referred to as the Moody diagram.[3] Chart 224-1 is a Moody diagram on which have been plotted experimental data obtained on concrete conduits. The terms involved are defined on the chart. Nikuradse's study on pipes coated with uniform sand grains demonstrated that the resistance factor decreases with an increase in Reynolds number. Prandtl and Von Karman based the smooth pipe formula (Chart 224-1) upon theoretical considerations adjusted to the Nikuradse data. The heavy dashed line on the chart represents the limit of the transition from the smooth pipe formula to rough pipes with full turbulence. The resistance factor then becomes independent of Reynolds number and is only a function of the relative roughness. The lines in the transition region represent the Colebrook-White function[4] based on experiments with mixed roughness contrasted to uniform sand grains. The Colebrook-White function has been extrapolated considerably beyond the limits of the basic experimental data $R_e = 6 \times 10^5$. Observed values of f for the prototype flood-control conduits at Oahe and Denison Dams are considerably less than those computed for comparable Reynolds numbers using the Colebrook-White equation and field roughness measurements of the interior surface of the conduits. However, the relation between physical measurements of surface roughness and the hydraulic effective roughness has yet to be firmly established.

3. The velocity-diameter product VD for water at 60 F is included as a scale across the top of the graph. The VD scale is convenient for most design problems in which the effect of water temperature on capacity is neglected. Chart 001-1 shows the relation between kinematic viscosity and water temperature for use when it is desired to compute the effect of temperature.

4. Effective Roughness. Available test data on concrete pipes and conduits have been analyzed to correlate the effective roughness k_s with construction practices in forming concrete conduits and in treatment of interior surfaces. The following tabulation gives information pertinent to the data plotted in Chart 224-1. The type of construction and the resulting effective roughness can be used as guides in specific design problems. However, the k_s values listed are not necessarily applicable to other conduits of greatly different diameters.

Symbol	Project	Ref No.	Shape*	Size ft	k_s ft	Construction
			Precast Pipe			
●	Asbestos cement	5	C	1.2	0.00016	Steel mandril
□	Asbestos cement	5	C	1.7	0.00008	Steel mandril
▽	Neyrpic	6	C	2.82	0.00030	19.7-ft steel form
⊖	Denver #10	7	C	4.5	0.00018	12-ft steel form
⊐	Umatilla River	8	C	3.83	0.00031	8-ft steel form
⊤	Prosser	8	C	2.54	0.00152	Oiled steel form
⊏	Umatilla Dam	8	C	2.5	0.00024	4-ft sheet steel on wood forms
⊥	Deer Flat	8	C	3.0	0.00043	6-ft steel form
×	Victoria	8	C	3.5	0.00056	4-ft oiled steel forms
▲	Denver #3	9	C	2.5	0.00011	12-ft steel form
◣	Denver #13	9	C	5.0	0.00016	12-ft steel form
◸	Spavinaw	2	C	5.0	0.00013	12-ft steel form
			Steel Form Conduits			
○	Denison	10	C	20	0.00012	
△	Ontario	8	O	18	0.00001	Hand rubbed
▼	Chelan	11	C	14	0.00061	
■	Adam Beck	12	C	45	0.00018	Invert screeded and troweled
⊟	Fort Peck	13	C	24.7	0.00014	

(Continued)

* C = circular, O = oblate, R = round, and H = horseshoe.

Symbol	Project	Ref No.	Shape	Size ft	k_s ft	Construction
				Wood Form Conduits		
◒	Oahe	14	C	18.3	0.00004	Joints ground
+	Enid	15	C	11	0.00160	
◑	Pine Flat 52	16	R	5 × 9	0.00103	Longitudinal planking
◐	Pine Flat 56	16	R	5 × 9	0.00397	Longitudinal planking
				Miscellaneous		
⊙	Quabbin	17	H	11 × 13	0.00015	Unknown

5. Design Criteria.

a. Capacity. Conservative values should be used in designing for conduit capacity. The k_s values listed below are based on the data presented in paragraph 4 and are recommended for capacity design computations.

Type	Size ft	k_s ft
Asbestos cement pipe	Under 2.0	0.0003
Concrete pipe, precast	Under 5.0	0.0010
Concrete conduits (circular)		0.0020
Concrete conduits (rectangular)		0.0030

b. Velocity. The smooth pipe curve in Chart 224-1 should be used for computing conduit flow velocity pertinent to the design of energy dissipators. It should also be used for all estimates for critically low pressures in transitions and bends, as well as for the effects of boundary offsets projecting into or away from the flow.

c. Model Studies. Experimental results indicate that the resistance coefficients of models made of plastic closely approximate the smooth pipe curve at model flow Reynolds numbers in Chart 224-1. The curve should be used in computing boundary resistance losses for models of concrete and steel conduits in order to make any required model length adjustment.

d. Conduit Shape Effects. A WES study[19] shows that the shape effects on resistance in noncircular conduits can be neglected for all practical purposes in the design of conduit shapes normally encountered in Corps of Engineers Civil Works projects. It is suggested that the concept of equivalent hydraulic diameter be used in the design of noncircular conduits unless the aspect ratio (width/height) is less than 0.5 or greater than 2. Where unusual shapes are involved, model testing to evaluate shape effects may be required.

e. Equivalent Diameter. The equivalent diameter concept assumes that the resistance loss and flow velocity in a noncircular conduit are equal to those in a circular conduit having a hydraulic radius, boundary roughness condition, and energy head equal to those of the noncircular conduit. The equivalent diameter is equal to four times the hydraulic radius of the noncircular conduit. The cross-section area of the noncircular conduit is used with the above-defined velocity to compute the flow discharge.

6. Acknowledgment is made to the following for permission to use the data shown in Chart 224-1.

a. Engineering News-Record, Spavinaw Aqueduct and Denver Conduit No. 10 data, References 2 and 7.

b. Journal, American Water Works Association, Denver Conduits Nos. 3 and 13 data, Reference 9.

c. American Society of Civil Engineers, Quabbin and Chelan data, References 11 and 17.

d. La Houille Blanche, Neyrpic tests, precast concrete data, Reference 6.

e. The Engineering Journal, Sir Adam Beck tunnel data, Reference 12.

f. The University of New South Wales, Asbestos cement data, Reference 5.

7. References.

(1) Horton, R. E., "Some better Kutter's formula coefficients." Engineering News, vol 75, No. 8 (24 February 1916), pp 373-374; discussion, vol 75, No. 18 (4 May 1916), pp 862-863.

(2) Scobey, F. C., "Flow of water in Tulsa 60-inch and 50-inch concrete pipe lines." Engineering News-Record, vol 94, No. 22 (May 28, 1925), pp 894-987.

(3) Moody, L. F., "Friction factors for pipe flows." Transactions, American Society of Mechanical Engineers, vol 66 (November 1944), pp 671-684.

(4) Colebrook, C. F., "Turbulent flow in pipes with particular reference to the transition region between smooth and rough pipe laws." Journal, Institute of Civil Engineering, London, vol 12, No. 4 (1939), pp 133-156.

(5) Foster, D. N., Field Study of Friction Loss in Asbestos Cement Pipe Lines. Water Research Laboratory Report No. 106, University of New South Wales, Australia, June 1968.

(6) Barbe, R., "La mesure dans un laboratorie des pertes de charge de conduites industrielles." La Houille Blanche (May-June 1947), pp 191-204.

(7) Scobey, F. C., "Flow of water in 54-inch concrete conduit, Denver, Colorado." Engineering News-Record, vol 96, No. 17 (April 29, 1926), pp 678-680.

(8) __________, The Flow of Water in Concrete Pipe. U. S. Department of Agriculture Bulletin No. 852, October 1920.

(9) Capen, C. H., "Trends in coefficients of large pressure pipes." Journal, American Water Works Association, vol 33, No. 1 (January 1941), pp 1-83.

(10) U. S. Army Engineer Waterways Experiment Station, CE, Pressure and Air Demand Tests in Flood-Control Conduit, Denison Dam, Red River, Oklahoma and Texas, by B. Guyton. Miscellaneous Paper No. 2-31, Vicksburg, Miss., April 1953.

(11) Fosdick, E. R., "Tunnel and penstock tests at Chelan Station, Washington." Transactions, American Society of Civil Engineers, vol 101, paper 1952 (1936), pp 1409-1439.

(12) Bryce, J. B. and Walker, R. A., "Head-loss coefficients for Niagara water supply tunnel." The Engineering Journal, Montreal, Canada (July 1955).

(13) U. S. Army Engineer Waterways Experiment Station, CE, Hydraulic Prototype Tests, Control Shaft 4, Fort Peck Dam, Missouri River, Montana, by B. Guyton. Technical Memorandum No. 2-402, Vicksburg, Miss., April 1955.

(14) __________, Prototype Performance and Model-Prototype Relationship, by F. B. Campbell and E. B. Pickett. Miscellaneous Paper No. 2-857, Vicksburg, Miss., November 1966.

(15) __________, Prototype Hydraulic Tests of Flood-Control Conduit, Enid Dam, Yocona River, Mississippi, by C. J. Huval. Technical Report No. 2-510, Vicksburg, Miss., June 1959.

(16) U. S. Army Engineer Waterways Experiment Station, CE, Vibration, Pressure and Air-Demand Tests in Flood-Control Sluice, Pine Flat Dam, Kings River, California, by B. Guyton. Miscellaneous Paper No. 2-75, Vicksburg, Miss., February 1954. Also unpublished data.

(17) Kennison, K. R., discussion of "Friction coefficients in a large tunnel," by G. H. Hickox, A. J. Peterka, and R. A. Elder. Transactions, American Society of Civil Engineers, vol 113 (1948), p 1053.

(18) U. S. Army, Office, Chief of Engineers, Engineering and Design; Hydraulic Design of Reservoir Outlet Structures. EM 1110-2-1602, Washington, D. C., 1 August 1963.

(19) U. S. Army Engineer Waterways Experiment Station, CE, Resistance Losses in Noncircular Flood Control Conduits and Sluices, by R. G. Cox. Miscellaneous Paper No. H-73-1, Vicksburg, Miss., February, 1973.

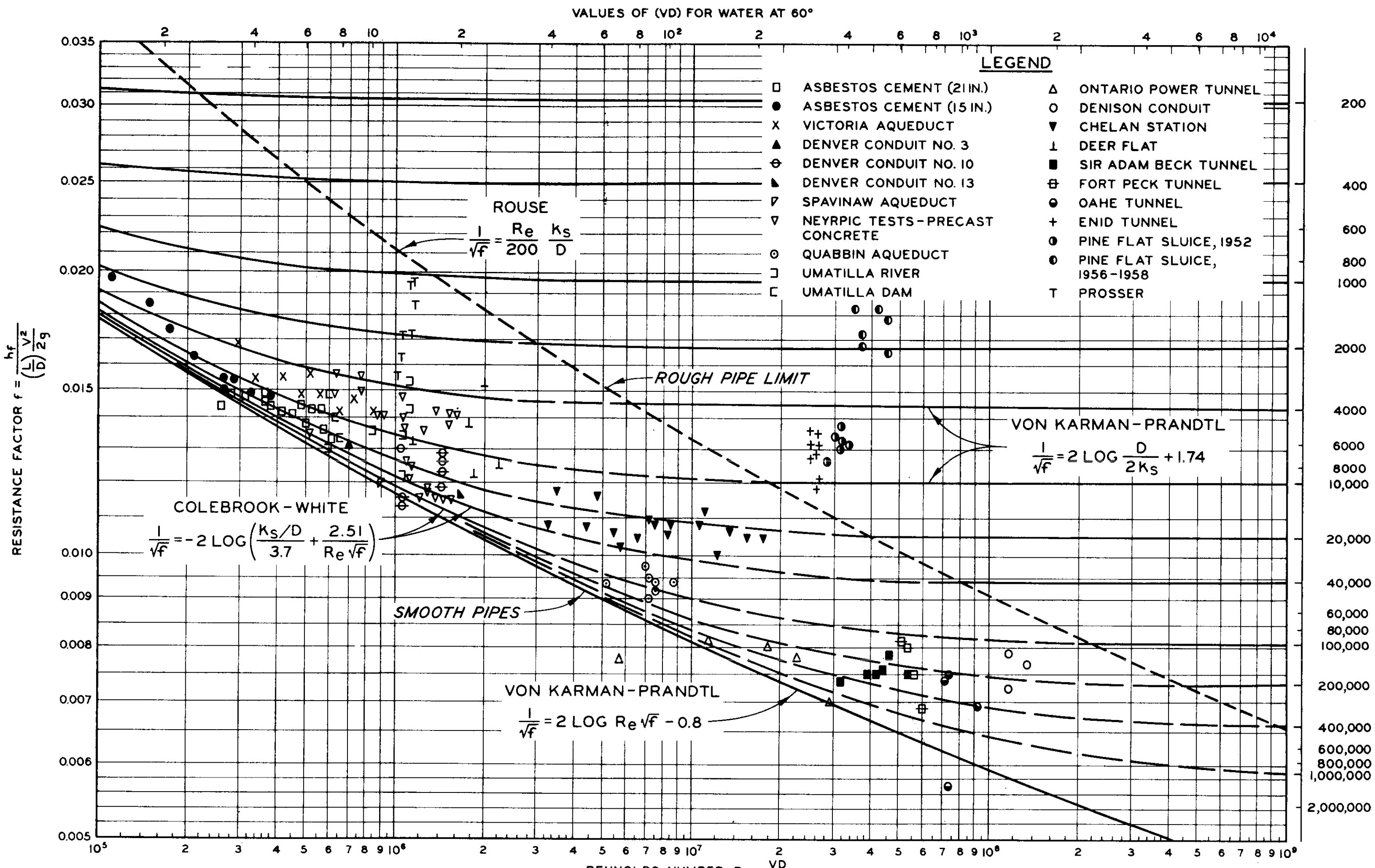

NOTE: h_f = RESISTANCE LOSS, FT
L = LENGTH OF CONDUIT, FT
D = DIAMETER, FT
k_s = EFFECTIVE ROUGHNESS, FT
V = VELOCITY, FPS
ν = KINEMATIC VISCOSITY, FT^2/SEC

RESISTANCE COEFFICIENTS
CONCRETE CONDUITS

HYDRAULIC DESIGN CHART 224-1

REV 6-57, 8-60, 1-64, 9-70 WES 1-53

PREPARED BY U. S. ARMY ENGINEER WATERWAYS EXPERIMENT STATION, VICKSBURG, MISSISSIPPI

SHEET 224-1/1

RESISTANCE COEFFICIENTS

STEEL CONDUITS

1. The magnitude of resistance (friction) loss in steel conduits is an important factor in the economics of design of pipelines, tunnels, and power penstocks. The concept of maximum and minimum design criteria is of importance in the design of flood-control outlet works and of surge tanks for power plants. It is desirable to use conservative resistance values in the design of flood-control conduits and water supply lines for hydraulic capacity and in the design of surge tanks for load acceptance. Conversely, minimum resistance values should be used for the design of stilling basins and of surge tanks for load rejection. The general comments in paragraphs 2 and 3 of HDC Sheet 224-1 apply to steel conduits.

2. Resistance Factors. Chart 224-1/1 is a plot of experimental data from tests made on steel conduits. The data are shown in the form of a Moody diagram where the resistance factor f is plotted as a function of the Reynolds number. The plotted points were selected principally from data compiled by the USBR.[1] The San Gabriel[2] test data were obtained from measurements on enamel-lined steel conduits and afford information for the higher Reynolds numbers. The Neyrpic tests,[3] the Milan tests,[4] and the Hoover Dam model tests[5] were hydraulic laboratory investigations involving fairly large Reynolds numbers. Corps of Engineers field tests at Fort Randall Dam in 1956[6] and 1959[7] afforded valuable information of the effects of surface treatment of 22-ft-diameter steel tunnels. The 1956 Fort Randall[6] and the 1957 Garrison[8] tests on vinyl-painted steel resulted in an average f value of 0.0075 for $R_e = 1.45 \times 10^7$ and an f value of 0.0071 for R_e of 2.5×10^7, respectively. The 1959 tests of brushed, tar-coated surface treatment resulted in an average f value of 0.0085 for $R_e = 1.01 \times 10^8$. The pipe flow theory indicates that experimental data should not plot below the smooth pipe curve in Chart 224-1/1.

3. Effective Roughness. The following tabulation summarizes the data plotted in Chart 224-1/1 and can be used as a guide in selecting k_s values for specific design problems. However, the k_s values listed do not necessarily apply to conduits having greatly different diameters.

Symbol	Project	Ref No.	Diameter ft	k_s ft	Remarks
□	Neyrpic	3	2.60	0.000010	Spun bitumastic coating
■	Neyrpic	3	2.61	0.000135	Uncoated
●	Milan	4	0.33	0.000039	Zinc coated
●	Milan	4	0.49	0.000026	Zinc coated

(Continued)

Symbol	Project	Ref No.	Diameter ft	k_s ft	Remarks
●	Milan	4	0.82	0.000071	Zinc coated
x	San Gabriel	2	10.25	0.000004	Enameled
Δ	San Gabriel	2	4.25	0.000152	Enameled
+	Hoover	5	0.83	0.000133	Galvanized pipe
▼	Fort Randall	9	22.00	0.000936	Tar coated
O	Fort Randall	7	22.00	0.000382	Tar coated
▲	Fort Randall	6	22.00	0.000008	Vinyl painted
∇	Garrison	8	24.00	0.000005	Vinyl painted

4. Design Criteria. The k_s values listed in the tabulation below are recommended for use in sizing cast iron and steel pipes and conduits to assure discharge capacity. The values for large steel conduits with treated interiors should also be useful in the design of surge tanks under load acceptance. The recommended values result from analysis of 500 k_s computations based on the data presented in Chart 224-1/1 and in table H of reference 1. The data are limited to continuous interior iron and steel pipe. The recommended values are approximately twice the average experimental values for the conditions indicated. The large increase in k_s values for large size tar- and asphalt-treated conduits results from heavy, brushed-on coatings.

Diameter ft	Treatment	k_s ft
Under 1.0	Tar dipped	0.0001
1 to 5	Tar coated	0.0003
Over 5	Tar brushed	0.0020
Under 6	Asphalt	0.0010
Over 6	Asphalt brushed	0.0100
All	Vinyl or enamel paint	0.0001
All	Galvanized, zinc coated or uncoated	0.0006

5. Velocity. The smooth pipe curve in Chart 224-1/1 is recommended for all design problems concerned with momentum and dynamic forces (water hammer, surge tanks for load rejection, critical low pressures at bends, branches, offsets, etc.).

6. Aging Effects. Interior treatment of pipes and conduits is of importance to their service life. Chemical, organic, and inorganic deposits in steel pipes and conduits can greatly affect the resistance losses and conduit capacity over a period of time. Data by Moore[10] indicate that over a 30-year period incrustation of iron bacteria up to 1 in. thick formed in uncoated 8-in. water pipe. Similar conditions prevailed in 10-in. pipe where the bond between the pipe and the interior coal tar enamel was poor. Computed k_s values for these pipes were 0.03 and 0.02 ft, respectively. Data compiled by Franke[11] indicate that organic and inorganic incrustations and deposits in steel conduits up to 6 ft in

diameter increased resistance losses by as much as 100 to 300 percent with k_s values increasing 100 percent. The data indicate that the interiors of some of the conduits were originally treated with a coat of bitumen. The changes occurred in periods of 5 to 17 years.

7. Conduit Shape Effects. (See paragraphs 5d and e, HDC Sheet 224-1.)

8. References.

(1) U. S. Bureau of Reclamation, Friction Factors for Large Conduits Flowing Full, by J. N. Bradley and L. R. Thompson. Engineering Monograph No. 7, Denver, Colo., March 1951 (revised 1965).

(2) Burke, M. F., High Velocity Tests in a Penstock. American Society of Civil Engineers Separate No. 297, October 1953.

(3) Barbe, R., "La mesure dans un laboratoire des pertes de charge de conduites industrielles." La Houille Blanche (May-June 1947), pp 191-204.

(4) Marchetti, A., "Perdite di carico per regime uniforme nelle condotte Dalmine di cemento-amianto con anima di acciaio, rivestite internamente di bitume centrifugato." Memorie e Studi del'Istituto di Idraulica e Costruzioni Idrauliche del Politecnico di Milano, No. 56, Milano (1944).

(5) U. S. Bureau of Reclamation, Part VI - Hydraulic Investigations; Bulletin 2, Model Studies of Penstocks and Outlet Works. Boulder Canyon Project Final Reports, Denver, Colo., 1938.

(6) U. S. Army Engineer District, Omaha, CE, Friction Loss Tests in Penstock No. 8, Fort Randall Power Plant. General Design Memorandum No. G-9, September 1956.

(7) U. S. Army Engineer Waterways Experiment Station, CE, Flow Characteristics in Flood-Control Tunnel 10, Fort Randall Dam, Missouri River, South Dakota; Hydraulic Prototype Tests, by J. V. Dawsey, Jr., C. J. Huval, and W. C. Blanton. Technical Report No. 2-626, Vicksburg, Miss., June 1963.

(8) U. S. Army Engineer District, Garrison, CE, Friction Loss Tests in Penstock No. 1, 1957.

(9) U. S. Army Engineer District, Omaha, CE, Friction Loss Tests in Penstock No. 7, Fort Randall Power Plant. General Design Memorandum No. G-7, 1955.

(10) Moore, M. O., "Incrustation in water pipelines." ASCE, Pipeline Division, Journal, vol 94, PL 1, paper 6161 (October 1968), pp 37-47.

(11) Franke, P. G., "Some roughness values of water pipelines." L'Energia Elettrica, vol 46, No. 2 (February 1969), pp 78-80.

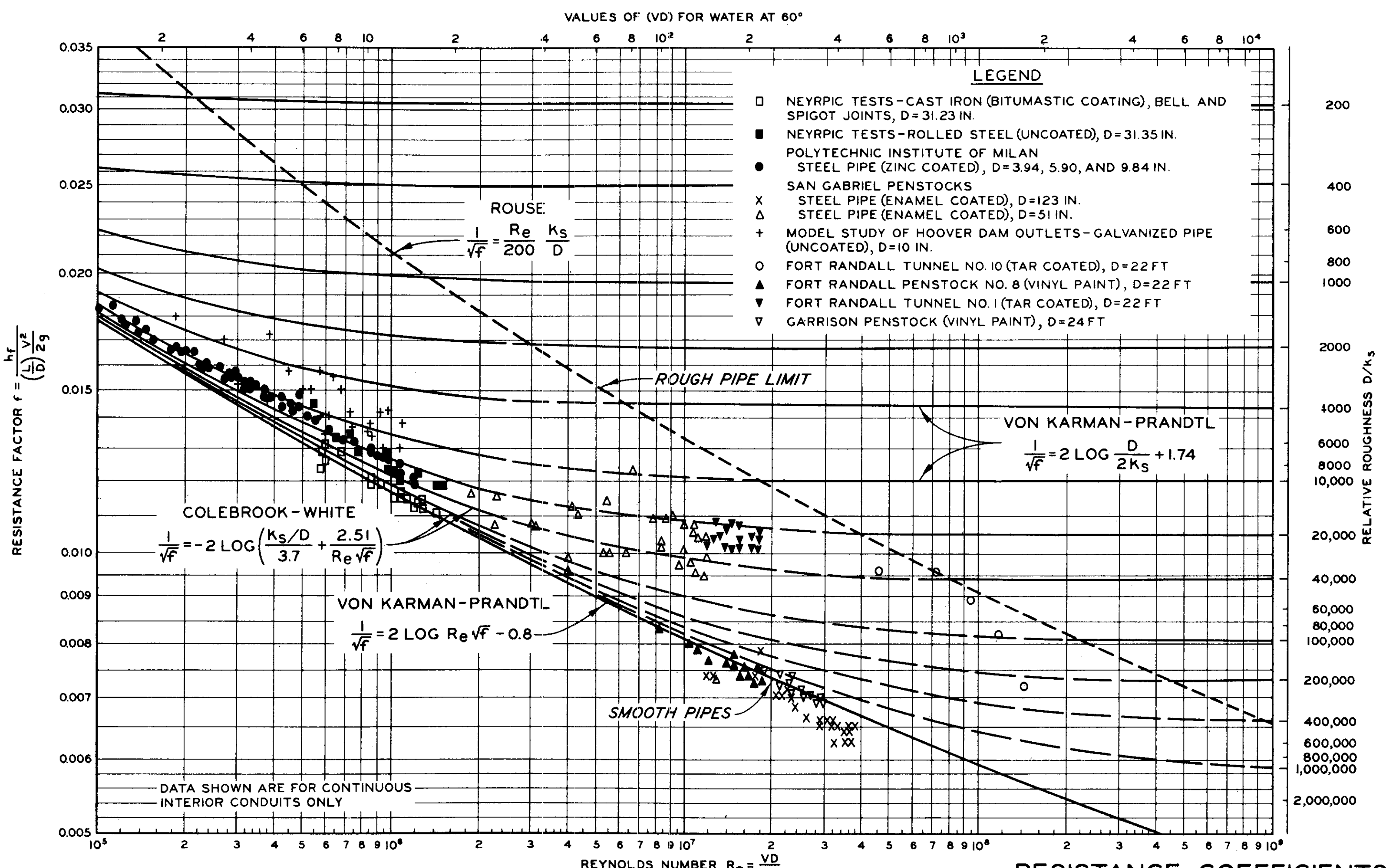

NOTE: h_f = RESISTANCE LOSS, FT
L = LENGTH OF CONDUIT, FT
D = DIAMETER, FT
k_s = EFFECTIVE ROUGHNESS, FT
V = VELOCITY, FPS
ν = KINEMATIC VISCOSITY, FT^2/SEC

RESISTANCE COEFFICIENTS
STEEL CONDUITS
SMOOTH INTERIOR

HYDRAULIC DESIGN CHART 224-1/1

REV 6-57, 1-64, 9-70 WES 3-55

PREPARED BY U. S. ARMY ENGINEER WATERWAYS EXPERIMENT STATION, VICKSBURG, MISSISSIPPI

HYDRAULIC DESIGN CRITERIA

SHEETS 224-1/2 TO 224-1/4

RESISTANCE COEFFICIENTS

CORRUGATED METAL PIPE

1. Known hydraulic head loss investigations for corrugated metal pipe in the United States date back to 1914.[1] Extensive U. S. Department of Agriculture tests at Iowa[2] were published in 1926. The results of more recent tests at St. Anthony Falls Hydraulic Laboratory,[3] Bonneville Hydraulic Laboratory,[4] the U. S. Army Engineer Waterways Experiment Station (WES),[5] and others[6,7,8] have been summarized in Charts 224-1/2 to 224-1/4. These data are for full-pipe flow and large length-diameter ratios. Resistance data obtained in the Bonneville tests with paved inverts are also shown.

2. Types of Corrugated Metal Pipe. Metal pipe with annular corrugations 0.5 in. deep spaced at intervals of 2.67 in. has been accepted as standard in the United States for many years (Chart 224-1/2). A new type of corrugated metal pipe having annular corrugations 1 in. deep spaced 3 in. apart is commercially available. Large diameter, field-assembled structural plate pipe having annular corrugations 2 in. deep spaced 6 in. apart has come into general use. Also, helical corrugated metal pipe in sizes of 6 to 96 in. is presently being manufactured.[9] The pitch and depth of the corrugations vary from 1.5 in. and 0.25 in., respectively, for the small size pipe to 3.0 in. and 1.0 in., respectively, for the large size pipe. Available limited test data indicate that the helical corrugated pipe is structurally superior to equivalent standard corrugated pipe.[10]

3. The available experimental data for standard corrugated metal pipe are generally for full-scale tests using commercially fabricated pipe. Available experimental data for structural plate and the new type of corrugated pipe are basically limited to large-scale model tests. The 1:4- or quarter-scale model tests of standard 5-ft-diameter corrugated pipe at WES indicate somewhat higher resistance coefficients than the Bonneville 5-ft-diameter prototype tests (Chart 224-1/2). This is attributed to a minor difference in the relative corrugation size in the model and the prototype. The full-scale Alberta structural plate pipe test data, $K/D = 0.0339$ (Chart 224-1/3) indicate about 10 percent higher f coefficients than comparable WES model test results adjusted 8 percent for field bolt effects.[5]

4. Charts 224-1/2 and 224-1/3 show values of the Darcy-Weisbach resistance coefficient (f) versus Reynolds number (R_e) computed from the observed test data. The equations used for the plots are

$$f = \frac{h_f}{\left(\frac{L}{D}\right)\frac{V^2}{2g}}$$

and

$$R_e = \frac{VD}{\nu}$$

The symbols are defined in Chart 224-1/2.

5. Values of the Manning's n versus pipe diameter resulting from the test data and recommended for design are shown in Chart 224-1/4. The basic Manning equation is

$$n = \frac{1.486 S^{1/2} R^{2/3}}{V}$$

The terms are defined in the chart. The relation between f and n is given in Sheets 224-3 to 224-7. Recommended design curves of Manning's n for various pipe diameters are given in Chart 224-1/4. Also shown are limited experimental data[3] for standard corrugated pipe arches. The n values plotted in this chart are computed from the average maximum values of f observed on corrugated pipe. The 3-ft-diameter f vs R_e curve shape in Chart 224-1/2 was used to extrapolate to maximum f values for the smaller pipe sizes. A similar procedure was used to extrapolate to the maximum values for the data curves in Chart 224-1/3. The curves for structural plate pipe shown in the charts are principally based on results of WES tests on model pipe having a corrugation depth-to-pitch ratio of 1 to 3. The Bossy[5] procedure was used to adjust the WES model data for the additional resistance attributable to bolts required in field assembly of prototype pipe.

6. Helical Corrugations. Resistance coefficients have been reported by Chamberlain,[7] Garde,[8] and Rice[11] on small size helical and standard corrugated pipe of comparable size. The following tabulation summarizes their findings.

Pipe Size, in.	Type	K/D	f	n	Ref No.
8	Helical	0.03	0.037	0.013	11
12	Helical	0.04	0.042	0.015	11
12	Helical	0.04	0.048	0.016	8
12	Standard	0.08	0.126	0.026	8
12	Standard	0.08	0.117	0.026	7
12	Helical	0.04	0.040	0.015	7

All tests were made with Reynolds numbers from 10^5 to 10^6. The resistance coefficient was found to be essentially constant for each pipe tested.

7. The tabulation above indicates that the resistance coefficient for small-diameter helical corrugated pipe is about 33 percent of that for comparable standard corrugated pipe and about 58 percent in terms of Manning's n. These percentages will be different for other size pipe depending upon the corrugation pitch, depth, and inclination with the pipe axis. Presently available data are limited to small size pipe having corrugations inclined about 65 deg to the pipe axis. For large diameter helical corrugated pipe the n values given in Chart 224-1/4 for standard unpaved corrugated pipe are recommended for design.

8. Application. The Manning's n curves presented in Chart 224-1/4 are recommended for preliminary design purposes. The data presented in Charts 224-1/2 and 224-1/3 permit more accurate evaluation of resistance losses when the design Reynolds number is significantly different from that resulting in the peak values of the resistance coefficients. Resistance coefficients based on the model data curves in Chart 224-1/3 should be increased by 8 percent when used for field-assembled pipe. Caution should be used in extrapolating the data to other types of corrugations.

9. References.

(1) Cone, V. M., Trimble, R. E., and Jones, P. S., Frictional Resistance in Artificial Waterways. Bulletin No. 194, Colorado Agricultural Experiment Station, Fort Collins, 1914.

(2) Yarnell, D. L., Nagler, F. A., and Woodward, S. M., Flow of Water Through Culverts. Bulletin 1, Studies in Engineering, University of Iowa, Iowa City, 1926.

(3) Straub, L. G., and Morris, H. M., Hydraulic Tests on Corrugated Metal Culvert Pipes. Technical Paper No. 5, Series B, St. Anthony Falls Hydraulic Laboratory, University of Minnesota, Minneapolis, 1950.

(4) Bonneville Hydraulic Laboratory, Portland District, CE, Friction Losses in Corrugated Metal Pipe; CWI 828. Report No. 40-1, Portland, Oreg., July 1955.

(5) U. S. Army Engineer Waterways Experiment Station, CE, Resistance Coefficients for Structural Plate Corrugated Pipe; Hydraulic Model Investigation, by J. L. Grace, Jr. Technical Report No. 2-715, Vicksburg, Miss., February 1966.

(6) Neill, C. R., "Hydraulic roughness of corrugated pipes." ASCE, Hydraulics Division, Journal, vol 88, HY 3 (May 1962), pp 23-44; vol 88, HY 6 (November 1962), Discussions; vol 89, HY 1 (January 1962), Discussions; vol 89, HY 4 (January 1963), Closure.

(7) Chamberlain, A. R., Effects of Boundary Form on Fine Sand Transport in Twelve-Inch Pipes. Report CER No. 55, ARC 6, Department of Civil Engineering, Colorado State University, Fort Collins, 1955.

(8) Garde, R. J., Sediment Transport Through Pipes. Report CER No. 56, RJG 19, Department of Civil Engineering, Colorado State University, Fort Collins, 1956.

(9) American Iron and Steel Institute, Handbook of Steel Drainage and Highway Construction Products. New York, 1967.

(10) Armco Drainage and Metal Products, Inc., Handbook of Drainage and Construction Products. Middletown, Ohio, 1958.

(11) U. S. Department of Agriculture, Friction Factors for Helical Corrugated Pipe, by C. E. Rice. ARS 41-119, Agricultural Research Service, Washington, D. C., February 1966.

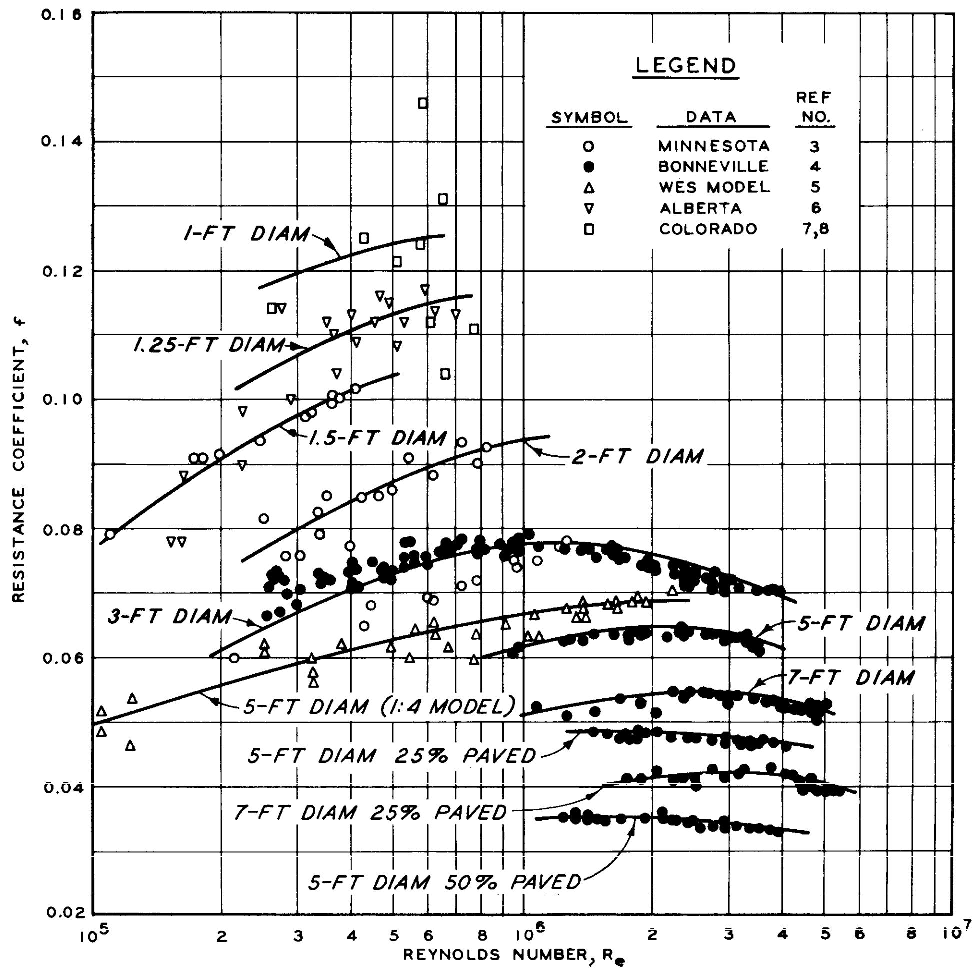

BASIC EQUATIONS

$$f = \frac{h_f}{\left(\frac{L}{D}\right)\frac{V^2}{2g}} \quad ; \quad R_e = \frac{VD}{\nu}$$

WHERE:

f = DARCY RESISTANCE COEFFICIENT
h_f = FRICTION LOSS, FT
L = PIPE LENGTH, FT
D = PIPE DIAMETER, FT
V = AVERAGE VELOCITY, FPS
g = ACCELERATION, GRAVITATIONAL, FT/SEC^2
ν = KINEMATIC VISCOSITY, FT^2/SEC

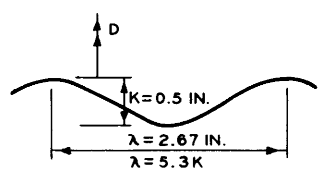

CORRUGATION DETAILS

RESISTANCE COEFFICIENTS

CORRUGATED METAL PIPE

$\lambda = 5.3\ K$

HYDRAULIC DESIGN CHART 224-1/2

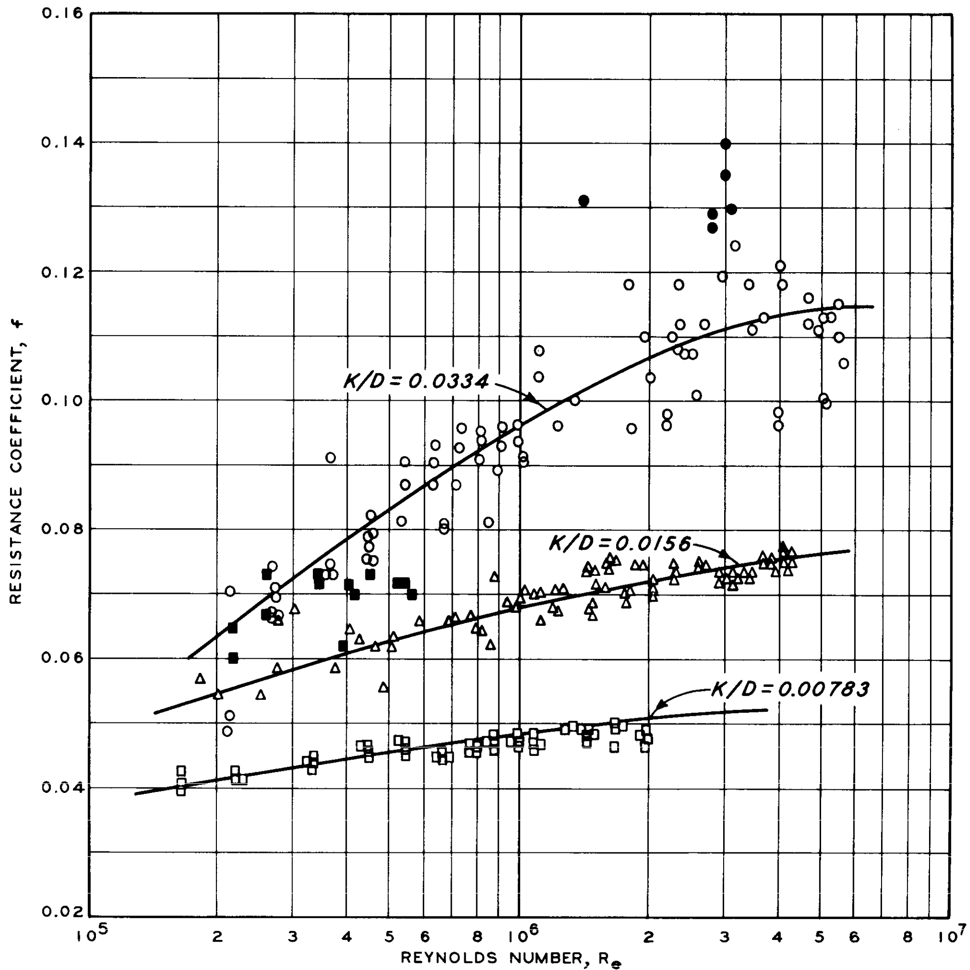

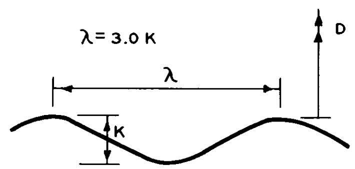

CORRUGATION DETAILS

	EQUIVALENT PIPE DIAMETER, FT	
K/D	1- X 3-IN. CORRUGATION	2- X 6-IN. CORRUGATION
0.00783	10	20
0.0156	5	10
0.0334	2.5	5

NOTE: CURVES ARE BASED ON MODEL DATA AND APPLY TO NEW TYPE SHOP-FABRICATED CORRUGATED METAL PIPE.

INCREASE MODEL f BY 8 PERCENT FOR FIELD-ASSEMBLED STRUCTURAL PLATE PIPE.

LEGEND

SYMBOL	DATA	REF NO.	MODEL SCALE	K/D
○	WES MODEL	5	1:2.2	0.0334
△	WES MODEL	5	1:8	0.0156
□	WES MODEL	5	1:16	0.00783
■	ALBERTA MODEL	6	1:16.6	0.0333
●	ALBERTA PROT.	6	1:1	0.0339

RESISTANCE COEFFICIENTS
CORRUGATED METAL PIPE
λ = 3.0 K

HYDRAULIC DESIGN CHART 224-1/3

REV. 1-68

WES 3-56

PREPARED BY U. S. ARMY ENGINEER WATERWAYS EXPERIMENT STATION, VICKSBURG, MISSISSIPPI

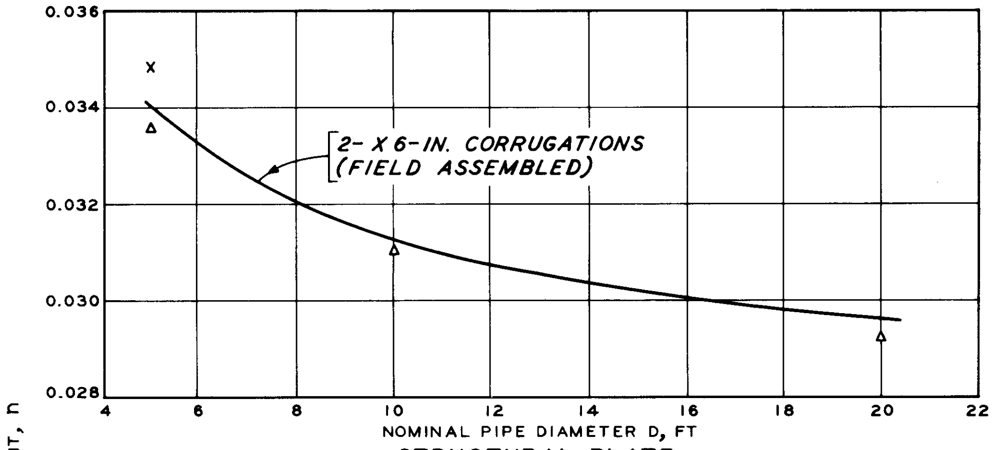

STRUCTURAL PLATE

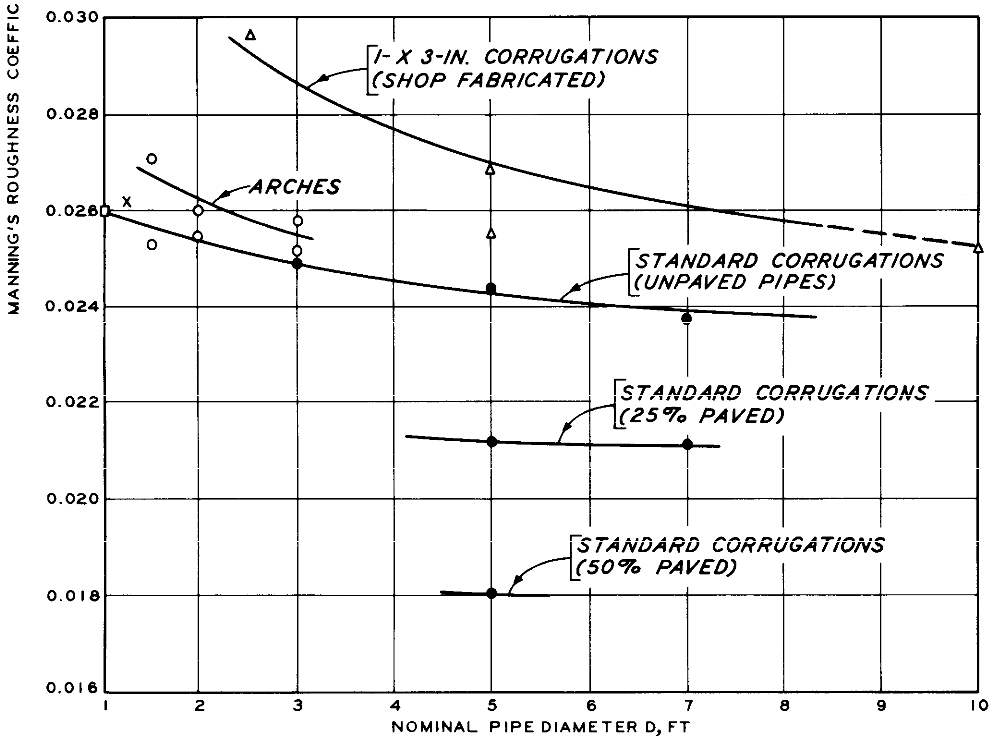

1- X 3-IN. AND STANDARD CORRUGATIONS

LEGEND		REF NO.
O	MINNESOTA	3
●	BONNEVILLE	4
Δ	WES MODELS	5
X	ALBERTA	6
□	COLORADO	7,8

BASIC EQUATION

$$n = \frac{1.486\ S^{1/2} R^{2/3}}{V}$$

WHERE:

n = MANNING'S ROUGHNESS COEFFICIENT
S = SLOPE OF ENERGY GRADIENT
R = HYDRAULIC RADIUS, FT
V = AVERAGE VELOCITY, FPS

RESISTANCE COEFFICIENTS
CORRUGATED METAL PIPES
MANNING'S n
FULL PIPE FLOW

HYDRAULIC DESIGN CHART 224-1/4

HYDRAULIC DESIGN CRITERIA

SHEETS 224-1/5 AND 224-1/6

RESISTANCE COEFFICIENTS

UNLINED ROCK TUNNELS

1. Purpose. Unlined rock tunnels have been built for flood flow diversion and for hydropower tunnels where the rock is of sound quality and not greatly jointed and fractured. Hydraulic Design Charts 224-1/5 and 224-1/6 summarize available flow resistance data for unlined rock tunnels and should be useful in estimating head losses resulting from boundary roughness.

2. General. The decision whether to line a water-carrying tunnel or to leave it unlined involves a number of factors that affect the economic aspects of a project. It will generally be found to be more economical to leave the tunnel unlined unless high flow velocities are involved, considerable rock remedial treatment is required, or lining in fractured rock zones is necessary. Operating experiences of over 60 years have shown that unlined power tunnels are economical both in initial construction and in maintenance.[1,2,3,4] However, the possibility of small rock falls resulting in turbine damage and penstock abrasion requires periodic tunnel inspection, especially during the first few years of operation.

3. Tunnel invert paving may be economically justified to (a) eliminate possible damage to downstream turbines or penstocks from migrating invert muck, thereby permitting greater flow velocities, and (b) facilitate tunnel inspection, maintenance, and rock trap clean out. In some cases it may be preferable to provide for tunnel invert cleanup using air and water jetting during construction. The proper balance between design velocity, provision of rock traps, and tunnel invert paving should be based on economic considerations.

4. Tunnel Stability and Shape. The determination of the structural stability of an unlined tunnel in rock and the need for partial or total tunnel lining depends on the findings of subsurface geologic exploration and a thorough study of the existing rock structure. The possible loss of flow through faults and fissures as well as heavy flows into the tunnel during construction should be investigated. Structural stability of the tunnel will usually require a rounded roof. A flat or nearly flat invert has been found to be advantageous for economical tunnel blasting and muck removal operations. The tunnel shape preferred by many contractors is the straight-legged horseshoe or some modified horseshoe shape.[5] The added hydraulic advantage of circular or nearly circular cross section has not generally justified the resulting increased tunneling complexity and cost. In the present study only one of 42 tunnels investigated was found to be circular in shape. Almost all the others were horseshoe or modified horseshoe shaped.

5. Overbreak. Overbreak as defined herein is the difference between the minimum allowable and the actual average tunnel dimensions. The sketch in Chart 224-1/6 graphically defines this terminology. The amount of overbreak determines to a great extent the tunnel roughness and thus resistance to the flow. There are many factors that influence the amount of overbreak, such as type and quality of rock, blasting technique, direction of driving relative to bedding planes, etc. The amount of overbreak varies from about 10 in. in the best granites to 18 in. in very blocky or laminated shales and sandstones.[5] More stringent control of overbreak usually results in higher costs.

6. Tunnel Hydraulics. Generally, velocities in unlined tunnels should not exceed 10 fps except during diversion flow when velocities to about 15 fps may be acceptable. For a tunnel with downstream turbines, penstocks, or valves, it has been recommended that velocities be limited to 5 fps or less[2] to prevent damage from migration of tunnel muck fines and rock falls. In addition, it is usually necessary to provide one or more rock or sand traps along the tunnel invert upstream of turbines to collect any migrating material. The development of satisfactory rock trap design and size is presented in references 6 and 7.

7. Theory. In unlined rock tunnels the resistance coefficient is independent of the Reynolds number because of the large relative roughness value usually obtained. Thus the Von Karman-Prandtl equation for fully rough flow based on the Nikuradse sand grain data should be applicable. This equation in terms of Darcy's f, pipe diameter D_m, and equivalent sand grain diameter k_s is

$$\frac{1}{\sqrt{f}} = 2 \log \left(\frac{D_m}{k_s}\right) + 1.14 \qquad (1)$$

A measure of overbreak k (see reference 8) in unlined tunnels can be expressed as

$$k = D_m - D_n = \sqrt{\frac{4}{\pi}}\left(\sqrt{A_m} - \sqrt{A_n}\right) \qquad (2)$$

where D_m and D_n are the equivalent diameters based on the areas A_m and A_n as shown in Chart 224-1/6. The relative roughness of the tunnel also can be expressed as

$$\frac{D_m}{k} = \frac{1}{1 - \sqrt{\frac{A_n}{A_m}}} \qquad (3)$$

The k dimension is approximately twice the mean overbreak thickness and, therefore, is a parameter similar to the Nikuradse sand grain diameter k_s.

8. Resistance Coefficients. Considerable information on resistance in unlined rock tunnels as well as field experience has been published since 1953 (references 1, 2, 4, 5, 6, 7, 9, and 10). Data published in references 1, 2, 6, and 9-15 have been analyzed in accordance with equation 3 above, summarized in Chart 224-1/5, and plotted in Chart 224-1/6. The relation between Darcy's f, Manning's n, and tunnel diameter given on page 1 of Sheets 224-3 to 224-7 was used to convert the published resistance coefficients as required for tabulating and plotting. The relation between f, D_m, and k_s expressed by equation 1 above is also shown in Chart 224-1/6. The experimental data correlate well with the theoretical curve and indicate that k (equation 2) is a reasonably good measure of the tunnel roughness. The user is cautioned that the data presented in Charts 224-1/5 and 224-1/6 are in terms of the mean driven ("as built" average) tunnel areas (A_m).

9. Application.

a. Preliminary design. The average of the Manning's n values tabulated in Chart 224-1/5 is 0.033 and is based on the mean driven area A_m. This value can be used in preliminary design and economic analyses for average rock and blasting conditions.

b. Final design. Once a preliminary mean driven area is established, the final design can proceed, using Chart 224-1/6. An estimate of tunnel overbreak or relative roughness (D_m/k) is required for estimating resistance losses. An estimate of the overbreak depth k can be obtained from previous tunnel experience in similar geologic areas or by studying the data tabulated in Chart 224-1/5. Detailed studies of the local geology as well as the blasting experience of potential contractors are useful in estimating the expected tunnel roughness. The area obtained in the preliminary design should be used in the first trial of the computation to determine the required diameter for the given discharge, energy gradient, and surface roughness. After tunnel driving begins, the overbreak can be measured and a value of D_m/k computed to check the final design assumptions. Low values of f should be used in computations made to determine power tunnel surge tank stability and surge tank levels during load rejection. High values of f should be used to compute surge tank levels during power tunnel load acceptance.

10. References.

(1) Rahm, L., Flow Problems with Respect to Intakes and Tunnels of Swedish Hydro-Electric Power Plants. Bulletin No. 36, Institution of Hydraulics, Royal Institute of Technology, Stockholm, Sweden, 1953.

(2) Spencer, R. W., Laverty, B. R., and Barber, D. A., "Unlined tunnels of the Southern California Edison Company." ASCE, Power Division, Journal, vol 90, PO 3, paper 4087 (October 1964), pp 105-132.

(3) Groner, C. F., Snettisham Project, Alaska, First Stage Development, Formal Report on Power Tunnel Design. Oslo, Norway, October 1967.

(4) Thomas, H. H., and Whitman, L. S., "Tunnels for hydroelectric power in Tasmania." ASCE, Power Division, Journal, vol 90, PO 3, paper 4065 (October 1964), pp 11-28.

(5) Petrofsky, A. M., "Contractor's view on unlined tunnels." ASCE, Power Division, Journal, vol 90, PO 3, paper 4086 (October 1964), pp 91-104.

(6) Dann, H. E., Hartwig, W. P., and Hunter, J. R., "Unlined tunnels of the Snowy Mountains Hydro-Electric Authority, Australia." ASCE, Power Division, Journal, vol 90, PO 3, paper 4071 (October 1964), pp 47-79.

(7) Mattimoe, J. J., Tinney, E. R., and Wolcott, W. W., "Rock trap experience in unlined tunnels." ASCE, Power Division, Journal, vol 90, PO 3, paper 4067 (October 1964), pp 29-45.

(8) U. S. Army Engineer Waterways Experiment Station, CE, Prototype Performance and Model-Prototype Relationship, by F. B. Campbell and E. B. Pickett. Miscellaneous Paper No. 2-857, Vicksburg, Miss., November 1966.

(9) Report of Task Force on Flow in Large Conduits of the Committee on Hydraulic Structures, "Factors influencing flow in large conduits." ASCE, Hydraulics Division, Journal, vol 91, HY 6 (November 1965), pp 123-152.

(10) Rahm, L., "Friction losses in Swedish rock tunnels." Water Power, vol 10, No. 12 (December 1958), pp 457-464.

(11) Discussion of reference 9: Wright, D. E.; Anderson, D., and Palmer, P. M.; Angelin, S., and Larsen, P.; ASCE, Hydraulics Division, Journal, vol 92, HY 4 (July 1966).

(12) Johansen, F., "Head loss investigations in unlined rock tunnels," in Model Tests Completed in 1965, Articles and Summary of Project Reports. Bulletin No. 8E, River and Harbour Research Laboratory, University of Norway, Trondheim, 1966.

(13) Laverty, B. R., and Ludwig, K. R., "Design and performance of Mammoth Pool power tunnel." ASCE, Power Division, Journal, vol 89, PO 1, paper 3642 (September 1963), pp 9-43.

(14) Discussion of reference 6: Rufenacht, A., ASCE, Power Division, Journal, vol 91, PO 1 (May 1965), pp 120-123.

(15) Hickox, G. H., Peterka, A. J., and Elder, R. A., "Friction coefficients in a large tunnel." Transactions, ASCE, vol 113 (1948), pp 1027-1076.

(16) Elder, R. A., "Friction measurements in the Apalachia Tunnel." Transactions, ASCE, vol 123 (1958), pp 1249-1274.

No.	Ref. No.	Project	Location	Type of Rock	Invert Lining	A_n, Nominal or Design Area, ft²	A_m, Mean Driven Area, ft²	D_m/k	n_m	f_m
1	1, 10	Alfta	Sweden	Granite-gneiss	Negligible	323	364	17.3	0.036	0.086
2	10	Blasjon	Sweden	Gneiss-mica-schist	Asphalt paved	581	615	35.9	0.028[a]	0.047
3	10	Donje	Sweden	Gneiss	Concrete arches	1345	1521	16.8	0.034[a]	0.070
4	1, 10	Jarpstrommen	Sweden	Upper silurian slate horizontally stratified	Negligible	1130	1230	24.1	0.029	0.048
5	10	Krokstrommen	Sweden	Granite, with large amount of feldspar	Negligible	969	1094	17.0	0.029	0.048
6	1, 10	Nissastrom	Sweden	Granite-gneiss	Concrete arches	323	394	10.6	0.037[a]	0.101
7	1, 10	Porjus I	Sweden	Granite-gneiss	Negligible	538	618	14.9	0.034	0.073
8	1, 10	Porjus II	Sweden	Granite-gneiss	Negligible	538	662	10.2	0.030	0.055
9	1, 10	Selsfors[b]	Sweden	Black slate with granite intrusions	NK[c]	753	866	14.8	0.044	0.114
10	1, 10	Sillre	Sweden	Vein gneiss	Negligible	54	71	7.7	0.034	0.102
11	1, 10	Sunnerstaholm	Sweden	Granite-gneiss	Minor	323	386	11.6	0.039	0.104
12[d]	10	Tasan	Sweden	Gneiss	Minor	183	185	170.6	0.033	0.081
13	1	Torpshammar	Sweden	Gneiss-granite and some diabase	NK	646	689	31.5	0.027	0.045
14	11	Stalon	Sweden	Sparagmite-quartzite	Negligible	645	705	23.0	0.030	0.055[a]
15	12	Tokke I	Norway	Variable-greenstone quartzite schist and metamorphic quartz sandstone	None	807	861	31.8	0.031	0.055[a]
16	12	Innset	Norway	NK	None	366	384	41.7	0.030	0.059[a]
17	12	Tunnsjo	Norway	Phyllite and mica schist	None	398	435	25.5	0.031	0.062[a]
18	12	Tunnsjodal	Norway	Greenstone, granite gabbro. Also phyllite and mica schist	None	484	508	41.7	0.030	0.055[a]
19	12	Tussa	Norway	NK	None	81	89	21.7	0.032	0.085[a]
20	12	Mykstufoss Head Race	Norway	Quartz, mica, and feldspar both granitic and gneissic	None	592	670	19.7	0.031	0.058[a]
21	12	Mykstufoss Tail Race	Norway	Gneiss, quartzite, and some micaceous amphibolite	None	592	639	26.9	0.035	0.074[a]
22[d]	12	Langvatn[g]	Norway	Silicates with lime-stone and dolomite sills	None	1507	1510	877	0.033	0.060[a]
23	6	Eucumbene-Tumut	Australia	36% granite, 64% metamorphized sedimentary	Concrete, paved flat	396	445	17.6	0.029	0.054
24	6	Tooma-Tumut	Australia	Granite	Concrete, paved flat	125	153	10.4	0.031	0.074
25	6	Murrumbidgee-Eucumbene[e]	Australia	10% granite, 90% metamorphized sedimentary	Smoothed muck	100	127	8.9	0.036	0.104
26	11	Eucumbene-Snowy[i]	Australia	94% granite, 6% metamorphized sedimentary	Concrete, paved flat	350	425	10.8	0.033	0.072
27	14	Kiewa No. 3	Australia	Granodiorite	Muck not sluiced	200	255	8.7	0.038	0.102[a]
28	14	Kiewa No. 4	Australia	Gneiss-intruded by granodiorite	Concrete	200	238	12.0	0.038	0.103[a]
29	14	Lower West Kiewa	Australia	Gneiss-intruded by granodiorite	Muck not sluiced, track left in	63	75	12.0	0.037	0.118[a]
30	14	Kiewa No. 1	Australia	Gneiss-intruded by granodiorite	Sluiced muck	150	200	7.5	0.041	0.122[a]
31	11	Telom	Malaysia	Closely-jointed granite	Compacted muck, track removed	87	105	11.0	0.030	0.081
32	9	Cresta	California	Granite	NK	578	656	16.3	0.035	0.075
33	9	West Point	California	Granite	NK	180	222	10.0	0.033	0.080
34	9	Bear River	California	Granite	NK	82	93	16.4	0.028	0.066
35	9	Balch	California	Granite	NK	144	169	13.0	0.032	0.079
36	9	Haas	California	Granite	NK	151	184	10.6	0.030	0.068
37	9	Cherry	California	Granite	NK	133	150	17.1	0.034	0.090
38	9	Jaybird	California	Granite	NK	177	195	21.0	0.032	0.077
39	2	Big Creek 3	California	Granite	Unlined	434	515	12.2	0.035	0.077[a]
40	2	Big Creek 4	California	Granite	Concrete paved	409	462	16.9	0.030	0.057[a]
41	2, 13	Mammoth Pool	California	Granite	Concrete paved	336	367	23.0	0.029	0.055[a]
42	15, 16	Apalachia	Tennessee	Quartzite and slate	Smoothed muck[h]	346[f]	403[f]	13.9	0.038	0.096

Notes:

a Computed from $f_m = \dfrac{185\, n_m^2}{D_m^{1/3}}$

b Cross-section shape not constant
c NK = not known
d Not plotted on HDC 224-1/6
e Tests may have been for free surface flow
f Average of 20- and 22-ft diameters
g Cross-section area and hydraulic measurements are believed to be in error
h Muck (except for large rocks) cleaned out by flow
i Discharge measurements may be in error. Data being reanalyzed by contributor.

RESISTANCE COEFFICIENTS

UNLINED ROCK TUNNELS
BASIC DATA

HYDRAULIC DESIGN CHART 224-1/5

WES 1-68

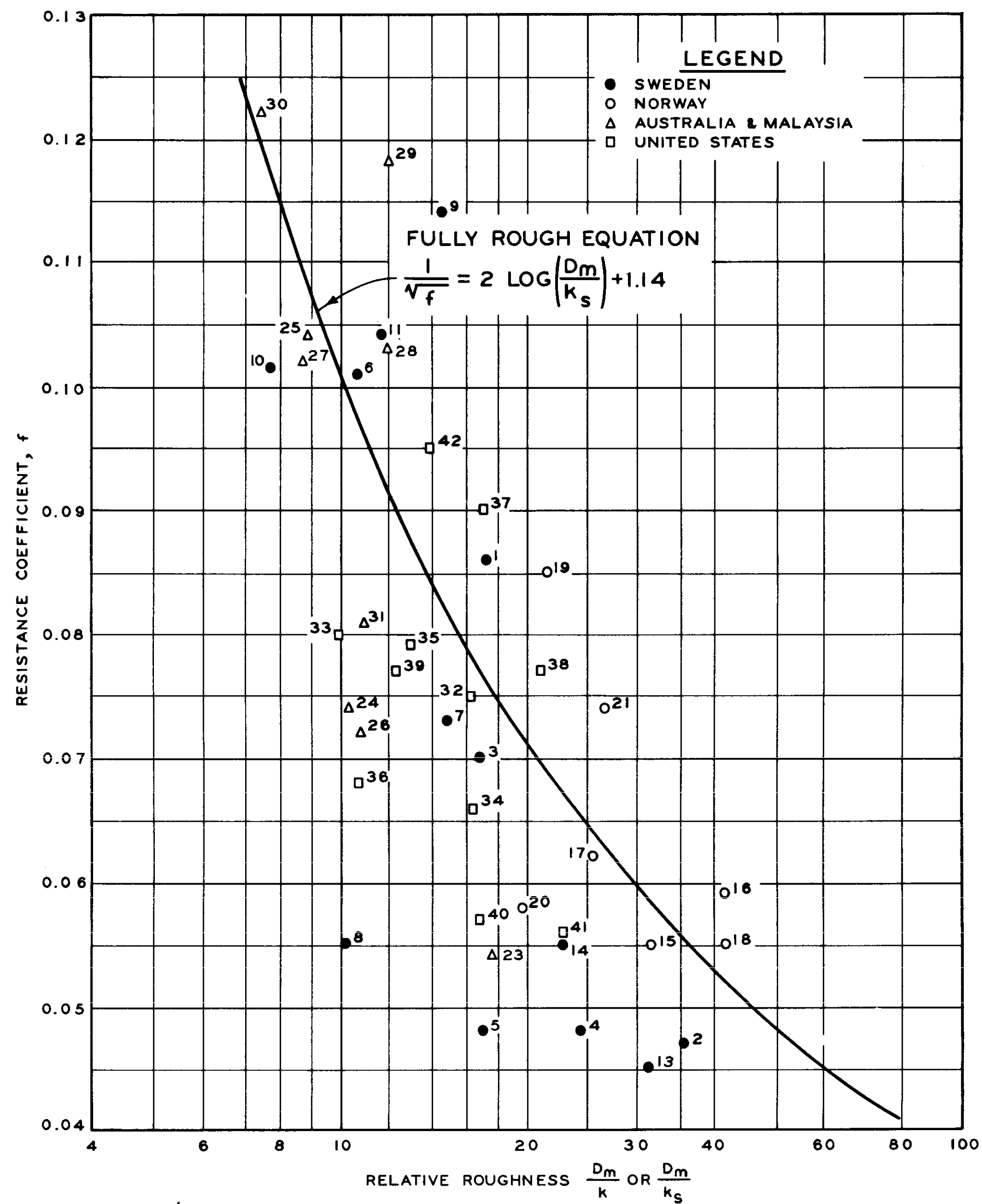

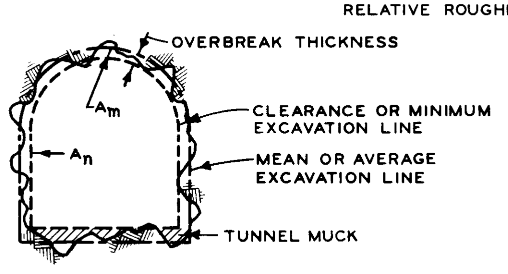

$D_m = \sqrt{4A_m/\pi}$

$D_n = \sqrt{4A_n/\pi}$

$k = D_m - D_n$

k_s = NIKURADSE'S SAND GRAIN ROUGHNESS

NOTE: SEE CHART 224-1/5 FOR IDENTIFICATION OF PROJECTS INDICATED BY NUMBERS

RESISTANCE COEFFICIENTS

UNLINED ROCK TUNNELS
f-RELATIVE ROUGHNESS

HYDRAULIC DESIGN CHART 224-1/6

HYDRAULIC DESIGN CRITERIA

SHEET 224-2

CONDUIT SECTIONS

HYDRAULIC ELEMENTS

PRESSURE FLOW

1. The Darcy resistance factor, being expressed in terms of conduit diameter, is theoretically applicable only to conduits of circular cross section. However, the concept of equivalent hydraulic diameter has been devised by Schiller and Nikuradse* to make the Darcy f applicable to noncircular sections. This concept assumes that the resistance losses in a noncircular conduit are the same as those in a circular conduit having an equivalent hydraulic radius and boundary roughness. A WES study** has shown that the equivalent hydraulic diameter concept is applicable to all conduit shapes normally encountered in hydraulic structure design.

2. The equivalent diameter is derived from

D =

$$D = 4R = \frac{4A}{WP}$$

where R is the hydraulic radius of the noncircular conduit, A is the cross-sectional area, WP is the wetted perimeter, and D is the diameter of a circular conduit having the same hydraulic radius. Hydraulic Design Chart 224-2 is presented as an aid in the computation of equivalent hydraulic diameter for various common conduit shapes.

---

* Schlichting, H., Boundary Layer Theory, English translation by J. Kestin, McGraw-Hill Book Co., Inc., New York, 1960.

** U. S. Army Engineer Waterways Experiment Station, CE, Resistance Losses in Noncircular Flood Control Conduits and Sluices, by R. G. Cox. Miscellaneous Paper H-73-1, Vicksburg, Miss. January 1973.

SECTION	AREA (A)	WETTED PERIMETER (WP)	HYDRAULIC RADIUS (R)
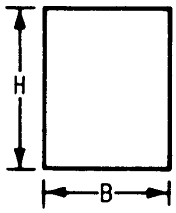	BH	$2(B+H)$	$\frac{BH}{2(B+H)}$
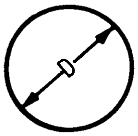	$\frac{\pi D^2}{4}$	πD	$\frac{D}{4}$
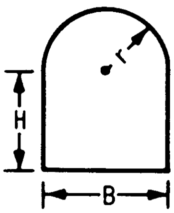	$BH + \frac{\pi r^2}{2}$	$B + 2H + \pi r$	$\frac{BH + \frac{\pi r^2}{2}}{B + 2H + \pi r}$
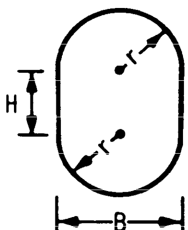	$BH + \pi r^2$	$2(H + \pi r)$	$\frac{BH + \pi r^2}{2(H + \pi r)}$
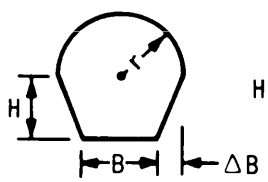	$H(B + \Delta B) + \frac{\pi r^2}{2}$	$B + 2(H^2 + (\Delta B)^2)^{1/2} + \pi r$	$\frac{H(B + \Delta B) + \frac{\pi r^2}{2}}{B + 2(H^2 + (\Delta B)^2)^{1/2} + \pi r}$
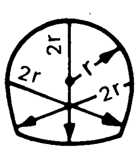	$3.3172\ r^2$	$6.5338\ r$	$0.5077\ r$

CONDUIT SECTIONS

HYDRAULIC ELEMENTS

PRESSURE FLOW

HYDRAULIC DESIGN CHART 224-2

REV 11--87 WES 5-75

PREPARED BY U.S. ARMY ENGINEER WATERWAYS EXPERIMENT STATION, VICKSBURG, MISSISSIPPI

HYDRAULIC DESIGN CRITERIA

SHEETS 224-3 TO 224-7

STRAIGHT CIRCULAR CONDUIT DISCHARGE

1. The basic equation for discharge in an outlet works tunnel or conduit is:

$$Q = A_c \sqrt{\frac{1}{K + K_f + 1.0}} \sqrt{2\ gH}$$

Where K is an intake coefficient which includes entrance losses, gate slot losses, and transition losses. The value K_f can be expressed in terms of the Darcy-Weisbach friction factor as follows:

$$K_f = \frac{fL}{D}$$

No simple equation is available for direct solution of the diameter required to pass a given discharge in view of the fact that the area of the conduit (A_c) and the friction coefficient (K_f) are both dependent upon the diameter (D). The design then requires successive approximations by computing the discharge for assumed values of diameter.

2. Hydraulic Design Chart 224-3 is a design aid for reducing the computation effort in determining the diameter required for passing a given discharge through a straight conduit. The Darcy-Weisbach friction factor "f" is used as the ordinate rather than Manning's "n" for simplicity in application. The f factor varies as the first power of the diameter whereas in Manning's formula, n varies as the two-thirds power of the diameter. The chart is prepared for an assumed K value of 0.10.

3. Many design engineers still prefer to use Manning's n instead of the Darcy-Weisbach friction factor f . Therefore, Hydraulic Design Chart 224-4 is included as an alternate design aid for reducing the computation effort in determining the diameter required for passing a given discharge. This chart presents a family of curves of various $L/D^{4/3}$ ratios plotted to show the relationship between Manning's n and the discharge coefficient K' .

4. Hydraulic Design Chart 224-5 is in the form of the Moody diagram with families of lines drawn to show the comparison of the Darcy-Weisbach f with the Manning's n for various values of the velocity-diameter ratio. The equation which relates f to n is expressed:

$$f = \frac{185n^2}{D^{1/3}}$$

This equation can be evaluated in terms of the VD product if the velocity is defined as so many diameters per second. The velocity-diameter product as used corresponds to a Reynolds number with water at 60° F.

5. A sample computation employing Charts 224-3 and 224-5 is given on Chart 224-6. An assumed diameter together with the required discharge fixes the velocity-diameter ratio and the velocity-diameter product. An alternate sample computation employing Chart 224-4 is given on Chart 224-7. The design aids presented facilitate an estimate of the required diameter, although it may be desirable to make the final determination of the discharge-head relationship analytically.

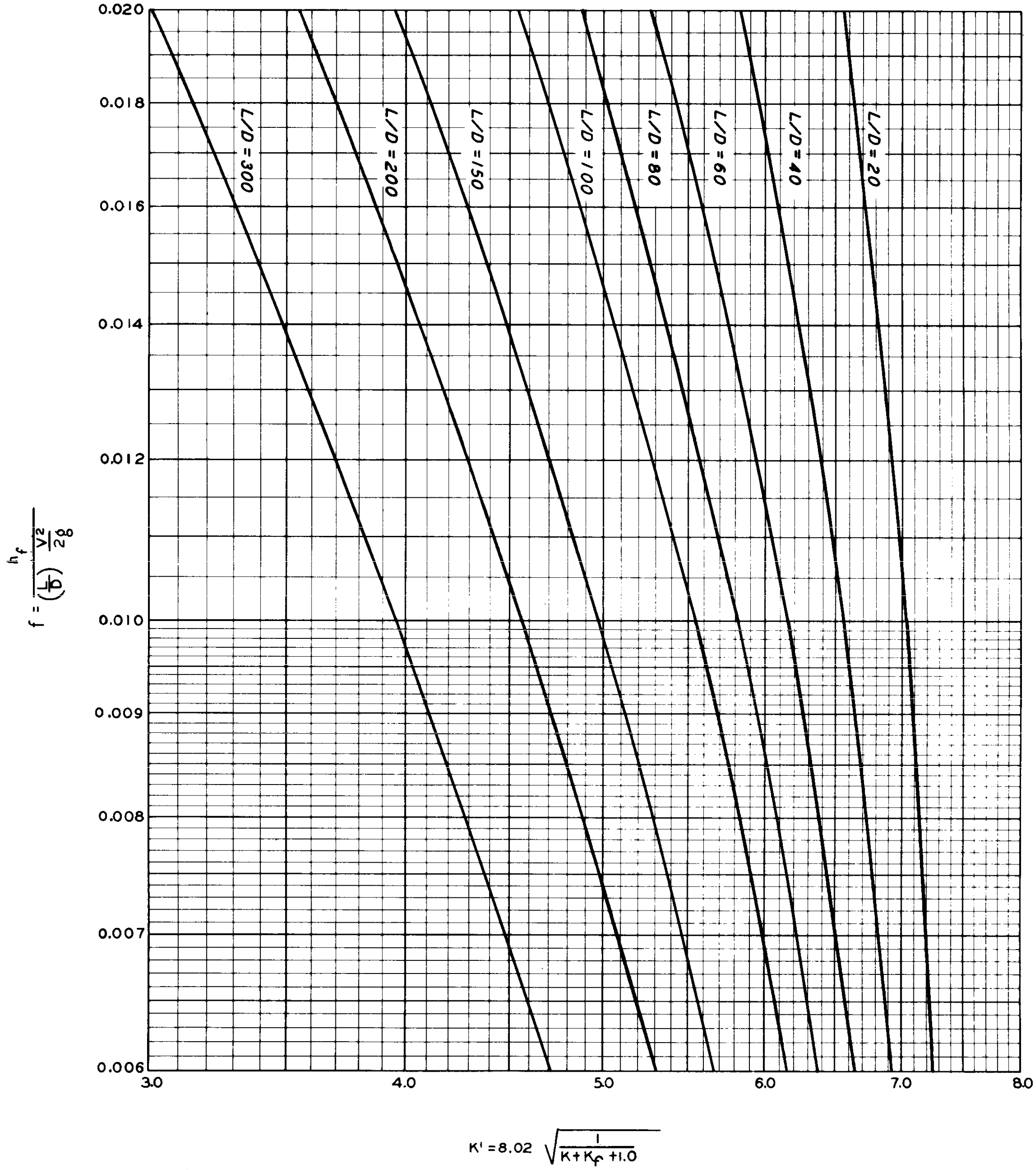

$$Q = A_C K' \sqrt{H}$$

WHERE

Q = DISCHARGE IN CFS

A_c = AREA OF CONDUIT IN SQ FT

K' = DISCHARGE COEFFICIENT

H = AVAILABLE HEAD

$K = 0.10$

STRAIGHT CIRCULAR CONDUITS

DISCHARGE COEFFICIENTS

HYDRAULIC DESIGN CHART 224-3

WES 4-1-53

HYDRAULIC DESIGN CRITERIA

SHEETS 224-3/1 TO 224-3/4

STRAIGHT CIRCULAR CONDUIT DISCHARGE

Hydraulic Design Charts 224-3/1 to 224-3/4 are design aids for reducing computation effort in determining the diameter required for a given discharge through a straight conduit. These charts are presented as supplements to Chart 224-3. Chart 224-3 presents various L/D ratios as a function of the Darcy-Weisbach friction factor "f" and a discharge coefficient "K'." Chart 224-3 was prepared for a combined loss coefficient other than friction of 0.10. Charts 224-3/1 to 224-3/4 are based on combined loss coefficients of 0.20, 0.30, 0.40, and 0.50.

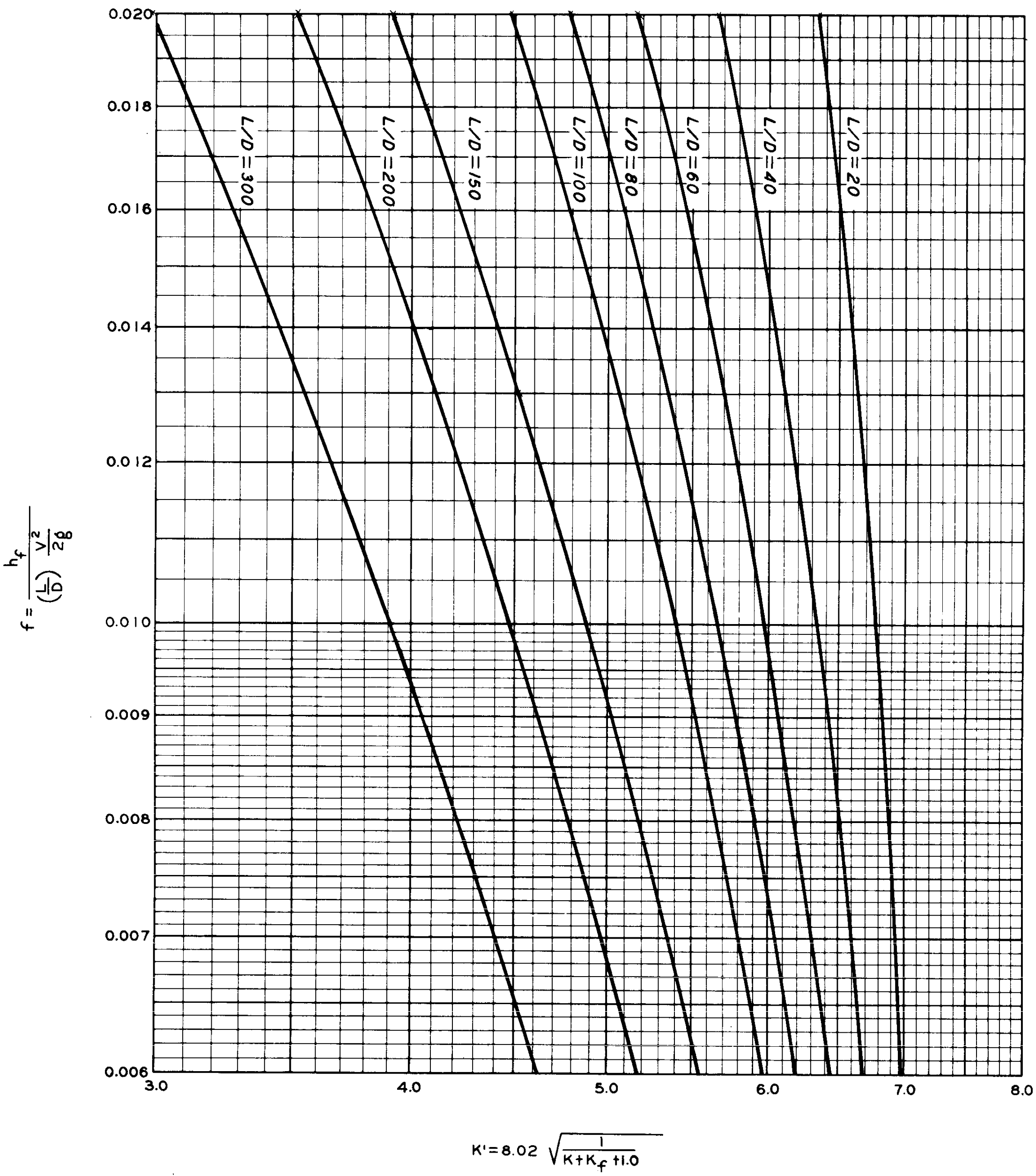

$Q = A_c K' \sqrt{H}$

WHERE:

Q = DISCHARGE IN CFS

A_c = AREA OF CONDUIT IN SQ FT

K' = DISCHARGE COEFFICIENT

H = AVAILABLE HEAD

$K = 0.20$

STRAIGHT CIRCULAR CONDUITS

DISCHARGE COEFFICIENTS

HYDRAULIC DESIGN CHART 224-3/1

WES 2-54

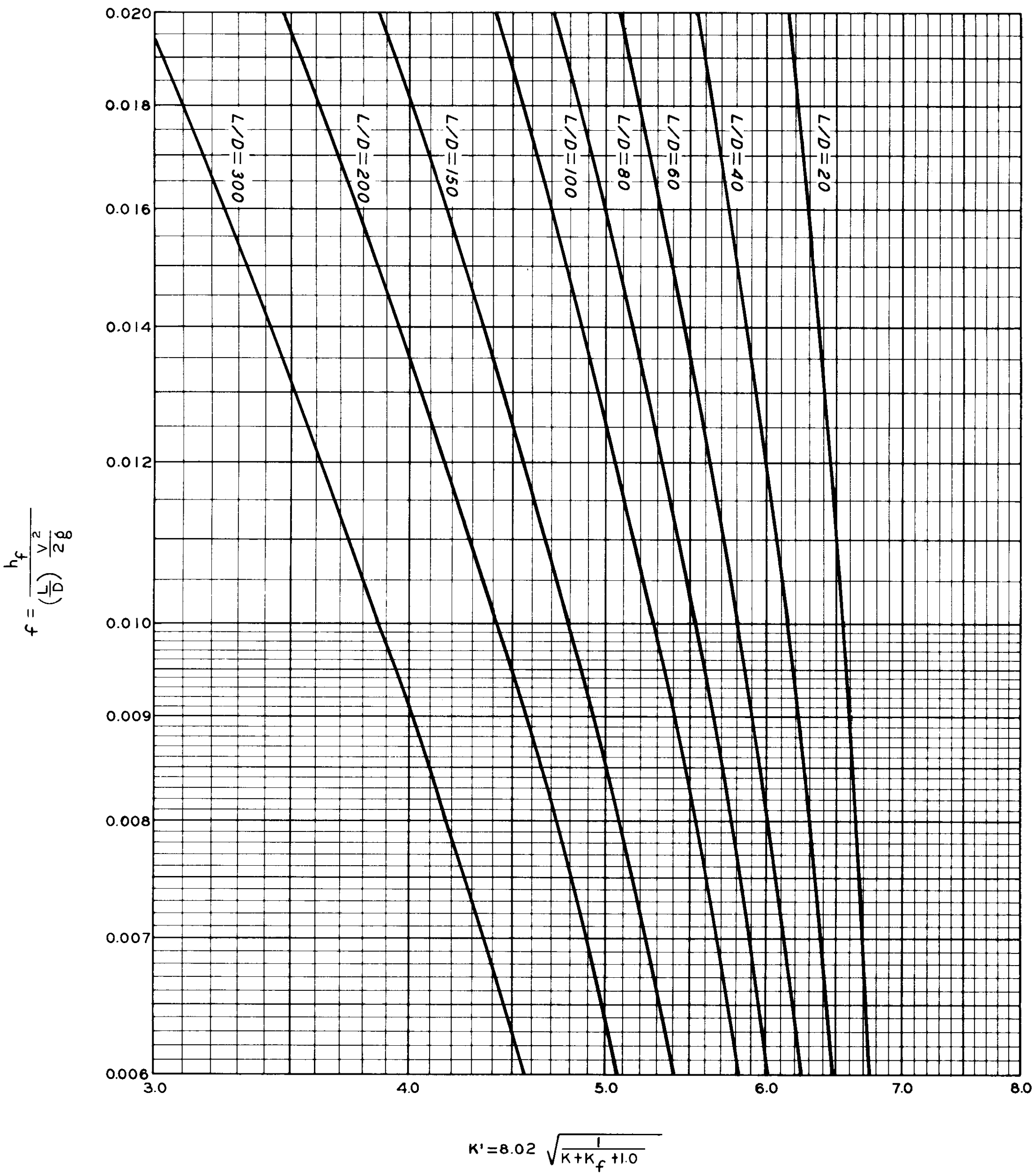

$Q = A_C K' \sqrt{H}$

WHERE:

Q = DISCHARGE IN CFS

A_C = AREA OF CONDUIT IN SQ FT

K' = DISCHARGE COEFFICIENT

H = AVAILABLE HEAD

$K = 0.30$

STRAIGHT CIRCULAR CONDUITS

DISCHARGE COEFFICIENTS

HYDRAULIC DESIGN CHART 224-3/2

WES 2-54

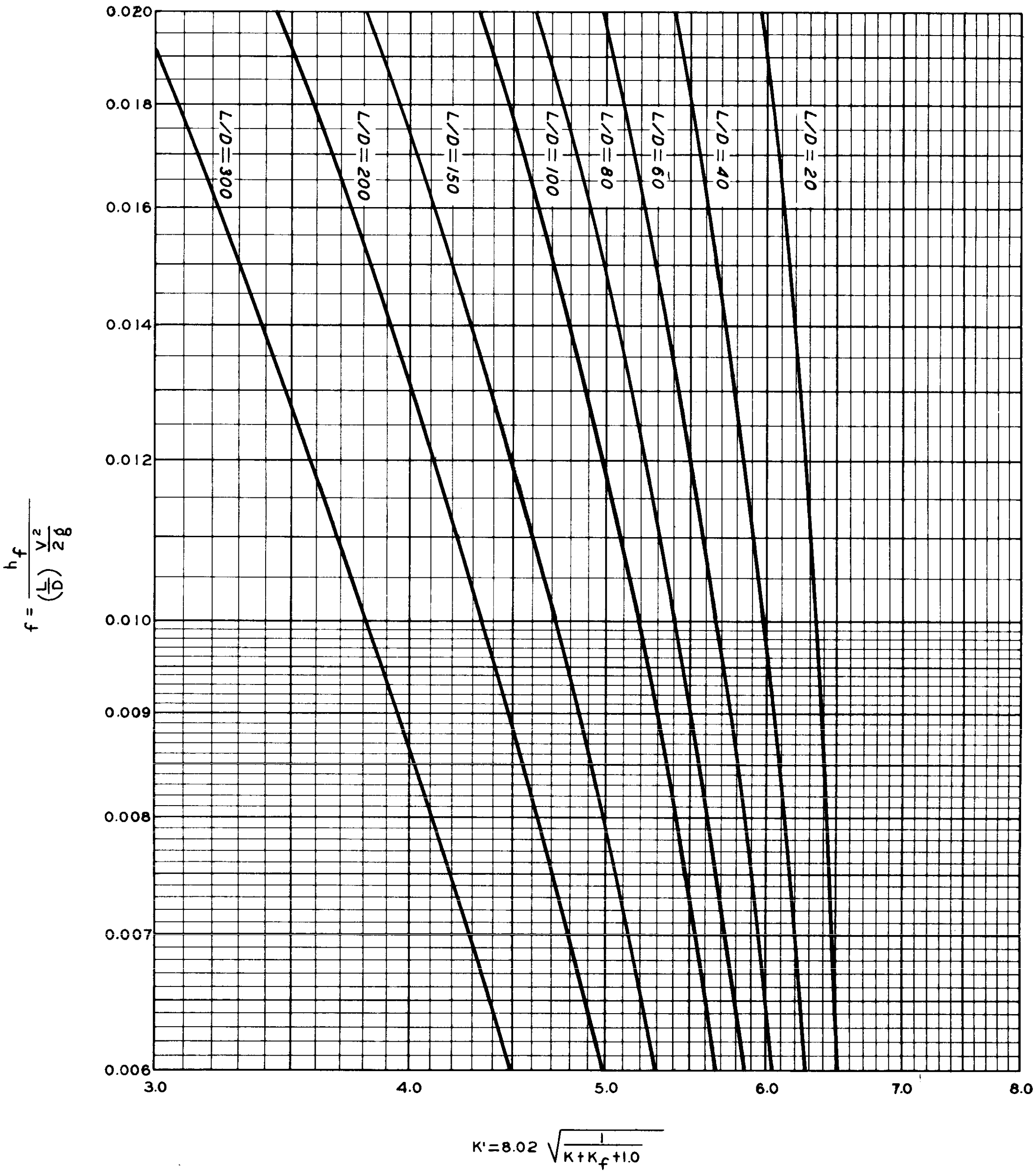

$$Q = A_C K' \sqrt{H}$$

WHERE:

Q = DISCHARGE IN CFS

A_C = AREA OF CONDUIT IN SQ FT

K' = DISCHARGE COEFFICIENT

H = AVAILABLE HEAD

$K = 0.40$

STRAIGHT CIRCULAR CONDUITS

DISCHARGE COEFFICIENTS

HYDRAULIC DESIGN CHART 224-3/3

WES 2-54

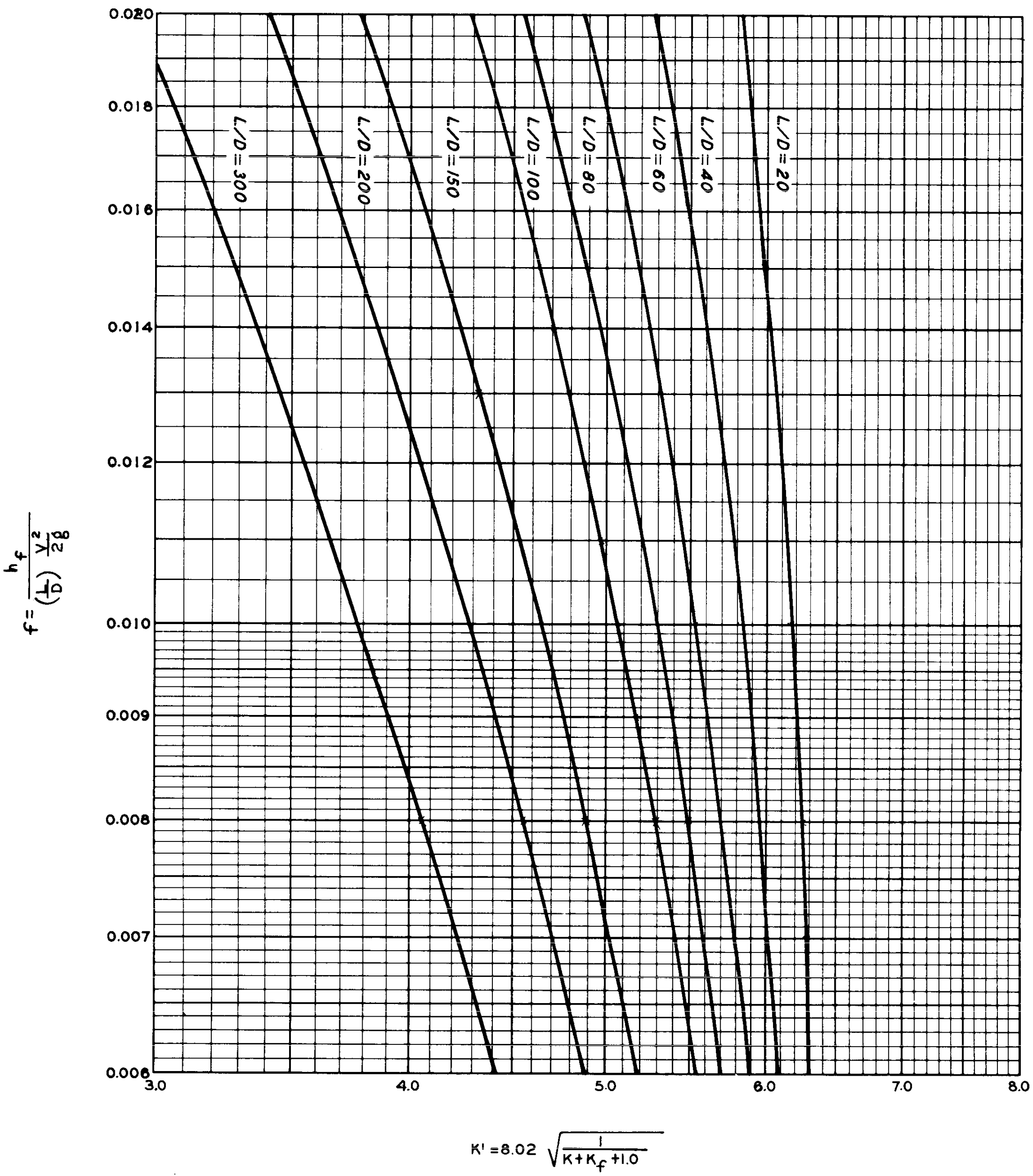

$$Q = A_C K' \sqrt{H}$$

WHERE:

Q = DISCHARGE IN CFS

A_c = AREA OF CONDUIT IN SQ FT

K' = DISCHARGE COEFFICIENT

H = AVAILABLE HEAD

$K = 0.50$

STRAIGHT CIRCULAR CONDUITS
DISCHARGE COEFFICIENTS

HYDRAULIC DESIGN CHART 224-3/4

WES 2-54

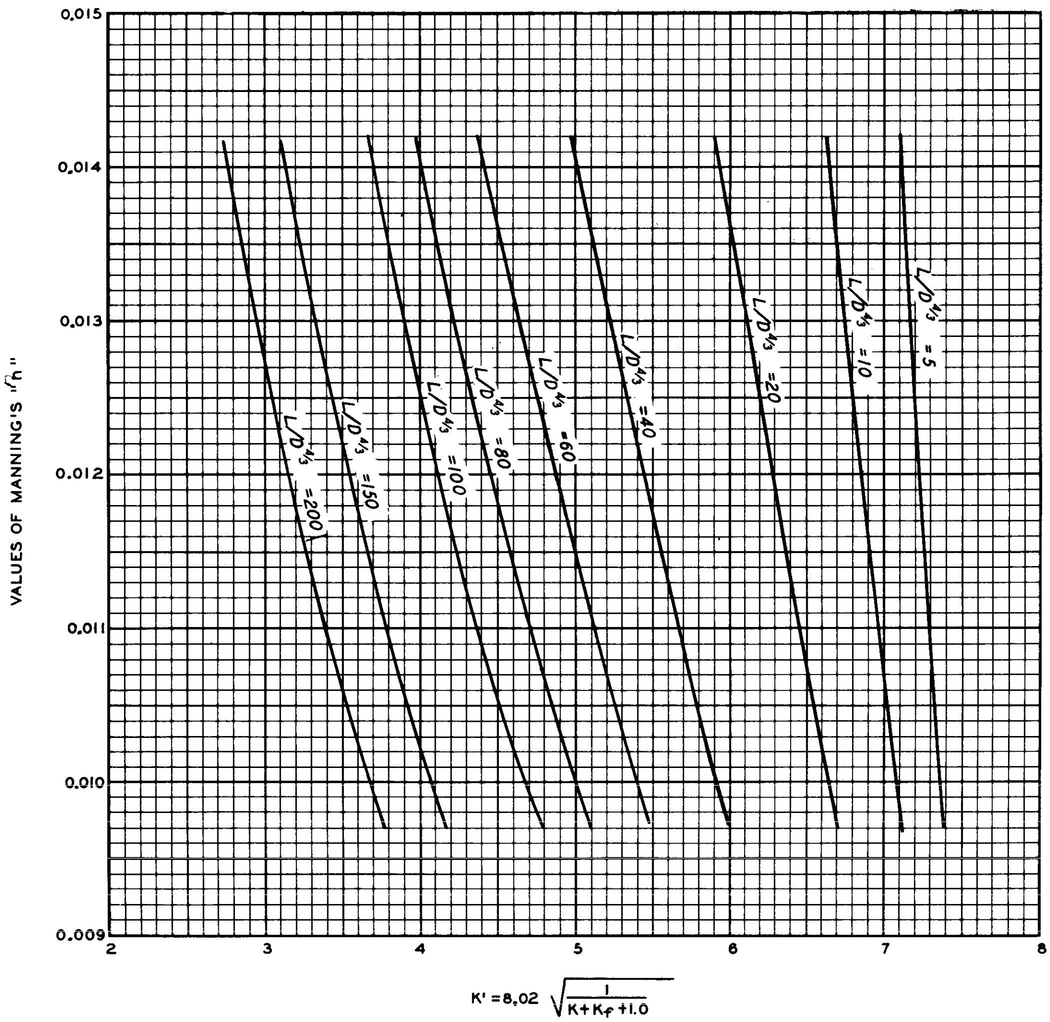

$$Q = A_C K' \sqrt{H}$$

WHERE

Q = DISCHARGE IN CFS

A_C = AREA OF CONDUIT IN SQ FT

K' = DISCHARGE COEFFICIENT

H = AVAILABLE HEAD

$K = 0.10$

STRAIGHT CIRCULAR CONDUITS

DISCHARGE COEFFICIENTS

HYDRAULIC DESIGN CHART 224-4

WES 4-1-53

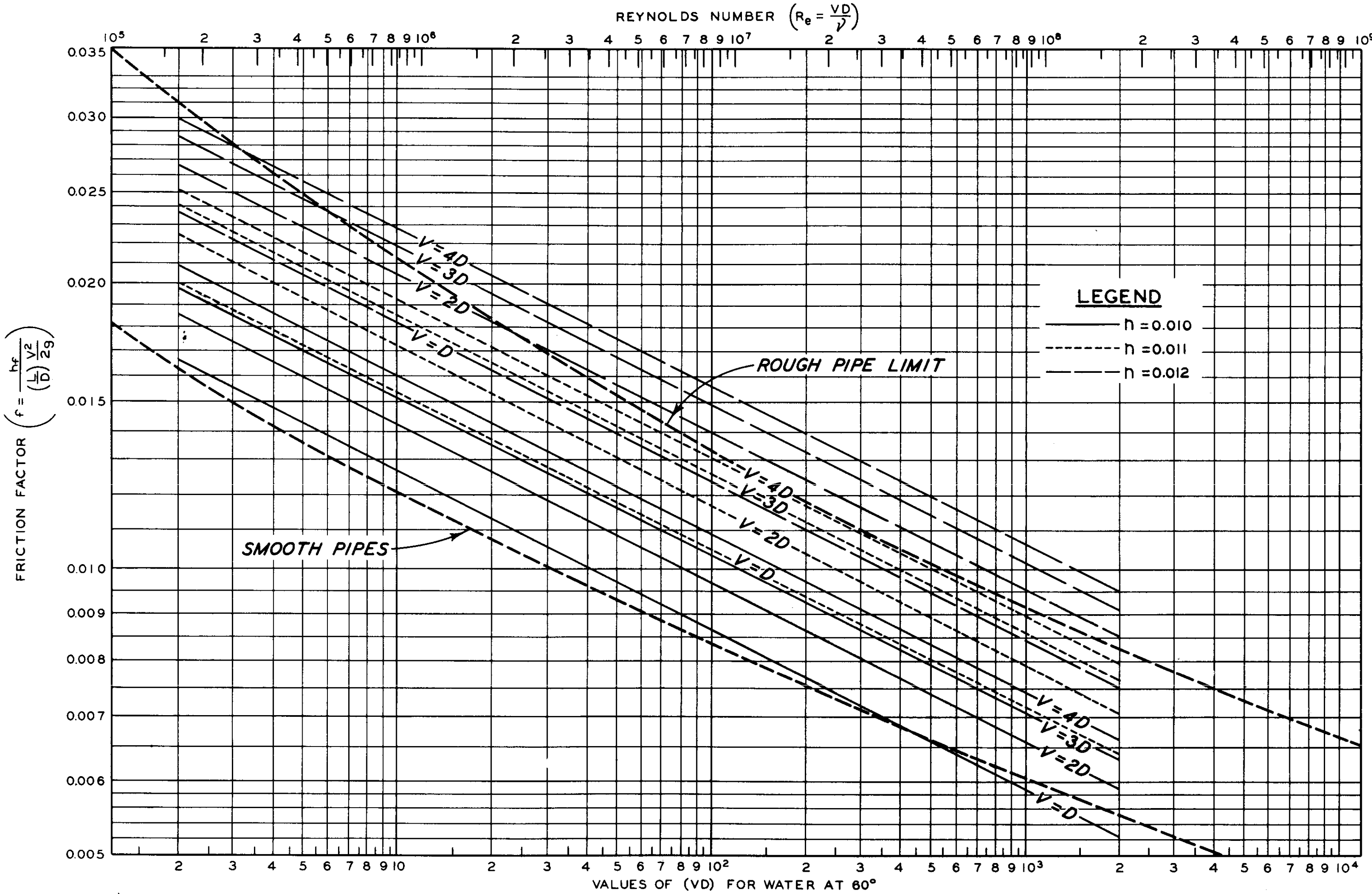

NOTE: h_f = FRICTION LOSS-FT
L = LENGTH OF CONDUIT-FT
D = DIAMETER-FT
V = VELOCITY-FPS
ν = KINEMATIC VISCOSITY-FT^2/SEC

CIRCULAR CONDUITS
FRICTION DESIGN GRAPH
HYDRAULIC DESIGN CHART 224-5

WES 4-1-53

WATERWAYS EXPERIMENT STATION

COMPUTATION SHEET

JOB: CW 804 PROJECT: JOHN DOE DAM SUBJECT: CIRCULAR CONDUITS

COMPUTATIONS: REQUIRED DIAMETER FOR DESIGN DISCHARGE

COMPUTED BY: RGC DATE: 10/22/52 CHECKED BY: AAMC DATE: 10-27-52

DESIGN REQUIREMENTS

Discharge (Q) = 20,000 cfs
Length of conduit (L) = 1,000 ft
Available head (H) = 100 ft
Required conduit diameter (D) to be determined

DESIGN ASSUMPTIONS

Composite coefficient (K) = 0.10
Manning's "n" = 0.012

TRIAL COMPUTATIONS – Charts 224-3 and 224-5

Assume D = 20 ft

Then:

Area of conduit (A_c) = 314 sq ft

$$\text{Velocity } (V) = \frac{20{,}000}{314} = 63.7 \text{ ft/sec}$$

$$\frac{V}{D} \text{ ratio} = \frac{63.7}{20} = 3.18$$

$$VD \text{ product} = 63.7 \times 20 = 1274$$

$$\frac{L}{D} \text{ ratio} = \frac{1000}{20} = 50$$

Enter Hydraulic Design Chart 224-5 on Ordinate VD = 1274 locating V/D ratio value = 3.18 between line V/D = 3 and V/D = 4 having "n" value = 0.012. Read friction factor (f) value of 0.010 on scale at left side of chart. Enter Hydraulic Design Chart 224-3 from left side at friction factor value (f) = 0.010. Follow this "f" value across chart to L/D value of 50 between lines L/D = 40 and L/D = 60. Read discharge coefficient value of (K') = 6.35 on scale at bottom of chart. Use discharge formula on chart to compute conduit discharge.

$$Q = A_c K' \sqrt{H}$$

$$Q = 314 \times 6.35 \sqrt{100} = 19{,}900 \text{ cfs}$$

NOTE: If the computed discharge does not approximate the required design discharge, successive trial computations are required varying D until the design discharge is obtained.

STRAIGHT CIRCULAR CONDUITS

SAMPLE DISCHARGE COMPUTATION

HYDRAULIC DESIGN CHART 224-6

WES 4/1/53

WATERWAYS EXPERIMENT STATION
COMPUTATION SHEET

JOB: CW 804 PROJECT: JOHN DOE DAM SUBJECT: CIRCULAR CONDUITS
COMPUTATIONS: REQUIRED DIAMETER FOR DESIGN DISCHARGE
COMPUTED BY: RGC DATE: 1/23/53 CHECKED BY: AAMC DATE: 2/3/53

DESIGN REQUIREMENTS

Discharge (Q) = 20,000 cfs
Length of conduit (L) = 1000 ft
Available head (H) = 100 ft
Required conduit diameter (D) to be determined

DESIGN ASSUMPTIONS

Composite coefficient (K) = 0.10
Manning's "n" = 0.012

TRIAL COMPUTATION — Chart 224-4

Assume D = 20 ft

Then:

Area of conduit (A_C) = 314

K = 0.10

$D^{4/3} = (20)^{4/3} = 54.3$

$$\frac{L}{D^{4/3}} = \frac{1000}{54.3} = 18.4$$

Enter Hydraulic Design Chart 224-4 at left side with "n" value of 0.012. Traverse chart to point $\frac{L}{D^{4/3}} = 18.4$ between lines $\frac{L}{D^{4/3}} = 10$ and $\frac{L}{D^{4/3}} = 20$. Read discharge coefficient (K') = 6.4 on scale at bottom of chart. Use discharge formula on Chart 224-4 to compute conduit discharge.

$$Q = A_C K' \sqrt{H}$$

$$Q = 314 \times 6.4 \times \sqrt{100} = 20{,}100 \text{ cfs}$$

NOTE: If computed discharge does not approximate the required design discharge successive trial computations are required varying D until the design discharge is obtained.

STRAIGHT CIRCULAR CONDUITS
SAMPLE DISCHARGE COMPUTATION
MANNING'S "N" METHOD
HYDRAULIC DESIGN CHART 224-7

HYDRAULIC DESIGN CRITERIA

SHEETS 224-8 AND 224-9

CIRCULAR SECTIONS

FREE-SURFACE FLOW

1. Hydraulic Design Charts 224-8 and 224-9 are aids for reducing the computation effort in design of channels of circular section. Chart 224-8 is designed for use with Charts 610-1 and 610-1/1. Chart 224-9 is complete within itself. These charts can be used in conjunction with the method for nonuniform flow presented on Chart 010-2.

2. Basic Equation. Chart 224-8 can be used to determine normal depths (y_o) for any circular section. The curves on Chart 224-8 were developed using the equations stated in paragraph 2 of Sheets 610-1 to 610-7. Functions of the area and hydraulic radius, necessary for the solution of the equations, were obtained from published tables(1).

3. Chart 224-9 can be used to determine the critical depth-diameter ratio from which the critical depth can be computed; these curves are based on the critical depth formula(2)

$$Q = CD^{5/2}$$

4. Application. The ratio of normal-depth to diameter (y_o/D) for various sections can be determined from Chart 224-8 in the manner described in paragraph 3a, b, and c, Sheets 610-1 to 610-7. The ratio of critical depth to diameter can be determined directly from Chart 224-9 for a given discharge and diameter.

---

(1) H. W. King, Handbook of Hydraulics, 3d ed., New York, N. Y., McGraw-Hill Book Company (1939), tables 100 and 101, p 299.

(2) Ibid., Table 130, p 441.

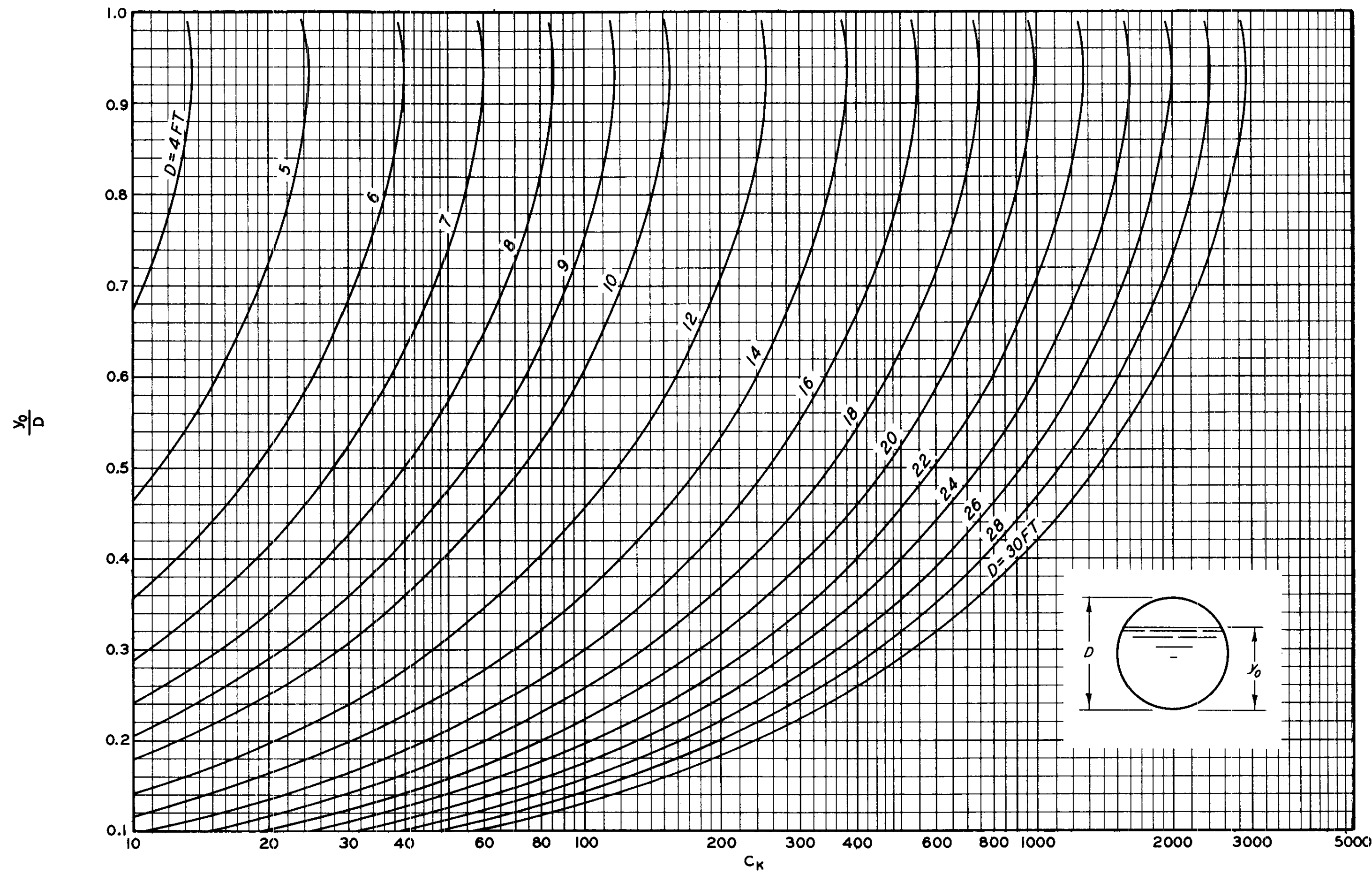

BASIC EQUATION

$Q = C_n C_K$

WHERE: Q = DISCHARGE IN CFS

$C_n = \frac{1.486\, S^{1/2}}{n}$ (CHART 610-1 AND 610-1/1)

$C_K = AR^{2/3}$

NOTE: FUNCTIONS OF "A" AND "R" TAKEN FROM KING'S HANDBOOK OF HYDRAULICS, TABLES 100 AND 101, PAGE 299, 3RD EDITION.

OPEN CHANNEL FLOW
CIRCULAR SECTIONS
y_0/D VS C_K

HYDRAULIC DESIGN CHART 224-8

WES 3-56

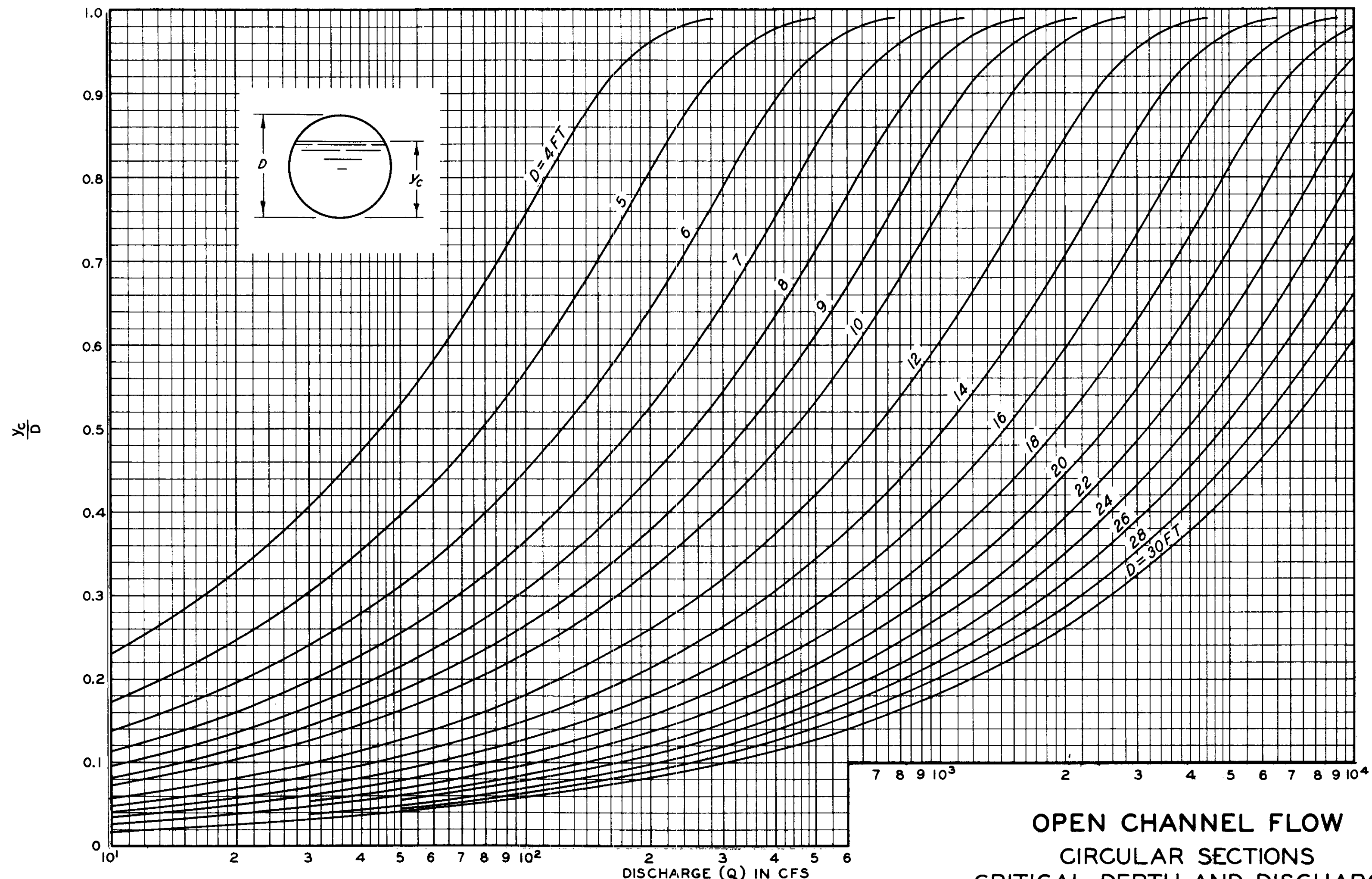

BASIC EQUATION

$Q = CD^{5/2}$

WHERE: Q = DISCHARGE IN CFS
D = DIAMETER IN FT
C = COEFFICIENT (KING'S HANDBOOK OF HYDRAULICS, TABLE 130, PAGE 441, 3RD EDITION)

OPEN CHANNEL FLOW
CIRCULAR SECTIONS
CRITICAL DEPTH AND DISCHARGE

HYDRAULIC DESIGN CHART 224-9

WES 3-56

HYDRAULIC DESIGN CRITERIA

SHEET 224-10

HORSESHOE CONDUITS

HYDRAULIC ELEMENTS

1. Hydraulic Design Chart 224-10 presents curves of hydraulic elements as computed by the U. S. Bureau of Reclamation* for a standard horseshoe tunnel cross section. This conduit shape is identical with that presented at the bottom of Hydraulic Design Chart 224-2.

2. The flow cross-sectional area A, water surface width T, and wetted perimeter P can be expressed in terms of y/H, in which y is the central flow depth and H is the central height and width, or in terms of the angle θ, which is the slope angle of the lower side arc radius line at the water surface intercept on the lower side arc. Angle θ equals $\sin^{-1}(0.5 - y/H)$. The flow section can be studied in three separate portions:

a. Value y varies from the bottom to the intersection of the lower side arcs, $0 \leq (y/H) \leq 0.0885$.

$$\frac{A}{H^2} = \cos^{-1}\left(1 - \frac{y}{H}\right) - \left(1 - \frac{y}{H}\right)\sqrt{\frac{y}{H}\left(2 - \frac{y}{H}\right)}$$

$$\frac{T}{H} = 2\sqrt{\frac{y}{H}\left(2 - \frac{y}{H}\right)}$$

$$\frac{P}{H} = 2\cos^{-1}\left(1 - \frac{y}{H}\right)$$

b. Value y varies from the intersection of the lower side arcs to half full, $0.0885 < (y/H) < 0.05$ or $0 < \theta < 0.4242$ rad.

---

* Hu, Walter W., "Hydraulic elements for the USBR standard horseshoe tunnel," Transportation Engineering Journal of ASCE, vol 99, No. TE4, November, 1973.

$$\frac{A}{H^2} = 0.4366 - \theta + \frac{1}{2} \sin \theta \left(1 - \sqrt{1 + 8 \sin^2 \frac{\theta}{2} - 4 \sin^2 \theta}\right)$$

$$\frac{T}{H} = \sqrt{1 + 8 \sin^2 \frac{\theta}{2} - 4 \sin^2 \theta}$$

$$\frac{P}{H} = 1.6962 - 2\theta$$

c. Value y varies from half full to full, $0.5 \leq (y/H) \leq 1.0$.

$$\frac{A}{H^2} = 0.8293 = \frac{1}{4} \cos^{-1} \left[2\left(\frac{y}{H}\right) - 1\right] + \left(\frac{y}{H} - 0.5\right)\sqrt{\frac{y}{H}\left(1 - \frac{y}{H}\right)}$$

$$\frac{T}{H} = 2\sqrt{\frac{y}{H}\left(1 - \frac{y}{H}\right)}$$

$$\frac{P}{H} = 3.2670 - \cos^{-1}\left[2\left(\frac{y}{H}\right) - 1\right]$$

3. Other hydraulic elements included in Chart 224-10 are the hydraulic radius, $R = A/P$; hydraulic depth, $D = A/T$; section factor, $Z = A\sqrt{D}$; conveyance of Manning's formula, $K = 1.486\ AR^{2/3}$; and the critical slope for a given normal depth, S_{cn} . All are expressed as dimensionless ratios with respect to H except S_{cn} , which is expressed in the form $S_{cn}/n^2 = 14.57P^{4/3}/A^{1/3}T$, where n is the Manning's roughness.

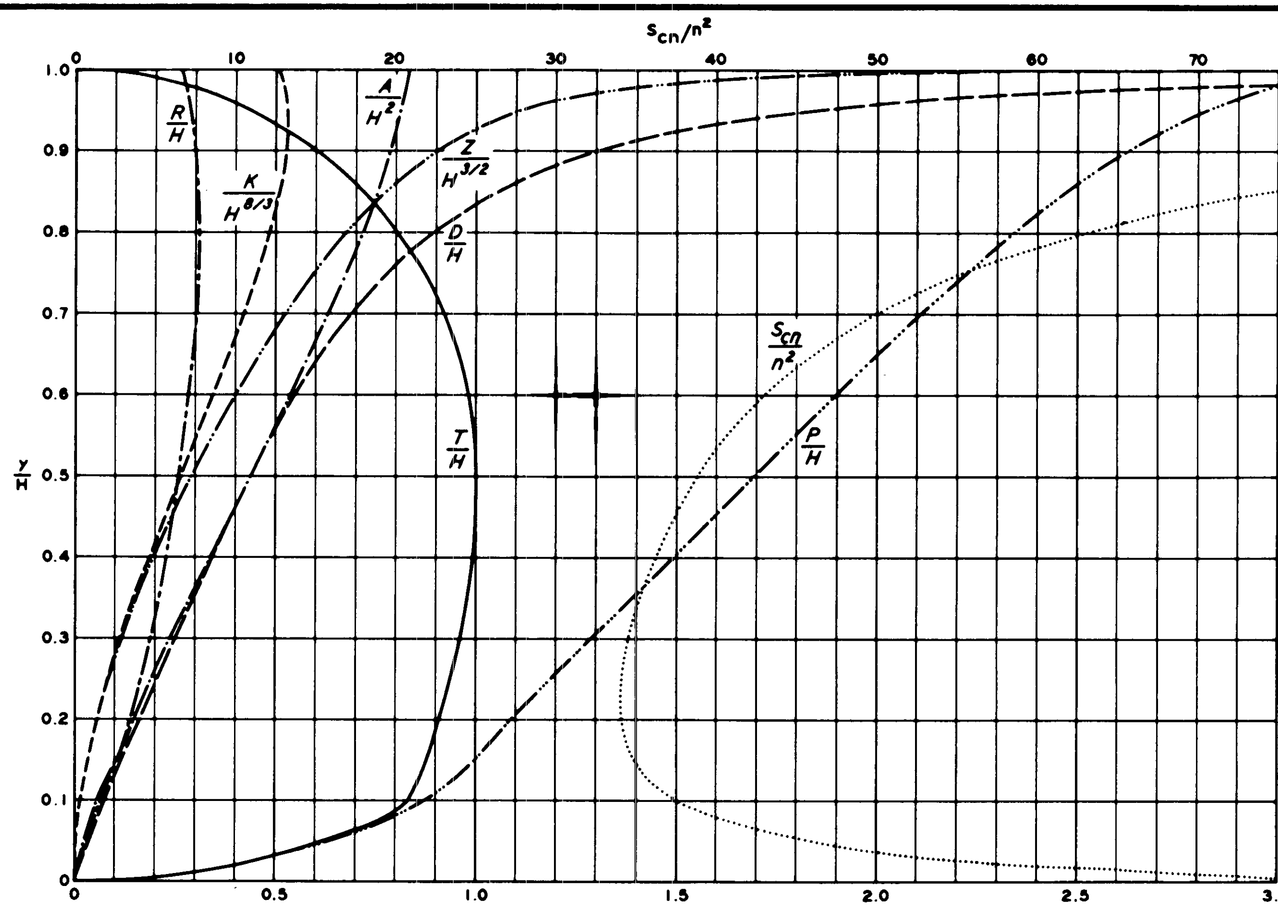

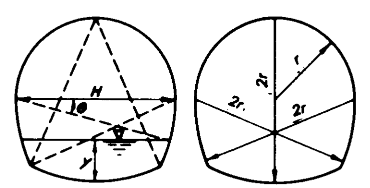

CROSS-SECTIONAL GEOMETRY

LEGEND

A=CROSS-SECTIONAL AREA
D=HYDRAULIC DEPTH
H=CENTRAL HEIGHT AND WIDTH
K=CONVEYANCE OF MANNING'S FORMULA
n=MANNING'S ROUGHNESS
P=WETTED PERIMETER
R=HYDRAULIC RADIUS
S_{cn}=CRITICAL SLOPE FOR GIVEN NORMAL DEPTH
T =FREE WATER SURFACE WIDTH
y =CENTRAL FLOW DEPTH
Z =SECTION FACTOR
θ =SLOPE ANGLE OF LOWER SIDE ARC RADIUS LINE AT WATER SURFACE INTERCEPT ON SIDE ARC

HORSESHOE CONDUITS
HYDRAULIC ELEMENTS

HYDRAULIC DESIGN CHART 224-10

WES 5-75
REV 11-87

HYDRAULIC DESIGN CRITERIA

SHEET 225-1

CIRCULAR EXIT PORTAL

PRESSURE GRADIENTS

1. The elevation of the intersection of the pressure gradient with the plane of the exit portal is a factor in the computation of the discharge capacity of a flood-control conduit. The use of the center of the portal as the position of the pressure gradient yields fairly accurate discharge determination for unconstricted flow where the conduit is relatively small in relation to the design head. However, a closer determination of the pressure gradient intersection is pertinent to the discharge-capacity design where the conduit size is large in relation to the head.

2. Theory. A number of investigations have been made of velocity and pressure distribution in the vicinity of exit portals. Each investigator concluded that the intersection of the pressure gradient with the plane of the exit portal did not coincide with the center of the portal for a free discharging jet. D. Rueda-Briceno(2) determined the location of the pressure gradient as a function of Froude's number.

3. Basic Data. HDC 225-1 shows the relative position of the pressure gradient at an exit portal of circular section (Y_p/D) with respect to Froude's number (F). The plotted data show that the position of the pressure gradient varies with the support of the jet downstream from the portal plane as well as with Froude's number. The geometry of the jet support for the various investigations is summarized below:

a. State University of Iowa (Rueda-Briceno).(2) Jet discharging into air.

b. Denison model.(4) Jet discharging into transition having level invert and sidewalls flared 1 on 5.

c. Denison prototype.(5) Jet discharging into transition having level invert and parallel sidewalls for 50 ft followed by 1-on-5 flared walls.

d. Garrison model.(6) Jet discharging into transition having parabolic invert and sidewalls flared 8 on 35.

e. Youghiogheny model.(1) Jet discharging into transition having 1-on-20 sloping invert and sidewalls flared 2 on 3 followed by elliptical curves.

f. Enid prototype.(7) Jet discharging into transition having parabolic invert and sidewalls flared with 100-ft radius for 20 ft followed by flare of 1 on 4.5.

g. Fort Randall model and prototype.[8,9] Jet discharging into primary stilling basin having level invert and sidewalls flared 1 on 6. The 500-ft-long primary basin is separated from the secondary basin by a 25-ft-high ogee weir.

h. Oahe prototype.[3] Jet discharging into transition having parabolic invert and sidewalls flared 1 on 7.42.

4. Application. The suggested design curve in HDC 225-1 applies to circular conduits with some form of jet support below the exit portal. The solid-line curve is applicable only to exit portals having a free-falling jet.

5. References.

(1) Carnegie Institute of Technology, Report on Hydraulic Model Tests of Spillway and Outlet Works of Youghiogheny River Dam, Confluence, Pennsylvania. Hydraulic Laboratory, Pittsburgh, Pa., March 1941.

(2) Rueda-Briceno, D., Pressure Conditions at the Outlet of a Pipe. State University of Iowa Master's Thesis, February 1954.

(3) U. S. Army Engineer District, Omaha, Oahe Outlet Tunnel Prototype Tests. (Unpublished data.)

(4) U. S. Army Engineer Waterways Experiment Station, CE, Hydraulic Model Studies of the Control Structures for the Denison Dam, Red River. Technical Memorandum No. 161-1, Vicksburg, Miss., April 1940.

(5) __________, Pressure and Air Demand Tests in Flood-Control Conduit, Denison Dam, Red River, Oklahoma and Texas. Miscellaneous Paper No. 2-31, Vicksburg, Miss., April 1953.

(6) __________, Outlet Works and Spillway for Garrison Dam, Missouri River, North Dakota; Hydraulic Model Investigation. Technical Memorandum No. 2-431, Vicksburg, Miss., March 1956.

(7) __________, Prototype Hydraulic Tests of Flood-Control Conduit, Enid Dam, Yocona River, Mississippi. Technical Report No. 2-510, Vicksburg, Miss., June 1959.

(8) __________, Spillway and Outlet Works, Fort Randall Dam, Missouri River, South Dakota; Hydraulic Model Investigation. Technical Report No. 2-528, Vicksburg, Miss., October 1959.

(9) __________, Flow Characteristics in Flood-Control Tunnel 10, Fort Randall Dam, Missouri River, South Dakota; Hydraulic Prototype Tests. Technical Report No. 2-626, Vicksburg, Miss., June 1963.

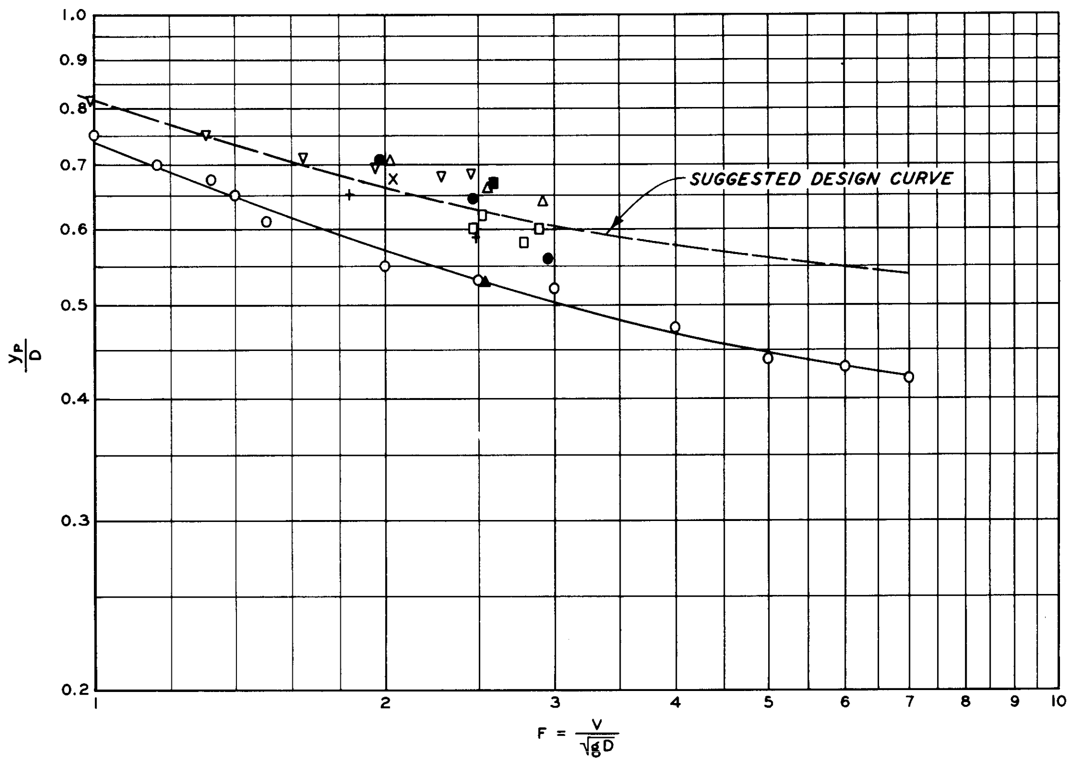

LEGEND

SYMBOL	DATA SOURCE	BOTTOM SUPPORT
—o—	STATE UNIVERSITY OF IOWA	NONE
□	DENISON MODEL	LEVEL
■	DENISON PROTOTYPE	LEVEL
●	GARRISON MODEL	PARABOLIC
▽	YOUGHIOGHENY MODEL	1 ON 20
X	ENID PROTOTYPE	PARABOLIC
△	FORT RANDALL MODEL	LEVEL
▲	FORT RANDALL PROTOTYPE	LEVEL
+	OAHE PROTOTYPE	PARABOLIC

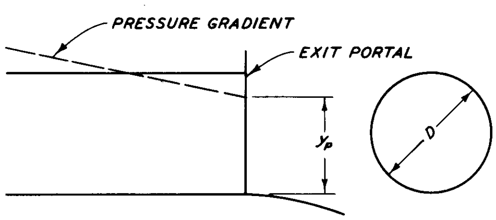

EXIT PORTALS

CIRCULAR CONDUITS

F VS y_P/D

HYDRAULIC DESIGN CHART 225-1

REVISED 1-64 REVISED 3-56 WES 9-54

SHEET 228-1

BEND LOSS COEFFICIENTS

1. The purpose of this chart is for use in the design of flood-control conduits and tunnels. Most of the research work which has been conducted on bend loss is based on right-angle bends and is applicable principally to the problems of mechanical engineering design. Flood-control conduits are usually designed with a deflection angle (α) much smaller than 90 degrees. The work of Wasielewski(1) at Munich was applicable to a wide range of deflection angles and ratio of bend radii to pipe diameters (r/D). These experiments formed the basis of the curves on the attached chart.

2. The broken lines are suggested design curves formulated from the Wasielewski curves shown as solid lines. The bend loss coefficient (K_b) represents the loss in terms of velocity head caused by the bend only, excluding the friction loss within the bend. The experiments of Wasielewski employed approximately 55 diameters of pipe and should represent nearly complete decay of the turbulence caused by the bend. The Reynolds number for these tests was 225,000.

3. The maximum angle tested by Wasielewski was 75 degrees. His graph includes the data obtained by Hofmann(2) for losses caused by 90° bends. The design curves were adjusted by the use of the 90° curve shown in the upper right-hand corner of the chart. This curve also serves as an interpolation curve for the design curves on the chart. Although the coefficient K_b approaches zero very slowly as the r/D ratio becomes large, it was suggested by Professor J. S. McNown of State University of Iowa that a logarithmic function may fit the data. The equation shown produces a good fit for 90° with π used in the constants as indicated.

---

(1) Rudolph Wasielewski, "Loss in Smooth Pipe Bends with Bend Angles Less than 90°" (In German), Proceedings of the Hydraulic Institute of the Technical College of Munich, Issue 5 (1932), pp. 53-67.

(2) A. Hofmann, "Loss in 90 Degree Pipe Bends of Constant Circular Cross-Section," Transactions of the Hydraulic Institute of the Munich Technical University, Bulletin 3 (1929). Published in 1935 by the American Society of Mechanical Engineers, pp. 29-41.

4. The interpolation curve for 90° was developed independently on the basis of the Wasielewski data and was then compared with Anderson's and Straub's adjusted curve[3]. The two curves show a fair agreement. A careful analysis of Waterways Experiment Station data[4] for $r/D = 1.5$ and $\alpha = 90°$ gives a good verification of the design curve for that ratio. The experimental data by Beij[5] has been included on the graph. Dr. Beij has informed the Office, Chief of Engineers, that he considers his data applicable to rough pipe.

5. It was found further that the introduction of α in the equation as indicated, produced a family of curves which embraces the Wasielewski data fairly well. More experimental information is needed for the range of r/D greater than 4 and α less than 45°. These data indicate the bend loss only and estimated friction for the length of bend should be added.

6. The data from the various experimenters on 90° bends show wide discrepancies. However, bend losses are usually small compared to friction losses in tunnels or conduits of substantial length. In the interest of conservatism, it is recommended that safety factors be applied to the dashed curves. The values on the graph should be increased 25% to 50% in the design for hydraulic capacity. The values indicated on the graph should be decreased by a comparable percentage in determining the maximum velocity entering a stilling basin at the downstream end of a tunnel. The selection of the actual percentage between the range given would depend upon the relative importance of hydraulic capacity and the effect upon cost.

---

(3) A. G. Anderson and L. G. Straub, "Hydraulics of Conduit Bends," St. Anthony Falls Hydraulic Laboratory Bulletin No. 1 (Minneapolis, Minnesota, December 1948).

(4) "Experiments to Determine the Pressure Loss in Pipe Bends," Waterways Experiment Station, Technical Memorandum No. 21-1 (Vicksburg, Miss., January 1932).

(5) K. Hilding Beij, "Pressure Losses for Fluid Flow in 90° Pipe Bends," Research Paper RP 1110, Journal of Research, National Bureau of Standards, Vol. 21 (July 1938).

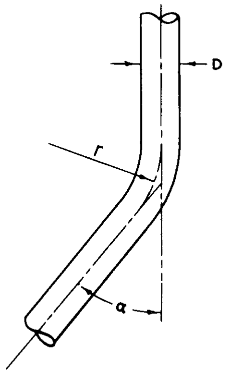

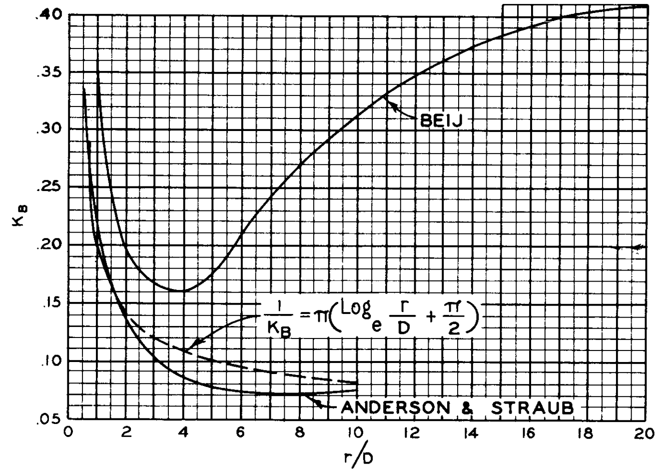

K_B VS r/D FOR 90° BENDS

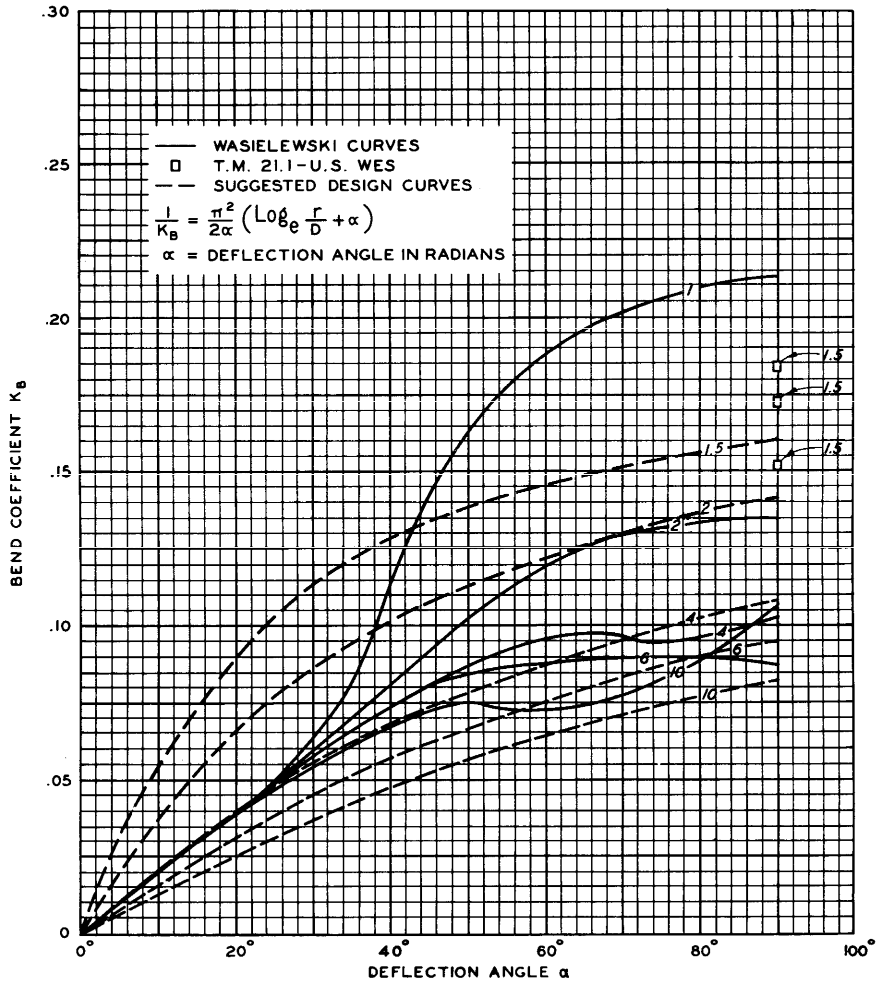

BASIC EQUATION = $h_L = K_B V^2/2g$

h_L = HEAD LOSS DUE TO BEND

K_B = BEND LOSS COEFFICIENT

V = VELOCITY IN PIPE

NOTE: FIGURES ON GRAPH INDICATE r/D RATIO.

BEND-LOSS COEFFICIENTS

HYDRAULIC DESIGN CHART 228-1

REVISED 8-58 WES 4-1-52

HYDRAULIC DESIGN CRITERIA

SHEETS 228-2 TO 228-2/1

MITER BENDS

BEND LOSS COEFFICIENTS

1. Hydraulic Design Chart 228-2 and 228-2/1 show bend loss coefficients (K_B) versus Reynolds number and deflection angle, respectively. The charts are based on laboratory tests made at Munich, Germany[(1)], and tests made on 90-degree bends at the Waterways Experiment Station[(2)]. The broken lines on Chart 228-2 are suggested design curves and are not the experimenters' interpretations. The bend loss coefficient (K_B) represents the loss in terms of velocity head caused by the bend only, excluding the friction loss within the bend.

2. Chart 228-2/1 is a plot of bend loss coefficients and deflection angles for three Reynolds numbers. The curves on this chart were used to establish the suggested design curves on Chart 228-2. The curves have been extended to assist the engineer in determining loss coefficients for smaller deflection angles.

---

(1) Hans Kirchbach, "Loss of Energy in Miter Bends," and Werner Schubart, "Energy Loss in Smooth and Rough Surfaced Bends and Curves in Pipe Lines," Transactions of the Hydraulic Institute of the Munich Tech. Univ. Bulletin 3, translation published by ASME, 1935.

(2) "Experiments To Determine the Pressure Loss in Pipe Bends," Waterways Experiment Station, Technical Memorandum No. 21-1, Vicksburg, Miss., January 1932.

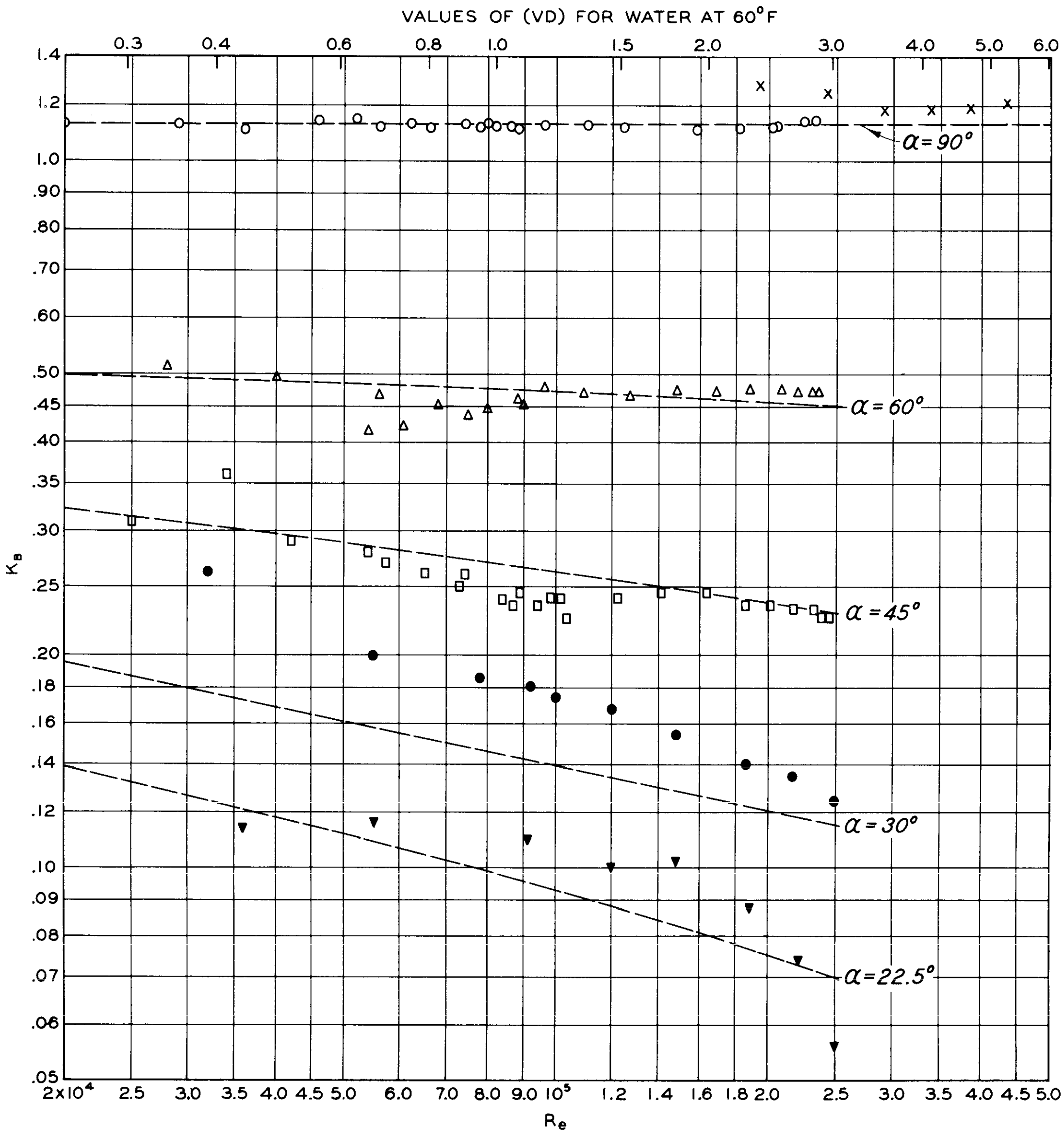

BASIC EQUATION

$$K_B = \frac{h_L}{V^2/2g}$$

WHERE K_B = BEND LOSS COEFFICIENT

h_L = HEAD LOSS DUE TO BEND

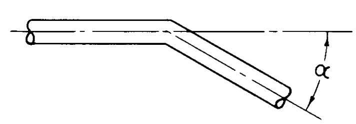

LEGEND

x WES DATA, α = 90°
o MUNICH DATA, α = 90°
△ MUNICH DATA, α = 60°
□ MUNICH DATA, α = 45°
● MUNICH DATA, α = 30°
▼ MUNICH DATA, α = 22.5°
—— SUGGESTED DESIGN CURVES

NOTE: WES DATA FROM 8" PIPE.
MUNICH DATA FROM 1.69" PIPE.

SINGLE MITER

BEND LOSS COEFFICIENTS

K_B VS R_e

HYDRAULIC DESIGN CHART 228-2

WES 3-55

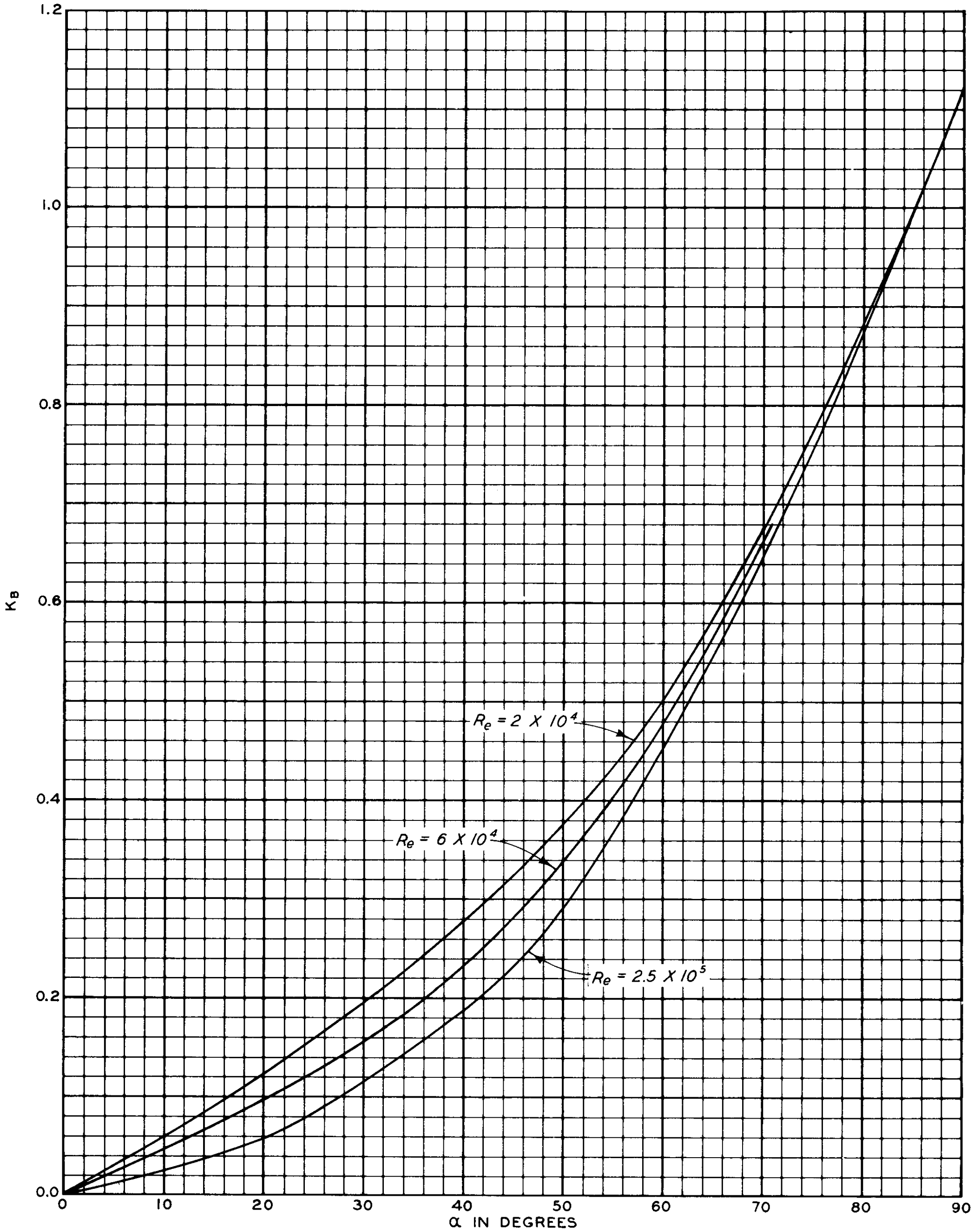

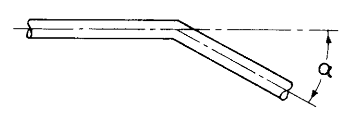

BASIC EQUATION

$$K_B = \frac{h_L}{V^2/2g}$$

WHERE K_B = BEND LOSS COEFFICIENT

h_L = HEAD LOSS DUE TO BEND

SINGLE MITER

BEND LOSS COEFFICIENTS

K_B VS α

HYDRAULIC DESIGN CHART 228-2/1

WES 3-55

SHEET 228-3

PRESSURE FLOW

PIPE BENDS

MINIMUM PRESSURE

1. Flow around pipe bends results in a velocity acceleration along the inside of the bend accompanied by a local pressure reduction. This pressure reduction may be sufficient to result in cavitation in low flow and water supply pipes conducting discharges from reservoirs. Hydraulic Design Chart 228-3 should serve for estimating minimum pressures in standard pipe bends.

2. Basic Data. Available experimental data on minimum pressures in pipe bends are limited to those on 6-in. pipe bends of 45 to 180 deg by Yarnell.[1] These data show that the minimum pressure occurs 22.5 deg from the point of curvature compared with its occurrence 45 deg from the point of curvature for rectangular section conduits (HDC Sheets and Charts 534-2 and 534-2/1). The analytical procedure suggested by McPherson and Strausser[2] for determining the magnitude of the minimum pressure in a circular bend of rectangular conduits has been applied to pipe bends. The theoretical curve, Yarnell's data, and points computed from elbow meter data compiled by Taylor and McPherson[3] are shown in Chart 228-3. The elbow meter data are based on studies by Lansford,[4] Addison,[5] and Taylor and McPherson[3] (Lehigh data). Yarnell's[1] study showed that the pressure 45 deg from the point of curvature is only slightly higher than the minimum pressure that occurs at the 22.5-deg point. This is confirmed by the Lehigh data points in Chart 228-3. Data for both the 22.5- and 45-deg points correlate with the theoretical curve as shown in the chart. The data cover a range of pipe diameters from 4 to 12 in. and indicate a range of Reynolds numbers (R_e) of 10^4 to 10^5.

3. Application. The minimum bend pressure can be computed from the equation

$$C_p = \frac{H - H_i}{\frac{V^2}{2g}}$$

The terms in the equation are defined in Chart 228-3. The equation for the theoretical curve shown in Chart 228-3 is given in Sheet 534-2.

4. The curve in Chart 228-3 can be used to estimate the minimum steady pressure in standard pipe bends of 45 to 180 deg. Cavitation occurs when the instantaneous pressure at any point in a flowing liquid drops to vapor pressure. Turbulence in flow causes local pressure

fluctuation. Therefore, an estimate should be made of the maximum expected fluctuation from the minimum computed steady pressure. A procedure for estimating the necessary average pressure or the permissible average velocity to prevent cavitation is given in paragraph 4 of Sheets 534-2 and 534-2/1. The sample computation shown in Chart 534-2/1 for rectangular conduits is also applicable to pipe bends.

5. References.

(1) U. S. Department of Agriculture, Flow of Water Through 6-Inch Pipe Bends, by D. L. Yarnell. Technical Bulletin No. 577, Washington, D. C. October 1937.

(2) McPherson, M. B., and Strausser, H. S., "Minimum pressures in rectangular bends." Proceedings, ASCE, vol 81, Separate Paper No. 747 (July 1955).

(3) Taylor, D. C., and McPherson, M. B., "Elbow meter performance." American Water Works Association Journal, vol 46, No. 11 (November 1954), pp 1087-1095. (Copyrighted by the American Water Works Association, Inc., N. Y.)

(4) Lansford, W. M., The Use of an Elbow in a Pipe Line for Determining the Rate of Flow in the Pipe. Bulletin No. 289, Engineering Experimental Station, University of Illinois, Urbana, December 1936.

(5) Addison, H., "The use of bends as flow meters." Engineering, vol 145 (4 March 1938), pp 227-229 (25 March 1938), p 324.

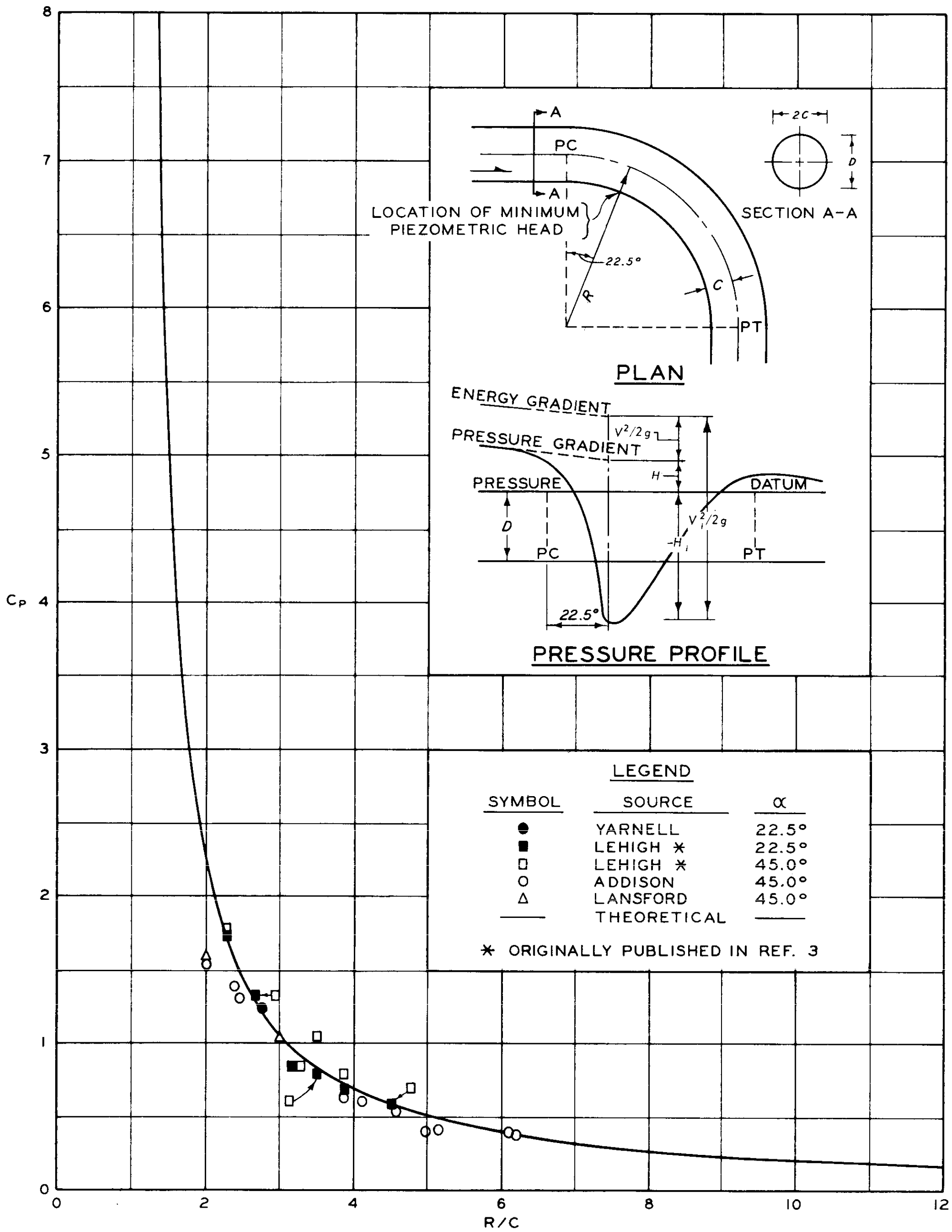

EQUATIONS

$$H + \frac{V^2}{2g} = H_i + \frac{V_i^2}{2g}, \qquad \frac{H - H_i}{\frac{V^2}{2g}} = C_P$$

NOTE: α IS BEND ANGLE TO POINT OF MEASUREMENT.

WHERE:

- H = PIEZOMETRIC HEAD FROM PRESSURE GRADIENT EXTENSION, FT
- V = AVERAGE VELOCITY, FT PER SEC
- g = ACCELERATION, GRAVITATIONAL, FT PER SEC^2
- H_i = MINIMUM PIEZOMETRIC HEAD, FT
- V_i = VELOCITY AT LOCATION OF H_i, FT PER SEC
- C_P = PRESSURE DROP PARAMETER

PRESSURE FLOW PIPE BENDS

MINIMUM PRESSURE

HYDRAULIC DESIGN CHART 228-3

PREPARED BY U. S. ARMY ENGINEER WATERWAYS EXPERIMENT STATION, VICKSBURG, MISSISSIPPI

HYDRAULIC DESIGN CRITERIA

SHEETS 228-4 TO 228-4/1

IN-LINE CONICAL TRANSITIONS AND ABRUPT TRANSITIONS

LOSS COEFFICIENTS

1. Purpose. Hydraulic Design Chart 228-4 presents coefficients for computing head losses through in-line expanding and contracting conical transitions frequently used in penstock and water supply design. This chart can also be used as a guide in estimating coefficients for computing head losses in flood control tunnel interior transitions. Chart 228-4/1 presents similar coefficients for abrupt transitions.

2. Background.

a. Expansions. Extensive data on energy losses in conical expansions were published by Gibson (reference 1) in 1912. Although additional data were published by Peters (reference 5) in 1934, design guidance given in Rouse (reference 7) was limited to the earlier work by Gibson. Kalinske (reference 3) and Robertson and Ross (reference 6) also have investigated flow characteristics in conical diffusers. However, it was 1964 before additional data for head loss coefficients were published by Huang (reference 2). His study included both smooth and artificially roughened pipe. Reynolds numbers tested were from 0.3 to 1.5×10^5. Huang found very little difference in loss coefficients for smooth and rough pipe flow and no effect of Reynolds number on losses for in-line transitions.

b. Contractions. Coefficient data for head losses in conical contractions are appreciably more limited than for expansions. The only known available study is that by Levin (reference 8) in 1970. Levin's data are for diameter ratios of D_2/D_1 of 1.2 to 2.1 and were made at Reynolds numbers of 1×10^5 to 1×10^6.

c. Other Shapes. Loss coefficient curves for expansion transitions of many other cross-section shapes and installation locations have been published by Miller (reference 4). Rouse (reference 7) also presents coefficient curves for abrupt expansions and contractions.

3. Theory. Loss coefficient curves for conical expansions

published by Rouse (reference 7) are based on Gibson's data and described by equation 1:

$$K = \frac{2gH_L}{\left(V_1 - V_2\right)^2} \tag{1}$$

Comparable loss coefficients published by Huang, based on Gibson's, Peters', and his own data are described by equation 2.

$$K_c = \frac{2gH_L}{V_1^2} \tag{2}$$

Loss coefficients published by Levin for conical contractions are also described by equation 2. In these equations, K and K_c are loss coefficients, H_L is the head loss effected by the transitions, V_1 is the average velocity in the smaller conduit (either upstream or downstream, respectively, depending upon whether the flow is expanding or contracting), V_2 is the average velocity in the larger conduit, and g is the acceleration of gravity.

4. Coefficient values from Rouse's plots of Gibson's data were transposed into terms comparable to Huang's by use of the following equation:

$$K_c = K\left[1 - \left(\frac{D_1}{D_2}\right)^2\right]^2 \tag{3}$$

where D_1 is the smaller conduit diameter and D_2 is the larger conduit diameter.

5. Design Criteria.

a. Expansion Coefficients, Conical Transition. Comparable plots of expansion loss coefficients based on tests by Gibson, Peters, and Huang are given in Chart 228-4a.

b. Contraction Coefficients, Conical Transition. Contraction loss coefficients reproduced from Levin's plots are given in Chart 228-4b.

c. Coefficients for Abrupt Transitions. Values based on reference 7 are provided in Chart 228-4/1.

6. References.

(1) Gibson, A. H., "The conversion of kinetic to potential energy in the flow of water through passages having divergent boundaries," Engineering, vol 93 (1912), p 205.

(2) Huang, T. T., Energy Losses in Pipe Expansions, Master of Science Dissertation, State University of Iowa, Iowa City, Iowa, 1964.

(3) Kalinske, A. A., "Conversion of kinetic to potential energy in flow expansions," Transactions, American Society of Civil Engineers, vol 111 (1946), pp 355-374.

(4) Miller, D. S., Internal Flow, A Guide to Losses in Pipes and Duct Systems, British Hydromechanics Research Association, Cranfield, Bedford, England, 1971.

(5) Peters, H., Conversion of Energy in Cross-Sectional Divergences Under Different Conditions of Inflow, Technical Memorandum No. 737 (Translation), National Advisory Committee for Aeronautics, Washington, D. C., March 1934.

(6) Robertson, J. M. and Ross, D., Water Tunnel Diffuser Flow Studies, Parts I and II, Ordnance Research Laboratory, Pennsylvania State College, Pa., 1949.

(7) Rouse, H., Engineering Hydraulics, John Wiley and Sons, Inc., New York, 1950, p 418.

(8) US Army Engineer Waterways Experiment Station, CE, Study of Peculiar Head Losses in Conical Convergences, by L. Levin, Translation No. 73-3, Vicksburg, Miss., January 1973.

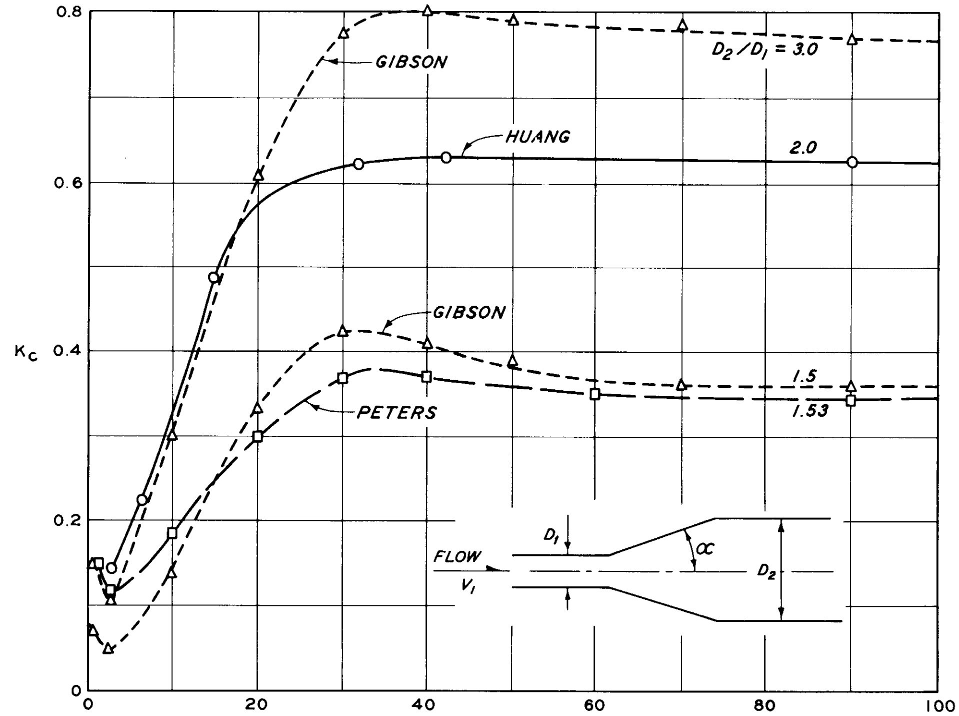

a. EXPANSIONS

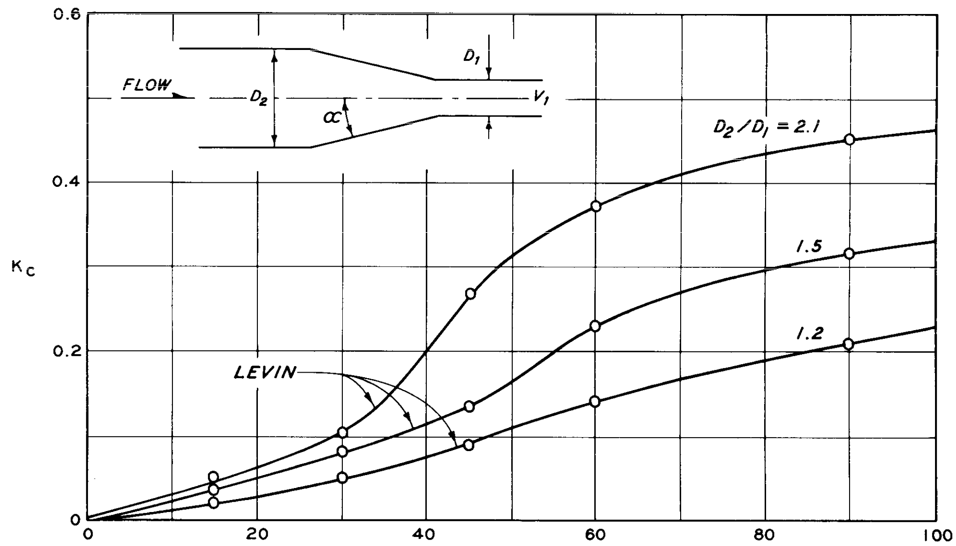

b. CONTRACTIONS

BASIC EQUATION

$K_C = 2gH_L/V_1^2$

WHERE:

H_L = HEAD LOSS, FT

g = ACCELERATION OF GRAVITY, FT/SEC^2

V_1 = AVERAGE VELOCITY IN THE SMALLER CONDUIT, FPS

CONITIONS TRANSITIONS

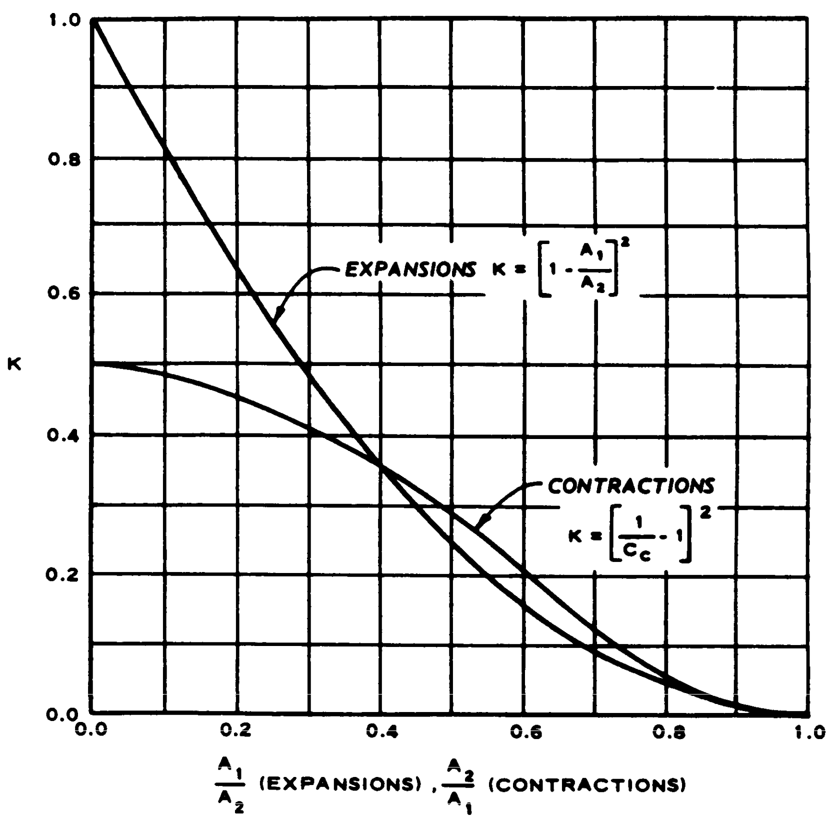

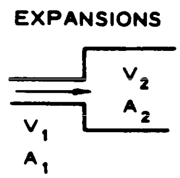

$$h_\ell = K \frac{V_1^2}{2g}$$

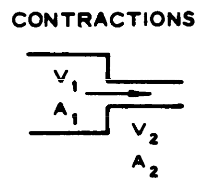

$$h_\ell = K \frac{V_2^2}{2g}$$

WHERE

h_ℓ = HEAD LOSS, FT

K = LOSS COEFFICIENT

V = REFERENCE CONDUIT VELOCITY, FPS

A = CROSS-SECTION AREA, FT^2

g = ACCELERATION OF GRAVITY, FT/SEC^2

C_C = CONTRACTION COEFFICIENT (FROM WEISBACH)

ABRUPT TRANSITIONS
HYDRAULIC DESIGN CHART 228 - 4/1

HYDRAULIC DESIGN CRITERIA

SHEET 228-5

PRESSURE CHANGE COEFFICIENTS

AND JUNCTION BOX HEAD LOSSES

FOR IN-LINE CIRCULAR CONDUITS

1. Purpose. Junction boxes are used extensively in the design of pressure storm drain systems where lateral drains flow into main-line drains. They are also included in long, continuous drains to provide ready access for conduit inspection and maintenance. In small, flow-control outlet works they have been used as wet wells for control gates. Hydraulic Design Chart (HDC) 228-5 presents design information on pressure change coefficients for junction boxes with in-line circular conduits. HDC 228-5a gives pressure change coefficients for junction boxes effecting expansions and contractions. HDC 228-5b shows the effects of box geometry on pressure change coefficient. A procedure for using these pressure change coefficients to compute junction box head losses is given in paragraph 5 below.

2. Background. Arbitrary loss coefficients were used for the design of junction boxes in storm drain systems for many years. In 1958 Sangster, et al.,[1] published the results of the first comprehensive hydraulic study on junction boxes for storm drain systems. In 1959 they published a selected summary of the basic tests.[2] The published reports also give design criteria applicable to multiple inflow junction boxes and to storm drain inlets.

3. Theory. Sangster applied the momentum theory to flows through junction boxes and developed the following equations describing pressure changes across a junction box with in-line conduits.

a. Expansions.

$$K = 2\left[1 - \left(\frac{D_1}{D_2}\right)^2\right] \tag{1}$$

b. Contractions.

$$K = 1 - \left(\frac{D_1}{D_2}\right)^4 + \left(\frac{1}{C_c} - 1\right)^2 \tag{2}$$

where

K = pressure change coefficient
D_1 = downstream conduit diameter, ft
D_2 = upstream conduit diameter, ft
C_c = downstream coefficient value for abrupt contraction according to Rouse[3]

4. Experimental Results. Experimental studies were undertaken by Sangster to evaluate the effects of junction box geometry on the pressure change coefficient K. In each test the upstream and downstream friction pressure gradients were extended to the center of the junction box. The difference between the extended pressure gradients was divided by the velocity head in the downstream conduit to obtain the pressure change coefficient K. HDC 228-5a shows that K is a function of ratio of the diameters of the upstream and downstream conduits and that the junction box width has little effect on the coefficient value. HDC 228-5b shows the effects of junction box shape on pressure changes for in-line conduits of equal size. These plotted data show that for large ratios of b/D_2, pressure change coefficients up to 0.25 were obtained.

5. Application. The pressure change H across the junction box can be computed using the following equation:

$$H = K\left(\frac{V_1^2}{2g}\right) \tag{3}$$

where

V_1 = downstream conduit velocity, fps
g = acceleration of gravity, ft/sec^2

The head loss H_L across the junction box can be computed by use of the Bernoulli equation as follows:

$$H_L = H + \frac{V_2^2 - V_1^2}{2g} \tag{4}$$

where

V_2 = velocity in the upstream conduit, fps

6. References.

(1) Sangster, W. M. et al., Pressure Changes at Storm Drain Junctions. Engineering Series Bulletin No. 41, vol 59, No. 35, University of Missouri, Columbia, Mo., 1958.

(2) Sangster, W. M. et al., "Pressure changes at open junctions in conduits." Journal of the Hydraulics Division, American Society of Civil Engineers, vol 85 (June 1959), pp 13-42.

(3) Rouse, H., Engineering Hydraulics. John Wiley and Sons, Inc., New York, N. Y., 1950, p 34.

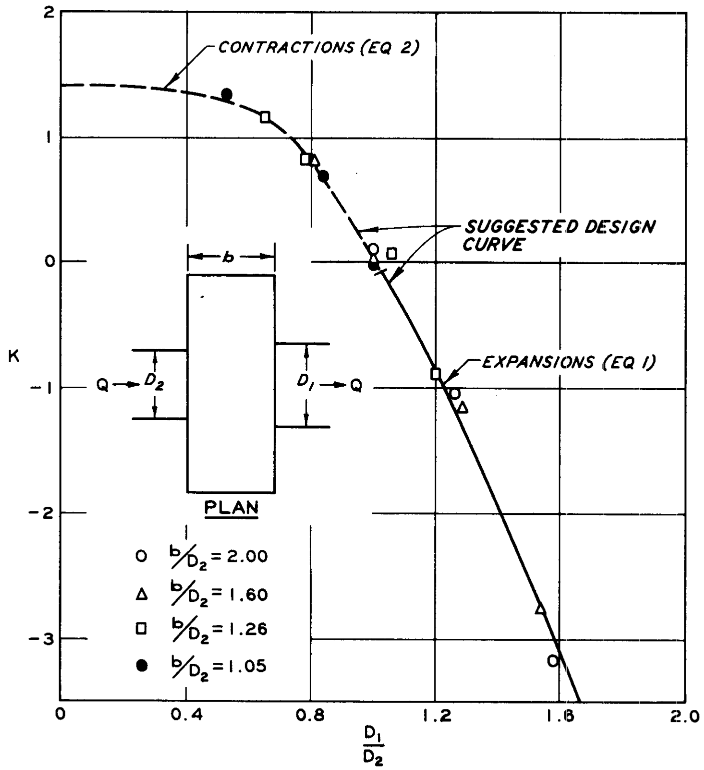

a. TWO CONDUITS IN-LINE

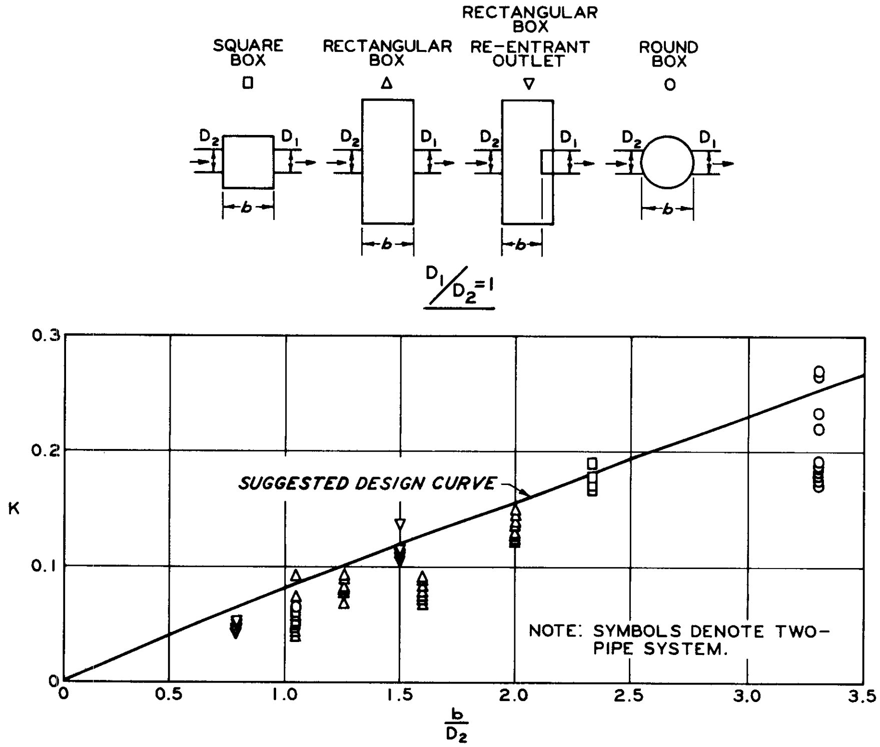

b. EQUAL SIZE CONDUITS

BASIC EQUATION

$K = 2gH/V_1^2$

WHERE:

K = PRESSURE CHANGE COEFFICIENT
g = ACCELERATION OF GRAVITY, FT/SEC^2
H = PRESSURE CHANGE, FT
V_1 = DOWNSTREAM CONDUIT VELOCITY, FPS

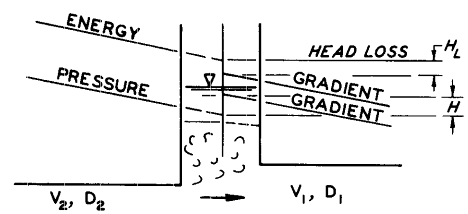

FLOW PROFILE

JUNCTION BOX

PRESSURE CHANGE COEFFICIENTS FOR IN-LINE CIRCULAR CONDUITS

HYDRAULIC DESIGN CHART 228-5

WES 7-73

HYDRAULIC DESIGN CRITERIA

SHEET 228-6

RECTANGULAR CONDUITS

TRIPLE BEND LOSS COEFFICIENTS

1. Purpose. Multiple conduit bends are encountered in water supply and air venting systems and to some extent in lock culvert systems. Appreciable data are available for head losses for circular and rectangular conduits with single bends.[1,2,3,4] Composite head loss coefficients for multiple bends have been investigated and reported by Sprenger[5] for a rectangular conduit with an aspect ratio of two in the plane of the bend. Hydraulic Design Chart (HDC) 228-6 reproduces Sprenger's coefficients for triple bend systems with intermediate straight conduit lengths from zero to five times the equivalent hydraulic diameter of the conduit. Sprenger's data from tests on a single 90-deg bend are shown for comparison. The basic report[5] also contains head loss coefficients for many 90-deg bends of various cross sections for aspect ratios of 0.5 and 2.0 in the plane of the bend. Interaction coefficient factors for bends separated by short tangent lengths have also been published by Miller.[6]

2. Theory. The head loss associated with a single or multiple bend is defined as the difference in elevation between the uniform upstream and downstream pressure gradients when extended on the longitudinal axis of the conduit to the middle of the bend or bend system. This procedure assumes that normal resistance loss exists throughout the bend system and is computed independently of the geometric head loss. The observed pressure differences (head losses) were divided by the velocity head in the conduit flow to obtain a dimensionless coefficient:

$$K = \frac{H_L}{\frac{V^2}{2g}} \tag{1}$$

where

- K = dimensionless head loss coefficient
- H_L = observed pressure difference, ft
- V = velocity of the conduit flow, fps
- g = acceleration of gravity, ft/sec^2

3. The bend loss coefficient is similar to other form resistance coefficients and is a function of the flow Reynolds number:

$$R_e = \frac{VD_h}{\nu} \tag{2}$$

where

R_e = Reynolds number
D_h = equivalent hydraulic diameter of the conduit, ft
ν = kinematic viscosity of the fluid, ft^2/sec

and V and g are as defined above.

4. The head loss coefficient decreases rapidly until it reaches a minimum value at a Reynolds number of about 2×10^5. From this point it increases in value until the Reynolds number reaches about 10^6, beyond which the coefficient probably remains fairly constant.[4]

5. Application. The head loss in a 90-deg rectangular bend with a large aspect ratio in the plane of the bend can be computed using equation 1 and the data given in HDC 228-6. Sprenger's experimental data on single 90-deg bends in rectangular conduits having aspect ratios of 0.5 in the plane of the bend indicate that head loss coefficients for this low aspect ratio are from 0.1 to 0.2 less than comparable values with high aspect ratios in the plane of the bend. It is recommended that the coefficient values given in HDC 228-6 be used for all rectangular conduits with multiple bends when designing for discharge.

6. References.

(1) Madison, R. D. and Parker, J. R., "Pressure losses in rectangular elbows." Transactions, American Society of Mechanical Engineers, vol 58 (1936), pp 167-176.

(2) Harper, J., "Tests on elbows of a special design." Journal of Aero Science (November 1947), pp 587-592.

(3) Silberman, E., The Nature of Flow in Elbows. Project Report No. 5, St. Anthony Falls Hydraulic Laboratory, University of Minnesota, Minneapolis, Minn., December 1947.

(4) Straub, L. G. and Anderson, A. G., Fluid Flow Diversion, A Summary and Bibliography of Literature. Project Report No. 1, St. Anthony Falls Hydraulic Laboratory, University of Minnesota, Minneapolis, Minn., August 1947, p 96.

(5) U. S. Army Engineer Waterways Experiment Station, CE, Head Losses in 90° Elbows for Rectangular Pipes, by H. Sprenger. Translation No. 70-3, Vicksburg, Miss., September 1970.

(6) Miller, D., Internal Flow, A Guide to Losses in Pipes and Duct Systems. British Hydromechanics Research Association, Cranfield, Bedford, England, 1971, p. 43.

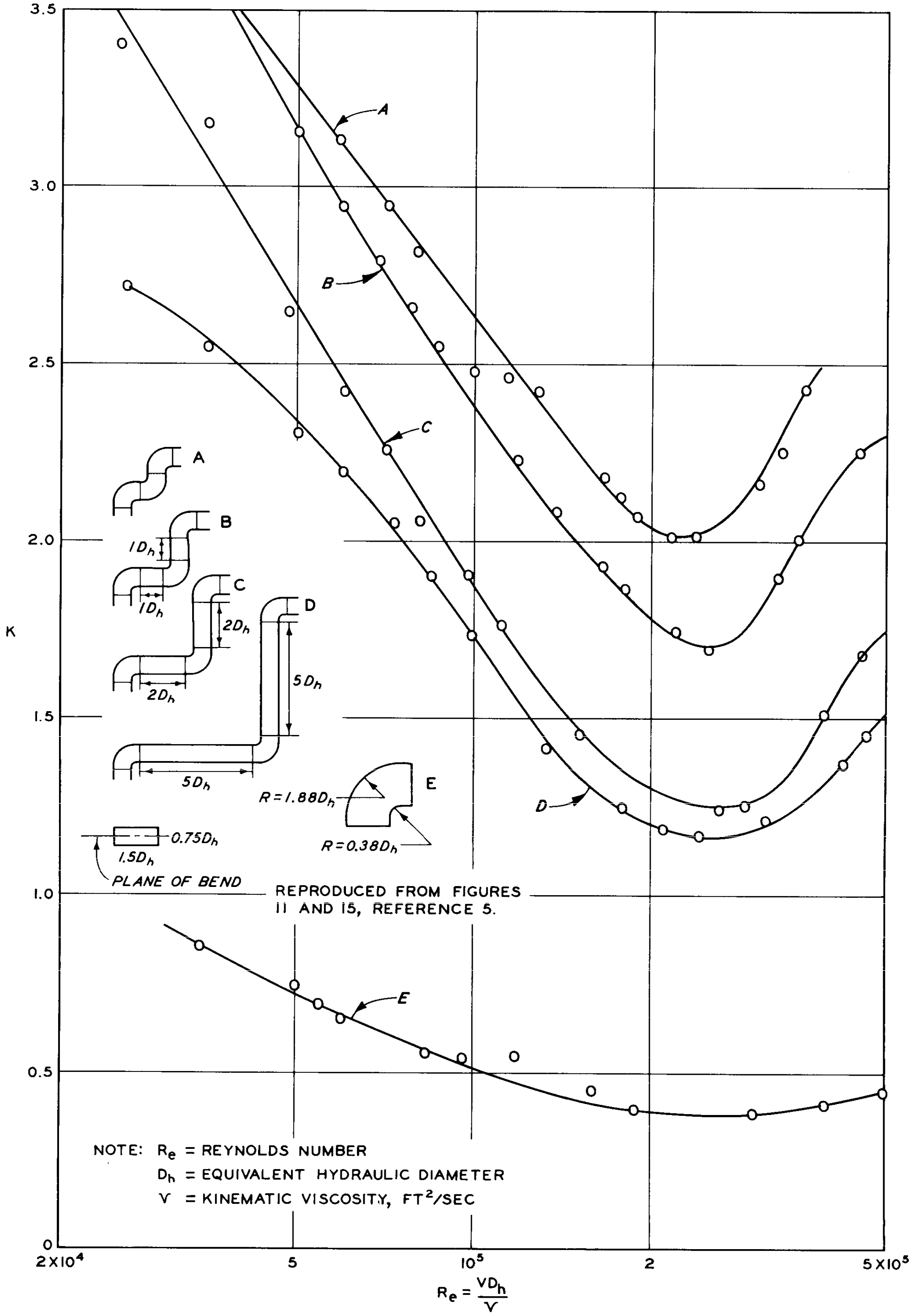

BASIC EQUATION

$H = KV^2/2g$

WHERE:

H = HEAD LOSS, FT
V = CONDUIT VELOCITY, FPS
K = LOSS COEFFICIENT
g = ACCELERATION OF GRAVITY, FT/SEC^2

RECTANGULAR CONDUITS
TRIPLE BEND LOSS COEFFICIENTS

HYDRAULIC DESIGN CHART 228-6

WES 7-73

HYDRAULIC DESIGN CRITERIA

SHEETS 230-1 TO 230-1/2

TWO-WAY DROP INLET STRUCTURES

1. Drop inlet structures for drainage and small dams have been studied for a number of years at the St. Anthony Falls Hydraulic Laboratory (references 1, 2, and 4). In order to adapt the results of this work to larger projects, two series of tests were conducted at the U. S. Army Engineer Waterways Experiment Station (References 5 and 6). The recommended design resulting from these studies is presented in Chart 230-1.

2. Two-way drop inlets are constructed in such a manner that water enters over two weirs that are parallel to the conduit axis (see Chart 230-1). The endwalls of the inlet are extended upward and laterally to support a horizontal antivortex plate. Trashracks can be mounted conveniently on these extended endwalls and outer edges of the antivortex plate. A divider wall between the weirs is extended downward from the antivortex plate to prevent nappe instability. The choice of design for the lower portion of the structure, which includes a hydraulically efficient transition, is based on performance. A design value of 0.2 times the conduit velocity head is used for the overall inlet loss coefficient K_e through the structure (from the pool to the downstream end of the transition). In addition to these characteristics, gated openings can be provided through the inlet riser for low flow outlets and emergency drainage of the reservoir (see reference 6).

3. As the discharge through a two-way drop inlet structure increases, the flow may pass through three phases: weir control, orifice control at the intake, and conduit control. Weir control and conduit control result in satisfactory flow conditions, but orifice control at the intake can produce unstable flow conditions. Designs should be prepared so that orifice flow control will not occur. Orifice control at the intake results when the nappes from the weirs intersect and seal air from the vertical shaft at a discharge less than that required for full pressure flow throughout the structure (conduit control). This leads to a siphonic condition in the shaft causing an increase in discharge. With this flow condition, air is periodically gulped into the inlet riser alternately making and breaking the siphon action. A rapid repetition of this siphonic cycle results in slug flow in the conduit along with surges and pressure variations in the shaft that can cause serious vibration of the entire structure.

4. Design Procedure. The objective of this design procedure is to determine the proper dimensions for a two-way drop inlet structure. Specifically, the weir lengths must be determined such that orifice control at the intake will not occur at any operating pool level. The

method proposed herein does not preset the antivortex plate height (reference 1). Instead, the curves for the three flow conditions are first graphed and analyzed for satisfactory performance (see Chart 230-1/2). The antivortex plate height is then set 1 foot higher than the pool elevation required for establishing conduit-controlled flow (reference 5).

5. Prior to intake design, the following dimensions must be established: (a) the outlet conduit length and its exit invert elevation, (b) the desired minimum reservoir pool elevation (this establishes the weir crest elevations), (c) the diameter of the outlet conduit as estimated by flood routing studies (a minimum of 3 feet is suggested to enable general maintenance (reference 6)), and (d) dimensions T and E based upon structural requirements (see Chart 230-1). Once this information has been determined, a weir length is chosen and discharge computations are made to ensure that orifice control at the intake does not occur. Curves for each of the three flow conditions (weir flow, orifice flow, and conduit flow) are plotted on the same graph, and an analysis is made to assure that orifice flow will not occur. Then the elevation of the antivortex plate is established. See example in Chart 230-1/2.

6. Flow Conditions.

a. Weir Control. Weir flow occurs when the drop inlet crests act as weirs. Satisfactory predictions of the weir flow head versus the discharge may be achieved using published weir flow equations (reference 1), such as:

$$Q = CL_wH_w^{3/2} \tag{1}$$

where

Q = the discharge through the structure, cfs

C = the weir discharge coefficient

L_w = the length of the weir crest for both sides of the structure, ft

H_w = the static head in relation to the crest elevation, ft

A semicircular-shaped crest is recommended to prevent separation of flow from the crest and subsequent periodic flutter of the nappe as observed with square or sharp-edged weirs (reference 5). The weir discharge coefficient for the semicircular shaped weir has been determined to be 3.8. See Chart 230-1 for recommended dimensions of the weir crest.

b. Orifice Control. For the development of an orifice flow head versus discharge relation without the influence of an antivortex plate, the following equation should be used:

$$Q = C'A_o\sqrt{2gH_w} \tag{2}$$

where

C' = orifice flow discharge coefficient

A_o = $(1/2)L_w(D - E)$ = orifice area, ft^2

D = conduit diameter, ft

E = separation wall thickness, ft

g = local gravitational acceleration, ft/sec^2

H_w = static head in relation to the crest elevation, ft

C' can be determined from

$$C' = C''\left(\frac{E}{D}\right)^{0.083}\left(\frac{L_w}{2D}\right)^{-0.2934} \tag{3}$$

where

$$C'' = -15.6993\left(\frac{T}{D}\right)^2 + 11.3136\left(\frac{T}{D}\right) - 0.2032 \tag{4}$$

and T is the width of weir, ft. Chart 230-1/1 presents a graphical solution of these equations.

c. Conduit Control. Conduit flow is developed when full pressure flow exists throughout the inlet structure. The equation for this flow is

$$Q = A\sqrt{\frac{2gH_c}{K}} \tag{5}$$

where

A = the conduit's cross-sectional area, ft^2

g = gravitational constant ($32.174\ ft/sec^2$)

H_c = difference between the pool elevation and the hydraulic grade line (HGL) elevation at the exit portal, ft. (For free flow, HGL elevation is established by Chart 225-1 and for submerged flow, HGL elevation is the tailwater elevation.)

$$K = K_e + f(L/D) + 1.0$$

The following symbols used in the expression for K are defined as follows:

K_e = entrance loss coefficient for the inlet structure in terms of the velocity head in the conduit (0.2 for structure shown in Chart 230-1). Refer to references 1, 2, and 4 for flush type shaft entrances.

$f(L/D)$ = equivalent to a loss coefficient as it is used in the Darcy-Weisbach formula.

f = Darcy-Weisbach friction factor

L = pipe length, ft

D = pipe diameter, ft

7. References.

(1) Agricultural Research Service, U. S. Department of Agriculture, Hydraulics of Closed Conduit Spillways; Part XII, The Two-Way Drop Inlet with a Flat Bottom, by Charles A. Donnelly, George G. Hebans, and Fred W. Blaisdell, ARS-NC-14, Minneapolis, Minn., September 1974.

(2) Agricultural Research Service, U. S. Department of Agriculture, Hydraulics of Closed Conduit Spillways; Part XIII, The Hood Drop Inlet, by Kesavarao Yalamanchili and Fred W. Blaisdell, ARS-NC-23, Minneapolis, Minn., August 1973.

(3) Office, Chief of Engineers, Department of the Army, Engineering and Design; Hydraulic Design of Reservoir Outlet Structures, Engineer Manual EM 1110-2-1602, Washington, D. C., 1 August 1963.

(4) Science and Education Administration, U. S. Department of Agriculture, Hydraulics of Closed Conduit Spillways; Part XVII, The Two-Way Drop Inlet with Semicylindrical Bottom, by Kesavarao Yalamanchili and Fred W. Blaisdell, AAT-NC-2, Minneapolis, Minn., May 1979.

(5) U. S. Army Engineer Waterways Experiment Station, CE, Outlet Works for Branches Oak and Cottonwood Springs Dams, Oak Creek, Nebraska, and Cottonwood Springs Creek, South Dakota, Hydraulic Model Investigation, by J. L. Grace, Technical Report H-72-1, Vicksburg, Miss., January 1972.

(6) __________. Outlet Works for Site 16, Papillion Creek and Tributaries, Nebraska, Hydraulic Model Investigation, by B. P. Fletcher, Technical Report H-73-17, Vicksburg, Miss., October 1973.

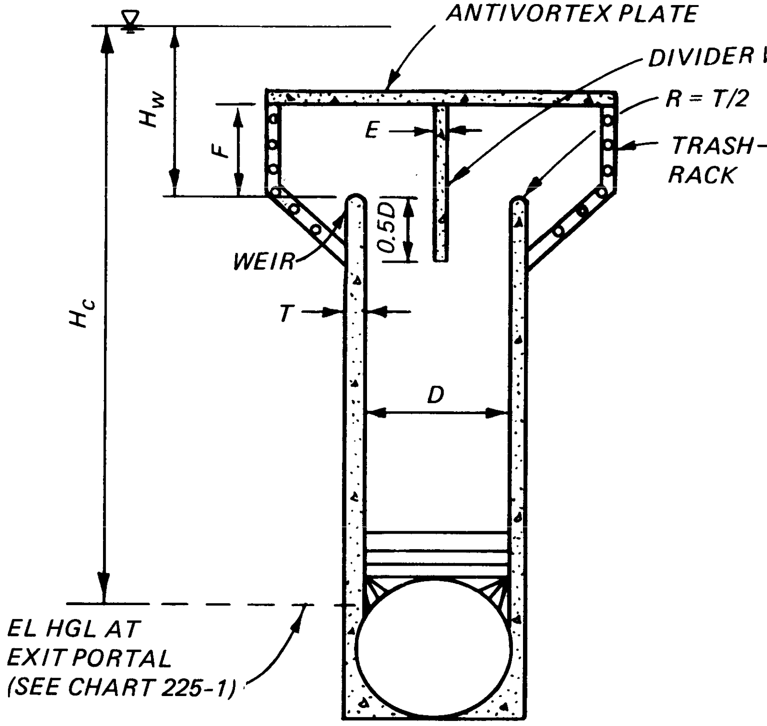

SECTION A - A *

$K_e = 0.2$

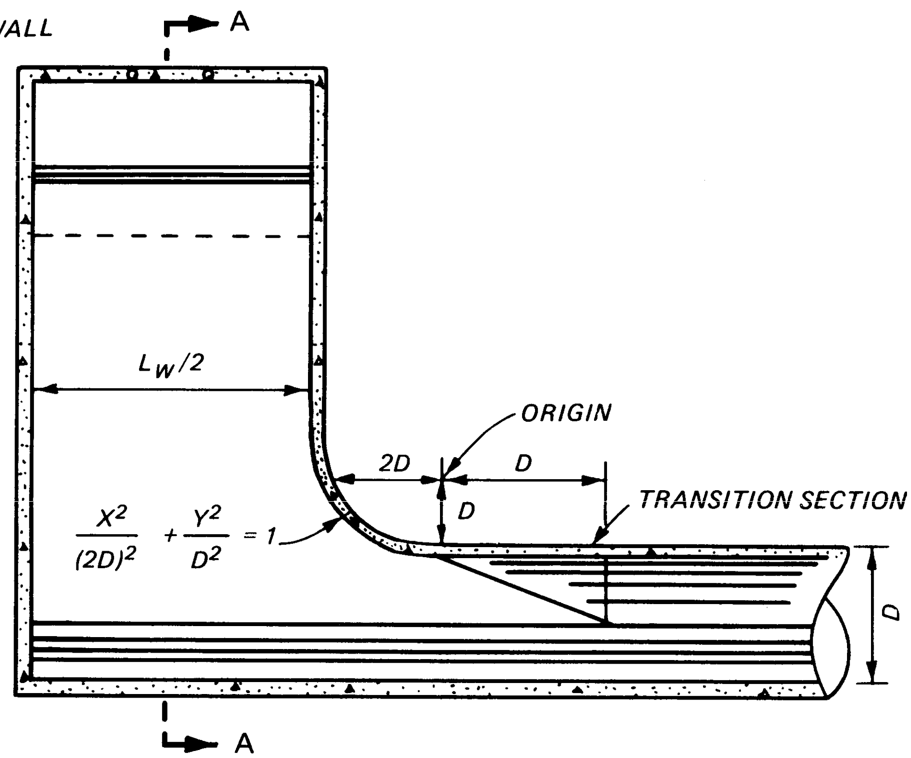

PROFILE *

*NOT TO SCALE

TWO-WAY DROP
INLET STRUCTURES
HDC CHART 230-1

PREPARED BY U.S. ARMY ENGINEER WATERWAYS EXPERIMENT STATION VICKSBURG, MISSISSIPPI

WES 11-87

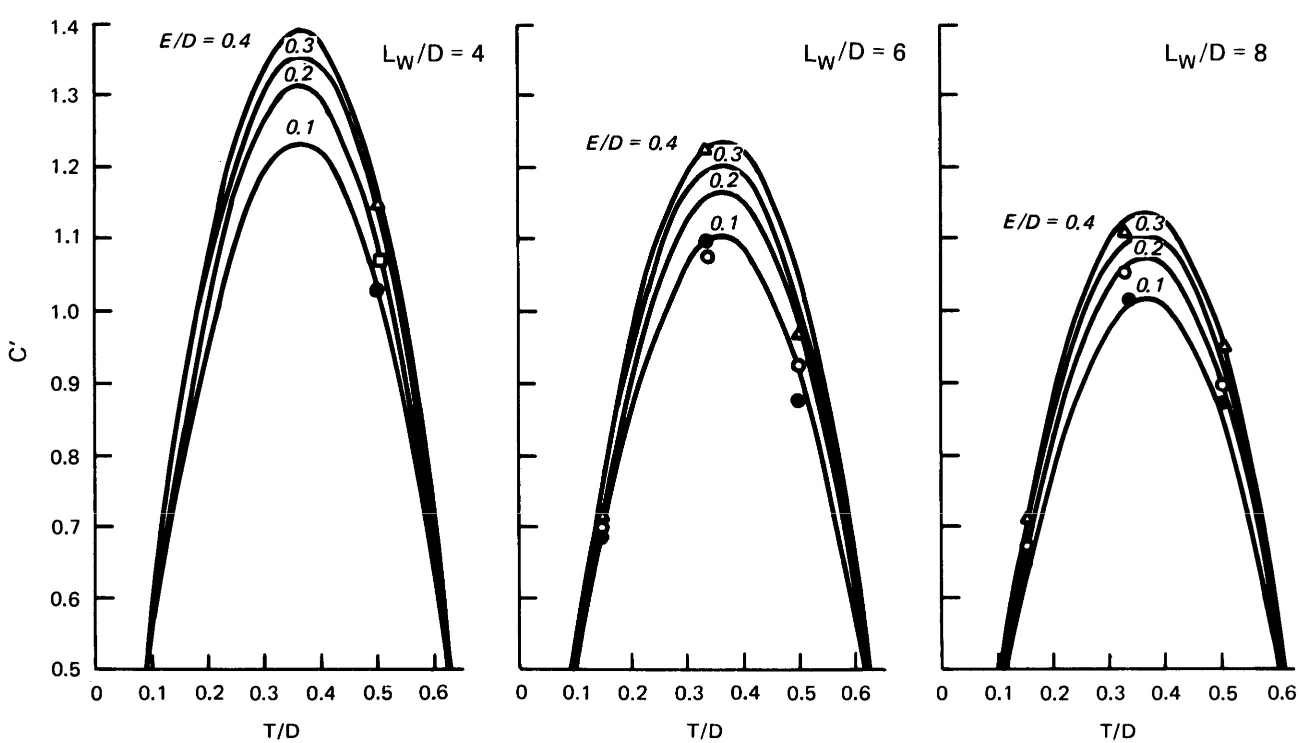

(SEE HDC CHART 230-1 FOR SKETCH)

BASIC EQN $Q = C'A_o\sqrt{2gH_W}$

Q = DISCHARGE, CFS

C' = DISCHARGE COEFFICIENT

A_o = AREA OF ORIFICE, SQ FT

g = LOCAL GRAVITATIONAL ACCELERATION, FT/SEC^2

H_W = STATIC HEAD ON ORIFICE

SYMBOL	E/D
●	0.10
o	0.15
△	0.33

E = SEPARATION WALL THICKNESS, FT

D = CONDUIT DIAMETER, FT

L_W = LENGTH OF WEIR CREST FOR BOTH SIDES OF THE STRUCTURE, FT

T = WIDTH OF WEIR, FT

TWO-WAY DROP INLET STRUCTURE

DISCHARGE COEFFICIENT
FOR ORIFICE FLOW
HDC CHART 230-1/1

WES 11-87

PREPARED BY U.S. ARMY ENGINEER WATERWAYS EXPERIMENT STATION, VICKSBURG, MISSISSIPPI

Example Use of Criteria

Given: $T = 1.0$ ft

$E = 0.75$ ft

$D = 5$ ft (concrete circular conduit)

Free flow at conduit outlet

Spillway conduit length = 600 ft

Elevation of conduit invert at outlet = 100 ft NGVD

Elevation of weir crests = 143 ft NGVD

Determine: Total weir length L_w

Solution:

(1) Initially assume $L_w = 4D$

(2) Weir Control:

$Q = CL_w H_w^{3/2}$

With $C = 3.8$ this becomes

$Q = 76.0\ H_w^{3/2}$.

For this case:

$H_w = P_e$ - weir crest elevation

$H_w = P_e - 143$

where

P_e = water surface elevation of the pool

(3) Orifice Control at Intake:

$$Q = C'\ A_o\sqrt{2gH_w} \text{ and } A_o = (1/2)L_w\ (D - E) = 42.5\ \text{ft}^2$$

From Chart 230-1/1, it is found that $C' = 0.998$

$$Q = (0.998)(42.5)\sqrt{2gH_w}$$

$$Q = 42.4\sqrt{2gH_w} \quad \text{and} \quad H_w = P_e - 143$$

(4) Conduit Control. Hydraulic Program H2045, Discharge in an Oblong or Circular Conduit Flowing Full, as found in the computer-aided design system (CORPS) is used to determine the pool elevation versus discharge curves for minimum and maximum losses. This program is run twice using an effective roughness K_s of 0 and 0.002 for minimum and maximum losses, respectively. The entrance loss coefficient of the two-way drop inlet structure with semicylindrical bottom and a transition at the outlet is chosen as 0.20. The following information results from using Program H2045:

Pipe Radius = 2.5 ft

Length of Conduit = 600.0 ft

Entrance Loss Coefficient = 0.20

Water Temperature = 60°F

Effective Roughness K_s = 0.002 (for maximum losses) EM 1110-2-1602 (reference 3) and Sheet 224-1 for Capacity of Concrete Conduits

= 0.00 (for minimum losses) Corresponds to Smooth Pipe Curve on Chart 224-1

Pool Elevation ft, NGVD	Energy Head ft	Discharge, cfs Maximum Loss Condition	Discharge, cfs Minimum Loss Condition
144.00	44.00	592.43	718.11
145.00	45.00	599.13	726.48
146.00	46.00	605.76	734.76
147.00	47.00	612.31	742.96
148.00	48.00	618.80	751.07
149.00	49.00	625.22	759.09
150.00	50.00	631.57	764.04
155.00	55.00	662.43	805.68

(5) Plots of the pool-discharge curves for weir control, orifice control at the intake, and conduit control (maximum and minimum losses) are presented in Chart 230-1/2a, Sheet 4. These plots reveal that orifice control at the intake may occur between pool elevations 147 and 148; thus, the assumed weir length is inadequate. Computations are therefore repeated for an assumed weir length of 4.4D.

(6) For $L_w = 4.4D$, calculations for weir control and orifice control result in the following:

$$Q = 83.6 H_w^{3/2} \text{ (Weir Control)}$$

$$Q = 45.3 \sqrt{2gH_w} \text{ (Orifice Control)}$$

and as before

$$H_w = P_e - 143$$

(7) Plots of the pool-discharge curves for weir control, orifice control at the intake, and conduit control (maximum and minimum losses) with $L_w = 4.4D$ are presented in Chart 230-1/2b, Sheet 4. These curves indicate that orifice control at the intake should not occur for this weir length and the design is acceptable. Chart 230-1/2b also illustrates how the elevation of the antivortex plate is established in accordance with guidance provided in paragraph 4 of Sheets 230-1 to 230-1/2.

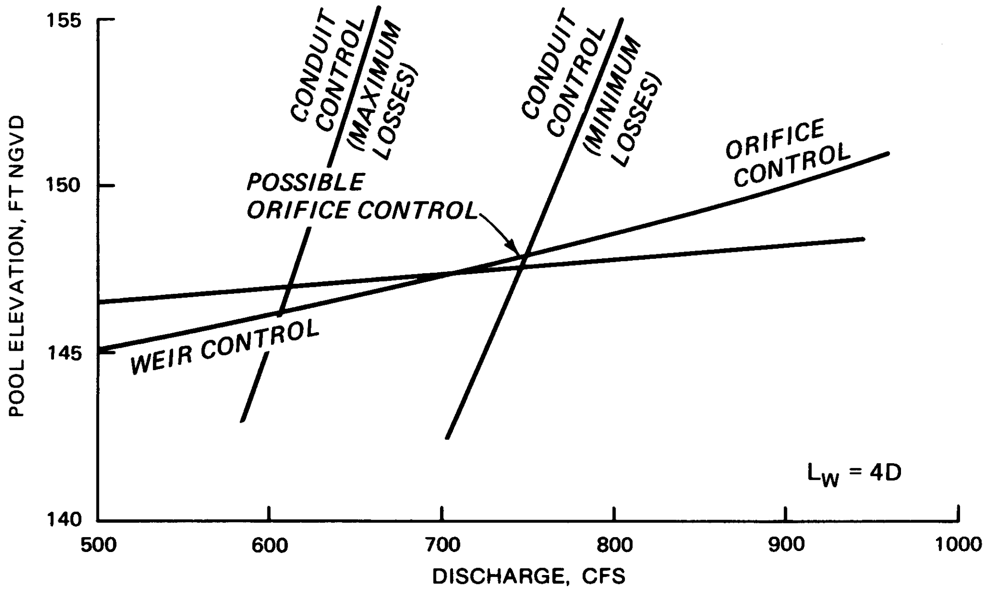

a. POOL DISCHARGE CURVES

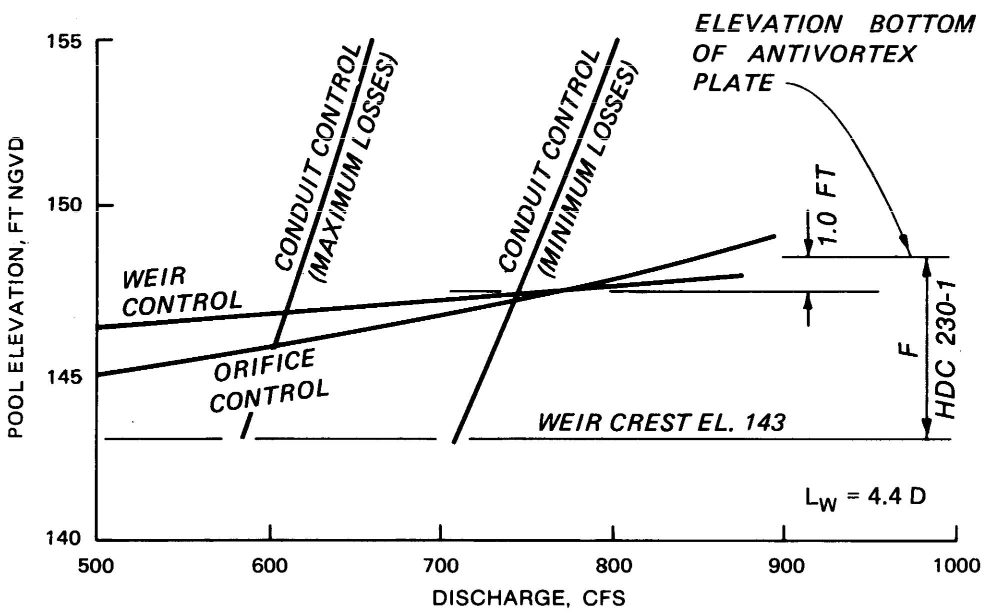

b. POOL DISCHARGE CURVES, ASSUMED WEIR LENGTH OF 4.4D

HDC CHART 230 - 1/2

(SHEET 4 OF 4)